Estimating and Forecasting the Smoking-Attributable Mortality Fraction for Both Sexes Jointly in 69 Countries[1]

Yicheng Li,
University of Washington

Working Paper no. 160
Center for Statistics and the Social Sciences
University of Washington

Feb 21, 2019

[1]Yicheng Li is Graduate Research Assistant and Adrian E. Raftery is Boeing International Professor of Statistics and Sociology, both at the Department of Statistics, Box 354322, University of Washington, Seattle, WA 98195-4322. This research was supported by NIH grants R01 HD054511 and R01 HD070936, and by the Center for Advanced Research in the Behavioral Sciences at Stanford University. The authors are grateful to John Bongaarts for helpful discussions.

Abstract

Smoking is one of the preventable threats to human health and is a major risk factor for lung cancer, upper aero-digestive cancer, and chronic obstructive pulmonary disease. Estimating and forecasting the smoking attributable fraction (SAF) of mortality can yield insights into smoking epidemics and also provide a basis for more accurate mortality and life expectancy projection. Peto et al. (1992) proposed a method to estimate the SAF using the lung cancer mortality rate as an indicator of exposure to smoking in the population of interest. Here we use the same method to estimate the all-age SAF (ASAF) for both sexes for 69 countries. We document a strong and cross-nationally consistent pattern of the evolution of the SAF over time. We use this as the basis for a new Bayesian hierarchical model to project future male and female ASAF from 69 countries simultaneously. This gives forecasts as well as predictive distributions that can be used to find uncertainty intervals for any quantities of interest. We assess the model using out-of-sample predictive validation, and find that it provides good forecasts and well calibrated forecast intervals.
Keywords: Smoking attributable fraction, Peto-Lopez method, Bayesian hierarchical model, double logistic curve, probabilislic projection

Contents

1 Introduction

Smoking is known to have adverse impacts on health and is one of the leading preventable causes of death (Peto et al., 1992; Bongaarts, 2014; Mons and Brenner, 2017). It is a major risk factor for lung cancer, chronic obstructive pulmonary disease (COPD), respiratory diseases, and vascular diseases, and tobacco use causes approximately 6 million deaths per year (Britton, 2017). For instance, tobacco use causes more than 480,000 deaths per year in the United States, accounting for about 20% of the total deaths of US adults, even though smoking prevalence in United States has declined from 42% in the 1960s to 14% in 2018 (Mons and Brenner, 2017).

As a result, estimating the smoking attributable fraction (SAF) of mortality is important for disease control and intervention policy planning. It can also help to improve mortality and life expectancy projections, because smoking can account for nonlinear trends, cohort effects and differentials between countries and between sexes in mortality (Rogers et al., 2005; Bongaarts, 2006; Wang and Preston, 2009; Preston et al., 2011; Janssen et al., 2013; Stoeldraijer et al., 2013; Bongaarts, 2014; Preston et al., 2014; Stoeldraijer et al., 2015; Peters et al., 2016).

The smoking attributable fraction (SAF) is the proportion by which mortality would be reduced if the population were not exposed to smoking. It is defined as

$$\text{SAF} = \frac{n_S}{n_D},$$

where n_S is the number of smokers who died because of their smoking habit and n_D is the total number of people who died. It can be shown that this is equivalent to

$$\text{SAF} = \frac{p(r-1)}{p(r-1)+1}, \tag{1}$$

where p is the underlying prevalence of smoking in the population and r is the risk of dying of smokers divided by the risk of dying of nonsmokers in the population (Rosen, 2013).

Estimating the SAF is not easy for several reasons (Bongaarts, 2014; Tachfouti et al., 2014). First, the smoking habits of individuals can differ in terms of smoking intensity, smoking history, types of tobacco used, as well as first-hand or second-hand smoking, so that estimating the prevalence of smoking (p in Eq. 1) based on smoking behavior data is not straightforward. Secondly, to estimate the relative risk of smoking (r in Eq. 1) requires accurate cohort data. Such data are challenging to collect because smoking is not a direct killer but rather has a lifelong impact, with deaths occurring mostly at older ages. The American Cancer Society's Cancer Prevention Study II (CPS-II), which began in 1982, is so far the largest study that collects such data (Tachfouti et al., 2014). Thirdly, the quality

of registration and survey data varies across countries and between sexes, which makes estimation and comparison of SAF across countries difficult.

Three categories of methods have been proposed to estimate SAF. The first is prevalence-based analysis in cohort studies (SAMMEC) (Levin, 1953). This uses estimated smoking prevalence from surveys and relative risk from CPS-II. The second method is prevalence-based analysis in case-control studies. This method is similar to the first one, except that the relative risk is estimated from a case-control study. It has been used for India (Gajalakshmi et al., 2003), Hong Kong (Lam et al., 2001), and China (Niu et al., 1998). The main drawback of prevalence-based methods is the scarcity of reliable historical data on smoking prevalence, especially for developing countries.

The third method, which overcomes this limitation, is an indirect method. It is called the Peto-Lopez method and was first proposed by Peto et al. (1992). This method estimates the proportion of the population exposed to smoking using lung cancer mortality data, since most lung cancer deaths are due to smoking in developed countries. We use this method to estimate the SAF and we describe the procedure in Section 2.3.

Another indirect method, the PGW method of Preston et al. (2009), also uses lung cancer mortality rate as an indicator of the cumulative hazard of smoking. Instead of using relative risks from the CPS-II as the Peto-Lopez method does, the PGW method adopts a regression-based procedure. We discuss these two methods in Section 5.1. More comparisons among different estimation methods of SAF can be found in Pérez-Ríos and Montes (2008), Tachfouti et al. (2014), Kong et al. (2016), and Peters et al. (2016).

Figure 1 plots the estimated all-age SAF (ASAF) of males and females for the United States from 1950 to 2015. It can be seen that the evolution of SAF over time follows a remarkably strong pattern, first rising and then falling. Qualitatively very similar patterns were found in most countries that we studied, although in countries with less good data, higher levels of measurement error can be seen. It seems intuitive to expect that such a regular pattern could be used to obtain good forecasts. Here we describe our method for doing this. It turns out that, indeed, good forecasts can be obtained, thanks to the strong and consistent pattern of SAF over time. Here we propose a new probabilistic projection method for the SAF using a Bayesian hierarchical model. Our method will provide estimates and projections of the SAF for both sexes jointly for more than 60 countries.

The paper is organized as follows. The data, the detailed SAF calculation based on the Peto-Lopez method, and the proposed Bayesian hierarchical model are described in Section 2. An out-of-sample validation experiment is reported in Section 3. We then discuss estimation and forecasting results for four countries chosen from North America, South America, Asia,

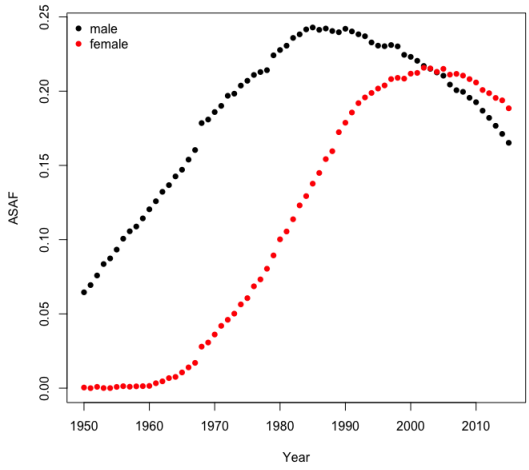

Figure 1: United States: Estimated all-age smoking attributable fractions of mortality for males and females from 1950 to 2015, estimated using the Peto-Lopez method.

and Europe in Section 4. We conclude with a discussion in Section 5.

2 Method

2.1 Notation

We use the symbol y to denote the estimated (observed) all-age smoking attributable fraction (ASAF), which is defined as the smoking attributable fraction for all age groups combined, and we use the symbol h to denote the true (unobserved) ASAF. All of these quantities are indexed by country c, sex s, and year t. The quantities of interest are the unobserved true past and present ASAF together with their future projections. Here the estimation time period is 1950–2015 and the projection time period is 2015–2050. Section 2.3 describes the estimation procedure for ASAF using the Peto-Lopez method for all available countries. A Bayesian hierarchical model will be used to model the estimated ASAF. In the Bayesian hierarchical model, the country-specific parameter vector determining the time evolution pattern of ASAF for country c and sex s is denoted by $\theta_{c,s}$, and the global parameters by ψ.

2.2 Data

We use the annual death counts by country, age group, sex, and cause of death from the WHO Mortality Database (World Health Organization, 2017) which covers data from 1950 to 2015 for more than 130 countries and regions around the world. This dataset comprises

Table 1: ICD codes for different cause of death categories across versions.

Causes	ICD-7 (A-list)	ICD-8 (A-list)	ICD-9 (09A, 09B)
Lung Cancer	A050	A051	B101
Upper Aero-digestive Cancer	A044, A045, A040	A045, A046, A050	B08, B090, B100
Other Cancer	rest of A044-A059	rest of A045-A060	rest of B08-B14
COPD	A092, A093	A093	B323, B324, B325
Other Respiratory	rest of A087-A097	rest of A089-A096	rest of B31-B32
Vascular Disease	A079-A086	A080-A088	B25-B30
Liver Cirrhosis	A105	A102	A347
Other non-med	A138-A150	A138-A150	B47-B56
Other medical	rest	rest	rest
All causes	A000	A000	B00
Causes	ICD-9 (09N)	ICD-10 (101)	ICD-10 (103, 104, 10M)
Lung Cancer	B101	1034	C33-C34
Upper Aero-digestive Cancer	B08, B090, B100	1027, 1028, 1033	C00-C15, C32
Other Cancer	rest of CH02	rest of 1027-1046	rest of C00-C97
COPD	B323, B324, B325	1076	J40-J47
Other Respiratory	rest of CH08	rest of 1072	J00-J99
Vascular Disease	CH07	1064	I00-I99
Liver Cirrhosis	S347	1080	K74, K70
Other non-med	CH17	1095	V00-Y89
Other medical	rest	rest	rest
All causes	B00	1000	AAA

death counts registered in national vital registration systems and is coded under the rules of the International Classification of Diseases (ICD). There are 5 raw datasets available by the most recent update on 11 April 2018. The first three datasets are labeled as ICD versions 7, 8, and 9 respectively, and the last two are labeled as ICD version 10.

Each version of ICD codes causes of death differently and a summary of the codes used for estimating ASAF in Section 2.3 is given in Table 1. For each country, the death counts data can differ by geographical coverage, number of years available and age group breakdown. Some countries such as China only have data from selected regions, and these countries will not be included here.

We use the quinquennial population by five-year age groups from the 2017 Revision of the World Population Prospects (United Nations, 2017) for each country, sex, and age group. Since this dataset provides population estimates at five-year intervals, we use linear interpolation to obtain annual population estimates for each five-year age group.

2.3 ASAF Estimation

We apply the original Peto-Lopez indirect method to estimate ASAF for male and female separately. This method uses the lung cancer mortality rate as an indicator of the accumulated hazard of smoking to estimate the proportion of population exposed to smoking. The original papers (Peto et al., 1992, 1994, 2006) applied the method to developed countries only, especially in West Europe and North America. With the shift of global smoking pattern, and diffusion of smoking in middle- and low-income countries, this method has been extended to less developed countries (Ezzati and Lopez, 2003, 2004; Pampel, 2006).

For estimating ASAF using the Peto-Lopez method, we need first to estimate age- and cause-of-death-specific SAF. The age groups used for estimation are 0-34, 35-59, 60-64, 65-69, 70-74, 75-79, and 80+. For each age group, annual death counts of the following nine categories of causes of death are obtained from the five raw datasets of WHO Mortality Database: lung cancer, upper aero-digestive cancer, other cancers, COPD, other respiratory diseases, vascular diseases, liver cirrhosis, non-medical causes, and all other medical causes. A detailed list of codes from ICD 7, 8, 9, and 10 for these nine categories is provided in Table 1.

The ICD categorizes death count data according to availability using so-called sublists, which can be one of A-list or several others; see Table 1. The sublists we use are those satisfying the minimum requirements for ASAF calculation. More specifically, for ICD 7 and 8, only countries whose ICD sublist is A-list are used. For ICD 9, only those countries whose ICD sublist is 09A-, 09B-, or 09N-list are used. For ICD 10, countries whose ICD sublist is one of 101-, 103-, 104-, 10M-list are used. In addition, we only calculate age-specific SAF for countries whose age group breakdown is finer than the following age group breakdown: 0-34, 35-39, 40-44, 45-49, 50-54, 55-59, 60-64, 65-69, 70-74, 75+. This corresponds to the age group format number 00, 01, 02, 03, 04 in the raw datasets.

To estimate the proportion of a population exposed to smoking, i.e., p in Eq. 1, the method compares the observed lung cancer mortality rate with the lung cancer mortality rate of smokers estimated from CPS-II. The estimated proportion, indexed by country c, age group a, sex s, and year t, is estimated by

$$p_{c,a,s,t} = \frac{d_{c,a,s,t} - d^S_{a,s}}{d^S_{a,s} - d^{NS}_{a,s}},$$

where $d_{c,a,s,t}$ is the observed country-age-sex-year-specific lung cancer mortality rate and $d^S_{a,s}$ and $d^{NS}_{a,s}$ are age-sex-specific lung cancer mortality rates for smokers and nonsmokers from the CPS-II respectively. Here the observed lung cancer mortality rate $d_{c,a,s,t}$ is the observed lung cancer death count divided by the population estimated from the 2017 Revision of the

World Population Prospects for country c, age group a, sex s, and year t.

The Peto-Lopez method uses the CPS-II to estimate the relative risk of dying for each cause of death for smokers and nonsmokers, i.e., r in Eq. 1. Specifically, the Cochran-Mantel-Haenszel method is used to estimate the relative risk for age group 35-59 by combining five sub-age groups (35-39, 40-44, 45-49, 50-54, 55-59). The relative risk is indexed by cause-of-death k, age group a, and sex s. Here k takes integer values 1-9 corresponding to the nine categories mentioned above.

The excess mortality rate attributable to smoking is denoted by $er_{k,a,s}$ for cause-of-death k, age group a, and sex s. For lung cancer, the excess mortality rate attributable to smoking is calculated as $er_{1,a,s} = r_{1,a,s} - 1$. For all other categories except liver cirrhosis ($k = 7$) and non-medical causes ($k = 8$), the excess risk is discounted by 50%, i.e., $er_{k,a,s} = 0.5(r_{k,a,s} - 1)$ for $k = 2, 3, 4, 5, 6, 9$, so as to control for confounding factors. The excess risks for liver cirrhosis and non-medical causes are set to 0, i.e., $er_{7,a,s} = er_{8,a,s} = 0$. The country-cause-age-sex-year-specific SAF, denoted by $y_{c,k,a,s,t}$, is then

$$y_{c,k,a,s,t} = \frac{p_{c,a,s,t} \times er_{k,a,s}}{p_{c,a,s,t} \times er_{k,a,s} + 1}.$$

Any estimated negative values are set to zero.

Since the hazard due to smoking is accumulated across years and mostly causes deaths at older ages, the fraction of deaths due to smoking for ages 0-34 is typically very small and is set to 0. In addition, the SAF for ages 80+ is set to the same value as that for ages 75-79 since smoking data are unreliable for very old ages. Finally, the country-sex-year-specific ASAF, denoted by $y_{c,s,t}$, is a weighted average of the age-specific smoking attributable fractions $y_{c,k,a,s,t}$. Thus

$$y_{c,s,t} = \sum_a \sum_k y_{c,k,a,s,t} \times d_{c,k,a,s,t},$$

where $d_{c,k,a,s,t}$ is the country-cause-age-sex-year-specific mortality rate.

We chose the Peto-Lopez method to estimate the ASAF because it has been validated and widely used (Preston et al., 2009; Bongaarts, 2014; Tachfouti et al., 2014; Kong et al., 2016). Also, the data required for the estimation are cause- and age-specific death counts and population, which are provided with high quality by the WHO Mortality Database and the 2017 Revision of the World Population Prospects.

There are some variants of the Peto-Lopez method, which also assume that the lung cancer mortality rate is a good indicator for measuring smoking exposure. Some of the modifications include using different relative risk estimation instead of the CPS-II to extend the method to developing countries (Ezzati and Lopez, 2003) or using a regression-based approach (Preston et al., 2009). Section 5.1 contains more detailed discussion and comparison of these methods.

2.4 Model

We develop a four-level Bayesian hierarchical framework to model male and female ASAF jointly for multiple regions simultaneously.

Random walk with drift for the true ASAF: The observed ASAF data show a strong and consistent pattern of increasing, then leveling, and then declining again for both sexes (Stoeldraijer et al., 2015) (see Figure 1 for the example of United States). This pattern can be captured by the following five-parameter double logistic curve:

$$g(t|\theta) = \frac{k}{1+\exp\{-a_1(t-1950-a_2)\}} - \frac{k}{1+\exp\{-a_3(t-1950-a_2-a_4)\}}, \qquad (2)$$

where t is the year of observation and θ is the double-logistic parameter vector, $\theta = (a_1, a_2, a_3, a_4, k)$. The double logistic curve has been widely used for modelling and projecting quantities that exhibit growth and decline, such as the rate of change of the total fertility rate (Alkema et al., 2011) and of life expectancy (Raftery et al., 2013). For the five-parameter double logistic function in Eq. 2, a_2 controls the first (left) inflection point of the curve and a_4 controls the distance between the first (left) and the second (right) inflection points. The rates of change at these inflection points are controlled by a_1 and a_3 respectively. The parameter k is an upper bound for the maximum value of the curve. See the upper panel of Figure 2 for an illustration.

To represent this and also take account of the observed pattern of variability, we modeled changes in the true ASAF between adjacent time points using a random walk with drift given by the difference between the double logistic curve at the two points. This takes the form

$$h_{c,s,t} = h_{c,s,t-1} + g(t|\theta_{c,s}) - g(t-1|\theta_{c,s}) + \varepsilon^h_{c,s,t}, \qquad (3)$$

where $g(\cdot|\theta_{c,s})$ (i.e., Eq. 2) quantifies the expected change of true ASAF governed by the country- and sex-specific parameters $\theta_{c,s} = (a_1^{c,s}, a_2^{c,s}, a_3^{c,s}, a_4^{c,s}, k^{c,s})$, and $\varepsilon^h_{c,s,t}$ are independent Gaussian noises. This random walk with drift model is designed to capture the variability of the true ASAF and allows the uncertainty of the forecast to increase when projecting further into the future.

Male-female joint model: Since the female smoking epidemic usually starts one to two decades after the male one, the start of the increase in female ASAF is also later than that of male ASAF. For most countries, the observed female ASAF is still in the increasing or leveling phase up to 2015. However, as the smoking epidemic diffuses from the male to the female population, it is reasonable to assume that the female ASAF will follow the

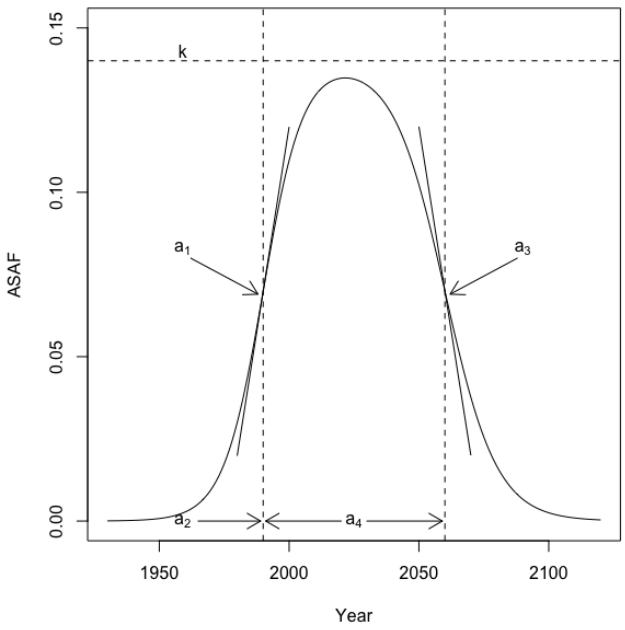

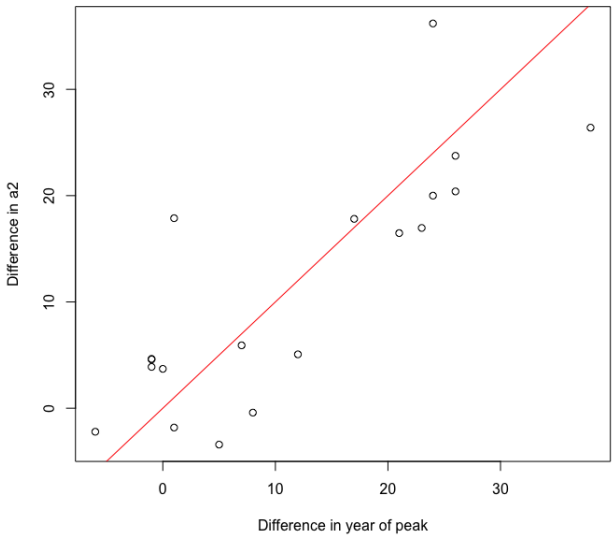

Figure 2: Upper: The five-parameter double logistic curve. a_2 controls the left inflection point, a_4 controls the distance between left and right inflections points, a_1, a_3 determine the rate of change at left and right inflection points, and k approximates the maximum value. Lower: The difference of country-specific a_2^m and a_2^f plotted against the difference between the country-specific peaks for males and females. The peak and a_2 are estimated from the countries whose male and female ASAF have all passed the maximum by 2015, according to the results of the non-linear least squares estimation. The red line is the 45 degree line.

same trend of increasing-leveling-declining as that of the male ASAF. This has already been observed for several countries with early smoking epidemics, such as the United Kingdom, Denmark, and Japan (Pampel, 2005; Peto et al., 2006; Janssen et al., 2013; Bongaarts, 2014; Stoeldraijer et al., 2015). For these countries, the female ASAF follows the same trend as that of the male ASAF, but differs mainly in terms of the rate of increase or decrease, the number of years taken to reach the peak, and the peak ASAF value.

For males, we need only estimate the rate of decline of the ASAF. For females, especially for those countries whose observed ASAF data have not levelled yet, one needs first to determine the time and value of leveling. By modeling male and female data jointly, the lower panel of Figure 2 shows that for countries whose male and female ASAF both passed the leveling period, the difference between the years of maximum of male and female is approximately the same as the difference in the a_2 parameter estimated from Eq. 2. The a_2 parameter represents the time point where the speed of the increasing part of the double logistic curve begins to slow down.

The difference between the times-to-peak of male and female ASAF also differs among countries. For example, the time-to-peak of the female ASAF in the United States is about 15 years later than that of the male ASAF, while the time-to-peak of the ASAF happened at about the same time for both sexes in Hong Kong. To incorporate these observations, we model the difference between male and female country-specific a_2^c using a Gaussian distribution:

$$a_2^{c,f} = a_2^{c,m} + \triangle_{a_2}^c, \qquad \triangle_{a_2}^c | \triangle_{a_2}, \sigma^2_{\triangle_{a_2}} \sim \mathcal{N}(\triangle_{a_2}, \sigma^2_{\triangle_{a_2}}), \tag{4}$$

where $a_2^{c,m}$ and $a_2^{c,f}$ are the country- and sex-specific values of a_2, and $\triangle_{a_2}^c$ is the country-specific difference between these two parameters with prior mean $\triangle_{a_2}$ and variance $\sigma^2_{\triangle_{a_2}}$.

Moreover, since there are very few countries whose female ASAF have begun to decline by 2015, while the male ASAF has been declining for many years in most countries, we set the same global parameters for the sex-specific parameters $a_4^{c,m}$ and $a_4^{c,f}$ for each country, namely,

$$a_4^{c,m}, a_4^{c,f} | a_4, \sigma^2_{a_4} \overset{\text{ind}}{\sim} \mathcal{N}(a_4, \sigma^2_{a_4}). \tag{5}$$

Except for a_4^c, the other four country-specific parameters of the double logistic curve are conditioned on their own sex-specific global parameters.

Measurement error model for observed ASAF: The observed country-sex-year-specific ASAF $y_{c,s,t}$ are modeled based on the true (unobserved) ASAF $h_{c,s,t}$ by incorporating

measurement error due to the variability of data quality across different countries:

$$y_{c,s,t}|h_{c,s,t}, \sigma_c^2 \sim_{ind} \mathcal{N}(h_{c,t,s}, \sigma_c^2). \tag{6}$$

We assume that the variance of observed ASAF for each country is time- and sex-invariant based on exploratory analyses that indicate that the data quality is consistent across time and between sexes within the same country.

Summary of Model: We combine the Bayesian hierarchical model and measurement error model into a four-level Bayesian hierarchical model. We model the observed ASAF estimates using the measurement error model in Level 1, conditional on the true (unobserved) ASAF data which are modeled with a random walk with drift in Level 2, conditional on the country-specific parameters. Country-specific parameters are modeled in Level 3, where parameters for male and female SAF are modelled jointly conditional on the global parameters, whose prior distributions are specified in Level 4.

The overall model is specified as follows:

$$\begin{aligned}
&\text{Level 1: } y_{c,s,t}|h_{c,s,t} \sim \mathcal{N}(h_{c,s,t}, \sigma_c^2);\\
&\text{Level 2: } h_{c,s,t_{0,c}} = g(t_{0,c}|\theta_{c,s}) + \varepsilon^h_{c,s,t_{0,c}},\\
&\qquad\qquad h_{c,s,t} = h_{c,s,t-1} + g(t|\theta_{c,s}) - g(t-1|\theta_{c,s}) + \varepsilon^h_{c,s,t} \text{ for } t > t_{0,c},\\
&\qquad\qquad \varepsilon^h_{c,s,t} \overset{\text{ind}}{\sim} \mathcal{N}(0, \sigma_h^2);\\
&\text{Level 3: } \theta_{c,s} \sim f(\cdot|\psi),\\
&\qquad\qquad \sigma_c^2 \sim \text{Lognormal}(\nu, \rho^2);\\
&\text{Level 4: } \psi, \nu, \rho^2, \sigma_h^2 \sim \pi(\cdot).
\end{aligned}$$

Here, $t_{0,c}$ is the year of the first available ASAF data for country c, g denotes the five-parameter double logistic curve in Eq. 2, f denotes the conditional distribution of the country-specific parameters $\theta_{c,s}$, and π denotes the hyperpriors for the global parameters $\psi, \nu, \rho^2, \sigma_h^2$. The country specific parameters $\theta_{c,s} = (a_1^{c,s}, a_2^{c,s}, a_3^{c,s}, a_4^{c,s}, k^{c,s})$ are sex-specific and the interaction between male and female parameters are governed by Eq. 4 and 5. The hyperparameters $\psi = (a_1^m, a_2^m, a_3^m, a_4, k^m, a_1^f, a_3^f, k^f, \triangle_{a_2}, \sigma^2_{a_2^m}, \sigma^2_{a_4}, \sigma^2_{k^m}, \sigma^2_{k^f}, \sigma^2_{\triangle_{a_2}})$ are also sex-specific except for $\triangle_{a_2}, \sigma^2_{\triangle_{a_2}}, a_4, \sigma^2_{a_4}$. More information about the specification of the full model is given in the Appendix A.

Estimation and prediction: Statistical analysis of the model is carried out in two phases, estimation and prediction. The goal of the estimation phase is to obtain the joint posterior

distribution of the true ASAF $h_{c,t,s}$ during the estimation period 1950–2015 and the country-specific parameters for the underlying double-logistic curve. The aim of the prediction phase is to forecast the future ASAF of both sexes for the prediction period 2015–2050 based on the observed ASAF for all 69 countries whose male ASAF data are classifed as clear-pattern (see Section 2.5 for the definition of clear-pattern).

The functional form of the prior distribution $\pi(\cdot)$ is assessed using results from nonlinear least squares estimation based on clear-pattern countries (see Section 2.5 for details). Specifically, the priors for $(a_1^m, a_2^m, a_3^m, a_4, k^m, \sigma^2_{a_2^m}, \sigma^2_{a_4}, \sigma^2_{k^m}, \sigma^2_{a_2^m}, \sigma^2_{a_4}, \sigma^2_{k^m})$ are based on non-linear least squares results from the male ASAF of 69 clear-pattern countries, the prior for a_1^f is estimated based on non-linear least squares results from the female ASAF of 52 clear-pattern countries, the priors for $(a_3^f, k^f, \sigma^2_{a_3^f})$ are set to the same priors as their counterparts for males, while the priors for $(\triangle_{a_2}, \sigma^2_{\triangle_{a_2}})$ are estimated based on 19 countries for which both male and female ASAF have passed the leveling stage by 2015. The priors for ν, ρ^2, σ_h^2 are estimated by pooling male and female ASAF from all clear-pattern countries.

2.5 ASAF Categorization

We categorize estimated ASAF for 127 countries and regions into two categories according to the data availability and quality: clear-pattern and non-clear-pattern. On one hand, the Peto-Lopez method is not guaranteed to produce reliable ASAF estimates for some less developed countries because of poor data quality. On the other hand, modeling only with clear-pattern countries can improve estimation and projection accuracy without introducing too much random noise.

The classification is based on non-linear least squares estimation of the following model for each country and sex separately:

$$y_t = g(t|\theta) + \varepsilon_t,$$

where $g(t|\theta)$ is as in Eq. 2 and ε_t are independent standard Gaussian errors. Its fit to the data in a given country provides an indication of data quality for that country.

Our categorization is based on the number of observations, maximum of observed values, and the R^2 value of the non-linear least squares fit. Due to the differences between the diffusion processes of smoking in the male and female populations (Pampel, 2006), we use different criteria for male and female data. For male data, we require that (1) the number of available annual observations up to 2015 be greater than 10; (2) at least one of the observations be greater than 0.05; and (3) that the R^2 value be greater than 0.5.

For female data, since the smoking epidemic in general started one to two decades later than the male one, the onset and the value of the ASAF is later and smaller than that of

the male epidemic (Pampel, 2005; Preston and Wang, 2006). The criterion for female data is that (1) the number of observations up to 2015 be greater than 10; (2) at least one of the observations be greater than 0.01; and (3) that the R^2 value be greater than 0.6.

By these rules, there are 69 countries whose male data are classifed as clear-pattern (2 in Africa, 16 in the Americas, 9 in Asia, 40 in Europe and 2 in Oceania), and 52 countries whose female data are classified as clear-pattern (12 in the Americas, 7 in Asia, 31 in Europe and 2 in Oceania).

2.6 Estimation

Estimation is based on the male and female ASAF data from the 69 countries whose male ASAF is classified as clear-pattern for the period 1950–2015. The reason why we chose clear-pattern ASAF data is that non-clear-pattern data either have too few observations, very low values, or their shapes are not identifiable.

We used the Rstan package (Version 2.18.2) in R to obtain the joint posterior distributions of the parameters of interest (Carpenter et al., 2017). Rstan uses a No-U-turn sampler, which is an adaptive variant of Hamiltonian Monte Carlo (Neal, 2011; Hoffman and Gelman, 2014). We ran 3 chains with different initial values, each of length 10,000 iterations with a burn-in of 2,000 without thining. This yielded a final, approximately independent sample of size 8,000 for each chain. We monitored convergence by inspecting trace plots and using standard convergence diagnostics. More information about the convergence diagnostics is given in the Appendix B.

2.7 Projection

We produce projections of future ASAF for the period 2015–2050 for the 69 countries whose male ASAF is classified as clear-pattern. The prediction of future ASAF for each country is based on past and present ASAF. We sample from the joint posterior distribution of the country-specific parameters $\theta_{c,s}$ and of the past, and present true ASAF $h_{c,s,t}$. We then use Eq. 3 and 6 to generate a sample of trajectories of future true and observed ASAF respectively from their joint posterior predictive distribution. It is possible that the quantity generated by Eq. 3 and Eq. 6 is negative, and we set such values to zero. This yields a sample from the joint posterior predictive distribution of future ASAF for all 69 countries, for both sexes, taking account of uncertainty about the past observations as well as the future evolution. We include the plots of projections ASAF for all 69 countries and both sexes in the Appendix C.

3 Results

We assess the predictive performance of our model using out-of-sample predictive validation.

3.1 Study Design

The data we used for out-of-sample validation cover the period 1950–2015. We assess the quality of our model based on different choices of estimation and validation data from the observed data. Since the trend of increasing-leveling-declining pattern plays an important role for estimation and projection, assessing how the model works when only part of the trend has been observed is crucial. We consider different choices for estimation and validation periods, namely (1) 1950– 2000 for estimation and 2000–2015 for validation; (2) 1950–2005 for estimation and 2005–2015 and for validation; and (3) 1950–2010 for estimation, 2010–2015 for validation. The countries used for validation in each time-split scenario are required to be clear-pattern countries based on the male ASAF, to contain more than 10 observations in the estimation period, and to have at least one observation in the prediction period. This results in 63, 66 and 66 countries used for validation under choices (1), (2) and (3), respectively.

Since we are making probabilistic projections, our evaluation is based on both accuracy of point prediction and calibration of prediction intervals. Our goal is not only to produce accurate point predictions, but also to account for variability of future predictions based on historic data, especially for those countries whose data in the estimation period reveal only part of the pattern. If the proposed model works well, we would expect the point predictor to have small sex-specific mean absolute error (MAE), which is defined as

$$\text{MAE}_s = \frac{1}{N} \sum_{c \in \mathcal{C}} \sum_{t \in \mathcal{T}_c} |\hat{y}_{c,s,t} - y_{c,s,t}|, \tag{7}$$

where $\mathcal{C}$ is the set of countries considered in the validation, $\mathcal{T}_c$ is the set of country-year combinations used for validation, $\hat{y}_{c,s,t}$ is the posterior median of the predictive distribution of ASAF at year t for country c and sex s, and N is the total number of data used for validation. In addition, we also expect the prediction to be well calibrated, i.e., the coverage of the prediction interval to be close to the nominal level.

3.2 Out-of-sample Validation Results

To our knowledge, no other method is available in the literature to produce probabilistic forecasts for male and female ASAF for developed and developing countries jointly. Janssen et al. (2013) and Stoeldraijer et al. (2015) developed methods for projection of age-specific

SAF and age-standardized SAF, and their methods are based on age-period-cohort analysis, which cannot be trivially extended to ASAF. See Section 5.2 for more discussion of their procedures and comparison to the present ones. As a benchmark against which to compare our method, we consider the persistence forecast, which takes the last observed value as the forecast for the prediction period.

We summarize the validation results in Table 2 for males and females separately, which records the MAE and coverage of the prediction interval (if available). For males, our method improves the prediction accuracy for all three scenarios over the persistence forecast. For forecasting one and two five-year periods ahead, our method improves the MAE by 30% and 21.4% respectively. Since most male ASAF levels had passed the leveling period by the year 2005 and had experienced declines for several years, the double logistic curve captures this trend well. For predictions three five-year periods into the future, during which the male ASAF data for some countries were just reaching the peak, our method still improves the MAE by 5.8%. For prediction intervals, the coverage of our method is close to the nominal level for one and two five-year predictions, while the coverage is reasonably close to nominal for the three five-year predictions.

Figure 3 shows validation results of four countries or regions for predictions three five-year periods ahead. We see that our method works quite well for the United States and Hong Kong, and the prediction interval captures the variability of male ASAF of Chile.

For females, we observe similar improvements. Table 2 shows that our method improves prediction accuracy over the persistence forecast. Specifically, our method decreases MAE by 22.2%, 16.7%, and 26.7% for predictions one, two, and three five-year periods ahead. On the other hand, since most female ASAF has not yet reached the leveling and decreasing stage, capturing the variability of future female ASAF is essential. The coverage of our method is very close to the nominal level, indicating that our method is well calibrated.

Figure 4 shows the results from Scenario (1) where most female ASAF of countries among the examples have not reached the peak by the year 2000. We see that the posterior median of the predictive distribution captures the general trend of future female ASAF of the United States, the Netherlands, and Chile reasonably well. For countries or regions like Hong Kong whose female ASAF already passed the peak, our method also accurately estimates the rate of decline.

Table 2: Predictive validation results for all-age smoking attributable fraction (ASAF). The first and second columns indicate the estimation and validation periods respectively. The "Sex" and "n" columns indicate the sex and the number of countries used for the validation respectively. In the "Model" column, "Bayes" represents the BHM model with measurement error and random walk with drift and "Persistence" represents the persistence forecast. The "MAE" column contains the mean absolute prediction error defined by Eq. 7. The "Coverage" columns show the proportion of validation observations contained in the 80%, 90%, 95% prediction intervals respectively.

Training Period	Test Period	Sex	n	Model	MAE	Coverage		
						80%	90%	95%
1950–2010	2010–2015	Male	66	Persistence	0.010	-	-	-
				Bayes	0.007	0.78	0.86	0.90
		Female	66	Persistence	0.009	-	-	-
				Bayes	0.007	0.83	0.93	0.96
1950–2005	2005–2015	Male	66	Persistence	0.014	-	-	-
				Bayes	0.011	0.72	0.83	0.89
		Female	66	Persistence	0.012	-	-	-
				Bayes	0.010	0.80	0.90	0.92
1950–2000	2000–2015	Male	63	Persistence	0.017	-	-	-
				Bayes	0.016	0.65	0.76	0.84
		Female	63	Persistence	0.015	-	-	-
				Bayes	0.011	0.81	0.90	0.95

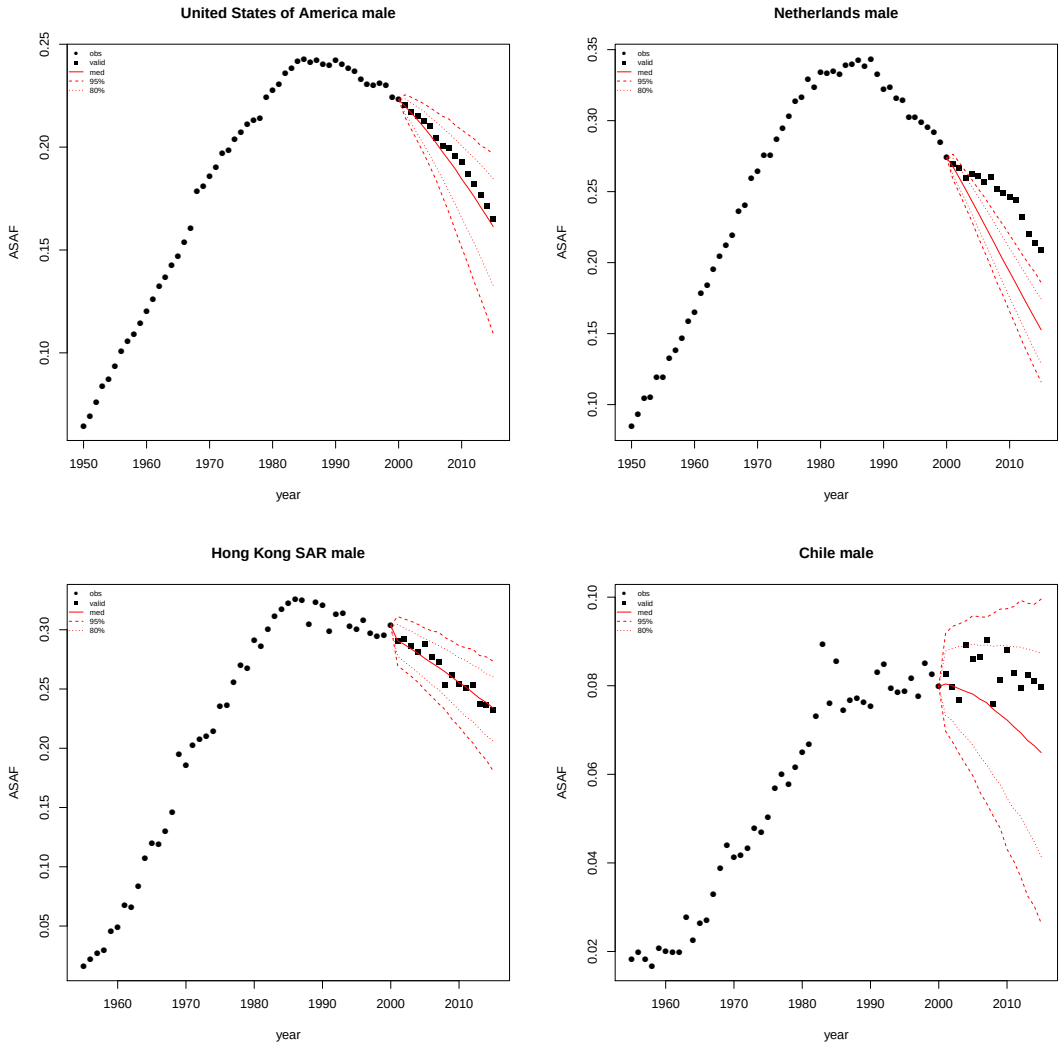

Figure 3: Validation of male all-age smoking attributable fraction for the United States, Netherlands, Hong Kong, and Chile. Past observed ASAF values are shown by black dots for 1950–2000 and by black squares for 2000–2015. The posterior median for 2000–2015 is shown by the red solid line, and the 80% and 95% prediction intervals are shown by the red dotted and dashed lines respectively.

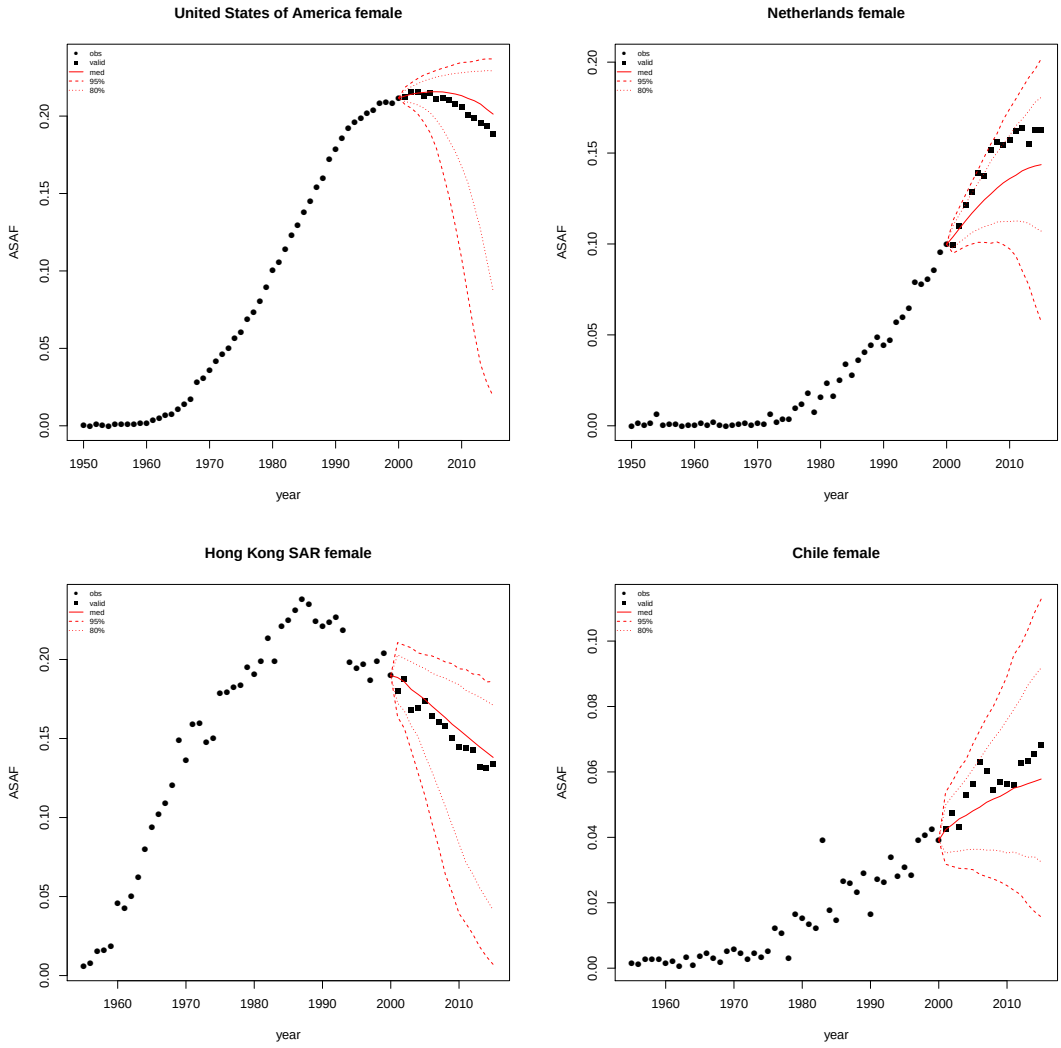

Figure 4: Validation of female all-age smoking attributable fraction for the United States, Netherlands, Hong Kong, and Chile. Past observed ASAF values are shown by black dots for 1950–2000 and by black squares for 2000–2015. The posterior median for 2000–2015 is shown by the red solid line, and the 80% and 95% prediction intervals are shown by the red dotted and dashed lines respectively.

4 Case Studies

We now give four cases studies which illustrate various aspects of the proposed method for estimating and forecasting ASAF.

4.1 United States

The annual ASAF for both male and female for the time period 1950–2015 is shown in Figure 1. The very clear pattern is due to the high quality of the data, reflecting the fact that the United States has one of the the best vital registration systems in the world.

The smoking epidemic in the male population in the United States started in the earlier 1900s, and there was a substantial decrease of smoking prevalence and lung cancer mortality rate after the 1950s. Smoking prevalence among US male adults was approximately 60% in 1950s, and went down to about 20% in the 1990s, and the general decline is still continuing (Burns et al., 1997; Islami et al., 2015). The observed ASAF levelled around the 1990s and declined afterwards. We forecast that by 2050, the median observed ASAF for US males will be around 4.3% (with 95% prediction interval [0.0%, 8.3%]). Because the measurement error for the U.S. is tiny, the projected true ASAF (green solid line for posterior mean and green dashed line for 95% predictive interval in Figure 5) for US males is almost equal to that of the observed ASAF.

The female smoking epidemic started two decades later than the male one and the maximum prevalence was around 30% in the 1960s, and then declined to about 20% in the 1990s (Burns et al., 1997). The pattern of smoking prevalence among US females is similar to that for males, but around 20 years behind (Burns et al., 1997; Islami et al., 2015). The female ASAF started to rise around the 1960s and reached its peak of 23% around 2005. We forecast that by 2050, the median observed ASAF for US females will be around 2.7% (with 95% prediction interval [0.0%, 9.3%]). Similarly, projected US female true ASAF follows closely with that of the observed ASAF. Figure 5 shows the historical records of observed male and female ASAF during the time period 1950–2015, along with projections up to 2050 with posterior median and prediction intervals.

4.2 The Netherlands

The Netherlands is a high-income western Europe country whose smoking epidemic started relatively early. Smoking prevalence reached 90% in the 1950s and dropped to 30% in the 2010s. The male observed ASAF in Netherlands passed its maximum ASAF around the 1990s and we project that it will go down to around 5.7% (with 95% prediction interval

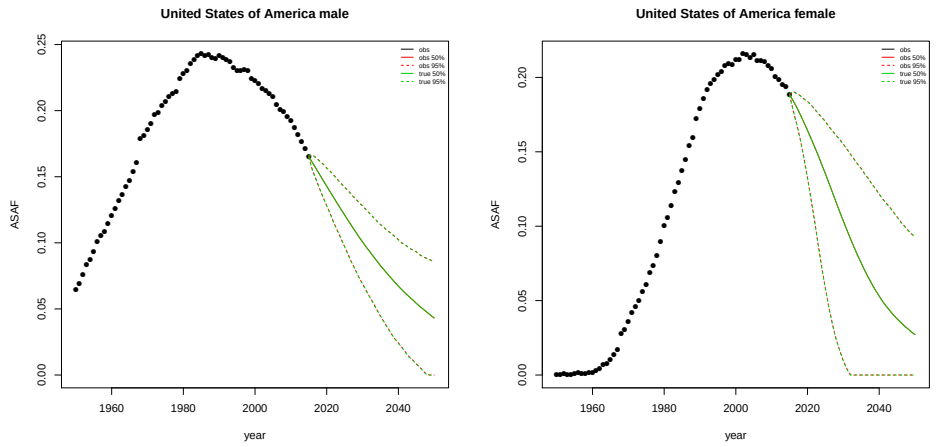

Figure 5: United States: The left and right panels show the projection of ASAF up to 2050 under the proposed model for male and female respectively. The red and green solid lines show the posterior median of projected observed ASAF and true ASAF respectively. The red and green dashed lines represent 95% prediction intervals for observed ASAF and true ASAF respectively.

[1.4%, 9.7%]) in 2050.

For females, smoking prevalence is also relatively high, and reached its peak of about 40% in the 1970s and dropped to 24% in the 2010s (Stoeldraijer et al., 2015). The female ASAF in Netherlands is among the few that is already experiencing the leveling stage. By our projection, the median year-to-peak for female ASAF will be around 2020, which is about 30 years after the male peak, and will reach 16.6% (with 95% prediction interval [12.4%, 18.5%]). By 2050, the median observed female ASAF will be 4.7% (with 95% prediction interval [0.0%, 19.3%]). Similarly to the case of US, the projected true ASAF follows that of the observed ASAF closely, due to the small measurement error. Figure 6 shows the historical records of observed male and female ASAF during time period 1950–2015, and projections are given up to 2050 with posterior median and prediction intervals for both observed and true ASAF.

4.3 Hong Kong

Hong Kong has an advanced smoking epidemic, but had a decrease in male smoking prevalence from about 40% in the 1980s to 22% in 2000. A decline has also been observed in female smoking prevalence, from 5.6% to 3.3% (Au et al., 2004). Like Japan, Singapore, and South Korea, both male and female ASAF have passed the leveling stage and have been declining for two decades. Unlike in most western developed countries, the time trend of

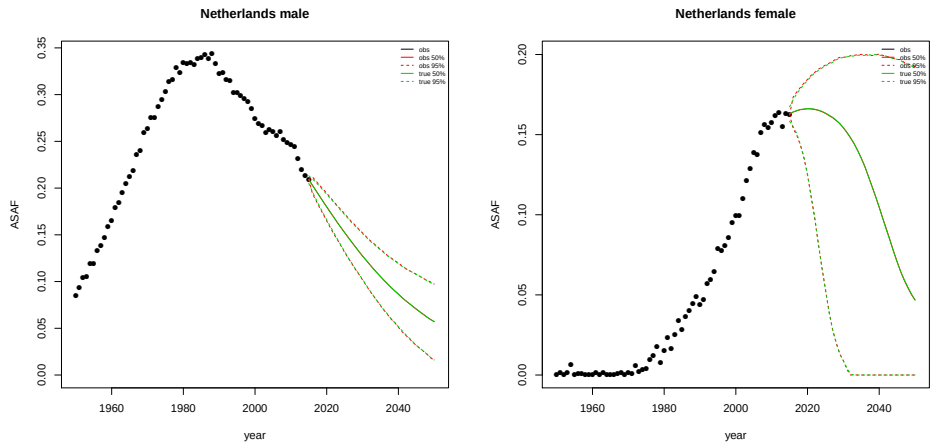

Figure 6: Netherlands: The left and right panels show the projection of ASAF up to 2050 under the proposed model for male and female respectively. The red and green solid lines show the posterior median of projected observed ASAF and true ASAF respectively. The red and green dashed lines represent 95% prediction intervals for observed ASAF and true ASAF respectively.

ASAF has been almost identical for males and females in Hong Kong, with similar times of onset and times-to-peak. Au et al. (2004) showed that the time trends of lung cancer incidence were similar for both genders.

By our projection, the observed ASAF will reach 9.7% for males (with 95% prediction interval [4.9%, 14.3%]) and 4.1% for females (with 95% prediction interval [0.0%, 8.1%]) by 2050. Compared with US and the Netherlands, the projected true ASAF of Hong Kong will have narrower predictor intervals than those of the observed ASAF due to larger measurement error exhibited in the historical data. However, the difference becomes less and less since the majority uncertainty of future ASAF will be account mainly by the variance from the random walk model of the true ASAF.

As discussed by Lam et al. (2001), Hong Kong may be a good indicator for the future development of the smoking epidemic and its impact on mortality in mainland China and other developing countries. Figure 7 shows the historical records of observed male and female ASAF during time period 1950–2015, along with projections up to 2050 with posterior median and prediction intervals.

4.4 Chile

Chile is one of the South America countries that have clear-pattern ASAF data for both males and females. It also has relatively high smoking prevalence. A decline in prevalence

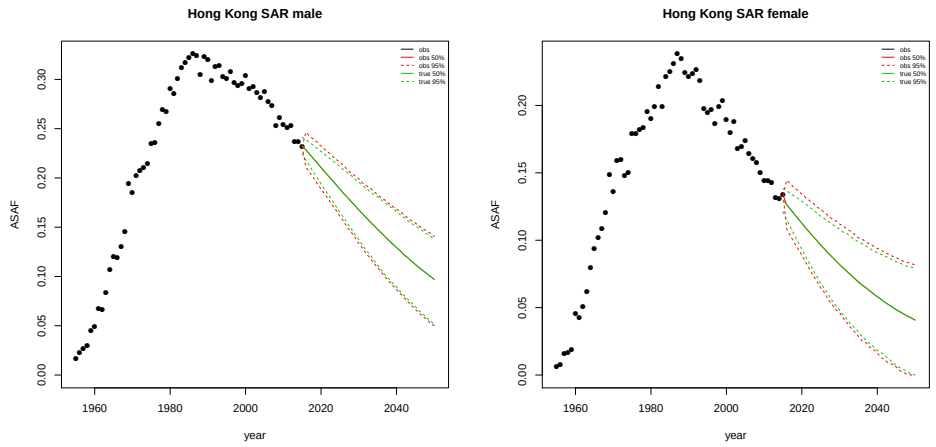

Figure 7: Hong Kong: The left and right panels show the projection of ASAF up to 2050 under the proposed model for male and female respectively. The red and green solid lines show the posterior median of projected observed ASAF and true ASAF respectively. The red and green dashed lines represent 95% prediction intervals for observed ASAF and true ASAF respectively.

among males and females has been observed in recent years but is modest compared to the decline in the United States (Islami et al., 2015). Also, female smoking prevalence is far behind that of males.

Our method projects that the male ASAF will decline gradually. By 2050, the projected median observed ASAF for the male population will be 4.3% (with 95% prediction interval [0.0%, 9.1%]). For females, we expect an increase for another 10 years with median observed ASAF reaching the maximum 7.6% (with 95% prediction interval [2.0%, 11.8%]) by 2030. By 2050, the median observed female ASAF be 5.36% (with 95% prediction interval [0.0%, 15.2%]); see Figure 8. Similarly to Hong Kong, Chile also has larger measurement error and the pattern is less clear, so that the projected true ASAF has wider predictive intervals compared with previous cases and the difference between true and observed projections also appears in the short term.

5 Discussion

5.1 Comparison between SAF Estimation Methods

In Section 1, we briefly described three categories of estimation methods for SAF. Prevalence-based methods depend heavily on smoking prevalence history. Since the lag between smoking prevalence and SAF is usually around two or three decades, in order to use smoking preva-

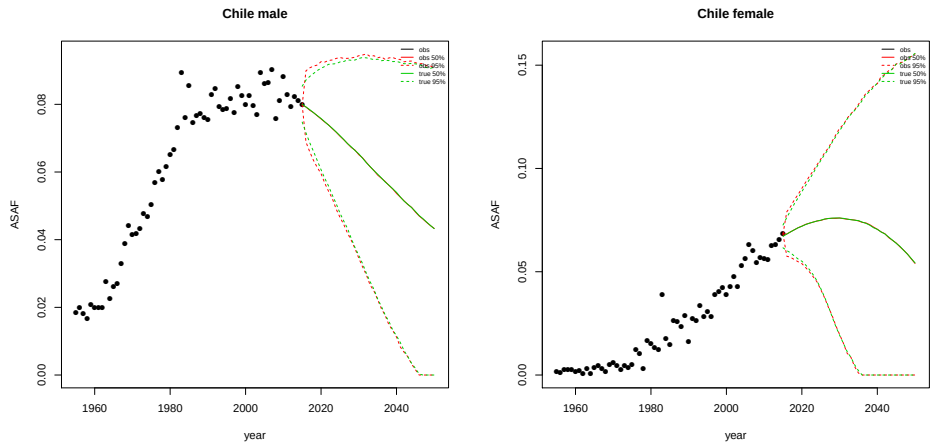

Figure 8: Chile: The left and right panels show the projection of ASAF up to 2050 under the proposed model for male and female respectively. The red and green solid lines show the posterior median of projected observed ASAF and true ASAF respectively. The red and green dashed lines represent 95% prediction intervals for observed ASAF and true ASAF respectively.

lence to estimate and predict SAF, especially for those countries whose onset of SAF is before 1950, one needs data at least back to the 1920s or 1930s. However, such smoking prevalence history is not available for most countries, and reconstruction of such data is challenging. Ng et al. (2014) provided estimates of smoking prevalence for many countries only from 1980 onwards.

Insufficient historical data is a major obstacle to using smoking prevalence for estimation and projection of SAF, and with currently available historical data, the predictive power using smoking prevalence data is not very high. In addition, smoking prevalence only reveals one aspect of the smoking epidemic, which cannot capture other aspects such as smoking intensity and duration and thus has been argued to be a poor indicator of the smoking exposure of the population (Shibuya et al., 2005; Luo et al., 2018). Prevalence-based estimation and projection have generally been applied only to specific countries on an individual basis, and examples include Taiwan (Wen et al., 2005) and the United States (Ma et al., 2018).

There are two main indirect methods used widely in the literature, which both use the lung cancer mortality rate as an indicator for the accumulated hazard of smoking. The first one is the Peto-Lopez method which we have used here. This has been widely used in the demographic literature, in part because its data requirements are relatively modest. It has been validated in many studies (Preston et al., 2009; Kong et al., 2016).

One drawback of the Peto-Lopez method is that it uses the CPS-II to estimate the relative risk. Since the CPS-II was conducted in 1982 with volunteer participants only from the

United States and most of them were middle-class, the CPS-II might not be fully representative and may potentially underestimate lung cancer mortality in nonsmokers (Tachfouti et al., 2014). Moreover, the Peto-Lopez method assumes that the relative risk is constant over time and homogeneous across nations. Mehta and Preston (2012), Teng et al. (2017), and Lariscy et al. (2018) have shown that the risks from smoking are changing over time. Also, in China and India, the lung cancer mortality rate among nonsmokers is higher than that of the developed countries such as that in CPS-II (Liu et al., 1998; Gajalakshmi et al., 2003). Another issue is that the original Peto-Lopez paper reduced the smoking excess risk of each cause-of-death except lung cancer by 50% to control for other confounders. As stated in their paper, this reduction is somewhat arbitrary. To avoid some of these issues, here we have used only data from clear-pattern countries, which avoids some countries for which the Peto-Lopez method may not give good estimates.

Some variants of the Peto-Lopez method have been proposed. For example, Ezzati and Lopez (2003) reduced the correction factor for excess risk from 50% to 30% for all countries and extended this method to less developed countries by estimating the non-smoker lung cancer mortality rate based on household use of coal in poorly-vented stoves. They also provided an analysis of uncertainty. Mackenbach et al. (2004) used a simplified version which only used the all-cause relative risk in the CPS-II study and avoided calculations for the nine disease categories separately. Janssen et al. (2013) used this version to calculate age-specific SAF to partition mortality into smoking and non-smoking attributable parts, and projected them separately.

Muszyńska et al. (2014) and Stoeldraijer et al. (2015) used the same method to calculate an age-standardized SAF, whose purposes are to compare the role of smoking in different regions of Poland, and to estimate and compare smoking attributable fraction of mortality among England & Wales, Denmark and the Netherlands, respectively. While age-standardization is used mainly to compare SAF among different populations, ASAF provides the all-cause SAF with all age-groups aggregated and is the main quantity reported in the iterature, e.g., Peto et al. (1992, 1994, 2006); Preston et al. (2009).

Based on these concerns about the Peto-Lopez method, Preston et al. (2009) and Preston et al. (2011) came up with the PGW method, which used a regression-based method to connect lung cancer mortality rate with other causes of death mortality rate instead of using the CPS-II. The PGW method avoids the relative risk problem faced by the Peto-Lopez method and provides estimates of uncentainty. However, its authors stated that the Peto-Lopez method might work better for countries where the cause-of-death structure is very different from that observed in developed countries, such as tropical African countries. They also pointed out that both methods would not work well for countries whose lung

cancer mortality rate is also influenced largely by some other factors such as air pollution. As discussed by Preston et al. (2009), the PGW method produces similar estimates to the Peto-Lopez method in general for both males and females.

5.2 Projection Methodology

To our knowledge, there are only two other methods available for projecting SAF based on the Peto-Lopez method. Janssen et al. (2013) proposed the first method to forecast age-specific SAF and to our knowledge it has so far been applied only to the Netherlands. For projecting male age-specific SAF, a constant decline rate (-1.5%) based on the current trend of all-age combined SAF is applied for each age group. For females, it first estimates the time-to-peak and value of peak of female SAF. It uses age-period-cohort (APC) analysis to find the cohort with the highest lung cancer mortality rate and then adds 68, which is the average age of dying from lung cancer, to that cohort to estimate the year which the all-age combined female SAF would reach the maximum. Then the difference between year-to-peak of male and female SAF with all ages combined is estimated and applied to get the time-to-peak and thus the age-specific female SAF. Finally, the rate of decline of female age-specific SAF is set to the same as that of the male.

The other method proposed for projecting SAF is to first estimate and project lung cancer mortality rate by considering the cohort effect, and use it to calculate the age-specific SAF. Stoeldraijer et al. (2015) used an APC model to estimate and forecast the lung cancer mortality rate of three countries: England & Wales, Denmark, and the Netherlands. For female data, they first estimated the time-to-peak for each age group by assuming that the time-to-peak of age-specific lung cancer mortality rate for females is when it reaches the corresponding rate for males. By assuming that the female lung cancer mortality will follow the same increasing-leveling-declining time trend as that for males for each age group, the authors argued that their method could provide long-term projections of lung cancer mortality rate, while previous work which only used historic trends in APC analysis could only provide short-term projections.

APC analysis is widely used, but it is also plagued by the unidentifiability issue resulting from the perfect linear relationship between the three effects. To resolve this requires extra constraints on the parameter space, many of which are not desirable (Luo, 2013; Smith and Wakefield, 2016). Also, projection of the future lung cancer mortality rate also requires the projection of age, period, and cohort effects, which introduces additional projection error, even more so for young cohorts for which historical data are not available.

Another way to resolve the unidentifiability issue in APC analysis is by introducing cohort explanatory variables (Smith and Wakefield, 2016). Cohort smoking history is one

such powerful tool for estimating and projecting mortality. Preston and Wang (2006) and Wang and Preston (2009) used the average year of smoking before 40 of a cohort as a covariate to explain the mortality differences between sexes and forecasted mortality of United States for both sexes up to 2035. Shibuya et al. (2005) and Luo et al. (2018) used APC anlaysis with selected smoking covariates such as cigarette tar exposure to estimate and project the lung cancer mortality rate. Cohort smoking history is a powerful tool, but it requires additional data (Burns et al., 1997) that are not available for many of the countries we considered.

5.3 China and India

According to Reitsma et al. (2017), China and India are the two countries that have seen the largest percentage increase in smoking prevalence. As a result, the ASAF for these two countries is important for understanding and projecting the world trend of the effect of smoking on mortality since the diffusion of the smoking epidemic from developed countries to developing countries has already started.

However, we have not included these two countries here for the following two reasons. Firstly, we do not have enough data to estimate the ASAF for China and India. Even though there are some records of lung cancer death count data in the WHO Mortality Database for China (World Health Organization, 2017), these are only regional data and so could be biased. India has a reasonably good vital registration system but it also has lung cancer mortality data only for selected regions and locations. Secondly, as pointed out by Preston et al. (2009), neither the Peto-Lopez original method nor the PGW method will provide reliable estimates of SAF for countries like China since smoking is not the only major factor that can cause lung cancer. The main assumptions of the Peto-Lopez and PGW methods are that lung cancer mortality is primarily caused by smoking and that the lung cancer mortailty rate is very low among nonsmokers. Therefore, as proposed by Ezzati and Lopez (2003) and others, some extra covariates such as household use of coal in poorly-vented stoves are used to adjust the estimates. Incorporating China and India in the joint model could be feasible in the future if better ASAF estimation methods and related data are available.

References

Alkema, L., Raftery, A. E., Gerland, P., Clark, S. J., Pelletier, F., Buettner, T., and Heilig, G. K. (2011). Probabilistic projections of the total fertility rate for all countries. *Demography*, 48(3):815–839.

Au, J. S., Mang, O. W., Foo, W., and Law, S. C. (2004). Time trends of lung cancer

incidence by histologic types and smoking prevalence in Hong Kong 1983–2000. *Lung Cancer*, 45(2):143–152.

Bongaarts, J. (2006). How long will we live? *Population and Development Review*, 32(4):605–628.

Bongaarts, J. (2014). Trends in causes of death in low-mortality countries: implications for mortality projections. *Population and Development Review*, 40(2):189–212.

Britton, J. (2017). Death, disease, and tobacco. *The Lancet*, 389(10082):1861–1862.

Burns, D. M., Lee, L., Shen, L. Z., Gilpin, E., Tolley, H. D., Vaughn, J., Shanks, T. G., et al. (1997). Cigarette smoking behavior in the United States. *Changes in cigarette-related disease risks and their implication for prevention and control. Smoking and Tobacco Control Monograph*, 8:13–42.

Carpenter, B., Gelman, A., Hoffman, M. D., Lee, D., Goodrich, B., Betancourt, M., Brubaker, M., Guo, J., Li, P., and Riddell, A. (2017). Stan: A probabilistic programming language. *Journal of Statistical Software*, 76(1).

Ezzati, M. and Lopez, A. D. (2003). Estimates of global mortality attributable to smoking in 2000. *The Lancet*, 362(9387):847–852.

Ezzati, M. and Lopez, A. D. (2004). Regional, disease specific patterns of smoking-attributable mortality in 2000. *Tobacco Control*, 13(4):388–395.

Gajalakshmi, V., Peto, R., Kanaka, T. S., and Jha, P. (2003). Smoking and mortality from tuberculosis and other diseases in India: retrospective study of 43000 adult male deaths and 35000 controls. *The Lancet*, 362(9383):507–515.

Gelman, A. and Rubin, D. B. (1992). Inference from iterative simulation using multiple sequences. *Statistical science*, 7(4):457–472.

Hoffman, M. D. and Gelman, A. (2014). The No-U-turn sampler: adaptively setting path lengths in Hamiltonian Monte Carlo. *Journal of Machine Learning Research*, 15(1):1593–1623.

Islami, F., Torre, L. A., and Jemal, A. (2015). Global trends of lung cancer mortality and smoking prevalence. *Translational Lung Cancer Research*, 4(4):327.

Janssen, F., van Wissen, L. J., and Kunst, A. E. (2013). Including the smoking epidemic in internationally coherent mortality projections. *Demography*, 50(4):1341–1362.

Kong, K. A., Jung-Choi, K.-H., Lim, D., Lee, H. A., Lee, W. K., Baik, S. J., Park, S. H., and Park, H. (2016). Comparison of prevalence-and smoking impact ratio-based methods of estimating smoking-attributable fractions of deaths. *Journal of Epidemiology*, 26(3):145–154.

Lam, T., Ho, S., Hedley, A., Mak, K., and Peto, R. (2001). Mortality and smoking in Hong Kong: case-control study of all adult deaths in 1998. *BMJ*, 323(7309):361.

Lariscy, J. T., Hummer, R. A., and Rogers, R. G. (2018). Cigarette smoking and all-cause and cause-specific adult mortality in the United States. *Demography*, 55(5):1855–1885.

Levin, M. L. (1953). The occurrence of lung cancer in man. *Acta Unio Int Contra Cancrum*, 9:531–941.

Liu, B.-Q., Peto, R., Chen, Z.-M., Boreham, J., Wu, Y.-P., Li, J.-Y., Campbell, T. C., and Chen, J.-S. (1998). Emerging tobacco hazards in China: 1. retrospective proportional mortality study of one million deaths. *BMJ*, 317(7170):1411–1422.

Luo, L. (2013). Assessing validity and application scope of the intrinsic estimator approach to the age-period-cohort problem (with discussion). *Demography*, 50:1945–1988.

Luo, Q., Yu, X. Q., Wade, S., Caruana, M., Pesola, F., Canfell, K., and O'Connell, D. L. (2018). Lung cancer mortality in Australia: Projected outcomes to 2040. *Lung Cancer*, 125:68–76.

Ma, J., Siegel, R. L., Jacobs, E. J., and Jemal, A. (2018). Smoking-attributable mortality by state in 2014, US. *American Journal of Preventive Medicine*, 54(5):661–670.

Mackenbach, J. P., Huisman, M., Andersen, O., Bopp, M., Borgan, J.-K., Borrell, C., Costa, G., Deboosere, P., Donkin, A., Gadeyne, S., et al. (2004). Inequalities in lung cancer mortality by the educational level in 10 european populations. *European Journal of Cancer*, 40(1):126–135.

Mehta, N. and Preston, S. H. (2012). Continued increases in the relative risk of death from smoking. *American Journal of Public Health*, 102(11):2181–2186.

Mons, U. and Brenner, H. (2017). Demographic ageing and the evolution of smoking-attributable mortality: the example of Germany. *Tobacco Control*, 26(4):455–457.

Muszyńska, M. M., Fihel, A., and Janssen, F. (2014). Role of smoking in regional variation in mortality in p oland. *Addiction*, 109(11):1931–1941.

Neal, R. M. (2011). MCMC using Hamiltonian dynamics. *Handbook of Markov Chain Monte Carlo*, 2(11):2.

Ng, M., Freeman, M. K., Fleming, T. D., Robinson, M., Dwyer-Lindgren, L., Thomson, B., Wollum, A., Sanman, E., Wulf, S., Lopez, A. D., et al. (2014). Smoking prevalence and cigarette consumption in 187 countries, 1980-2012. *Journal of the American Medical*, 311(2):183–192. Dataset last assess: Oct. 15, 2018 `http://www.healthdata.org/data-tools`.

Niu, S.-R., Yang, G.-H., Chen, Z.-M., Wang, J.-L., Wang, G.-H., He, X.-Z., Schoepff, H., Boreham, J., Pan, H.-C., and Peto, R. (1998). Emerging tobacco hazards in China: 2. early mortality results from a prospective study. *BMJ*, 317(7170):1423–1424.

Pampel, F. (2005). Forecasting sex differences in mortality in high income nations: The contribution of smoking. *Demographic Research*, 13(18):455.

Pampel, F. C. (2006). Global patterns and determinants of sex differences in smoking. *International Journal of Comparative Sociology*, 47(6):466–487.

Pérez-Ríos, M. and Montes, A. (2008). Methodologies used to estimate tobacco-attributable mortality: a review. *BMC public health*, 8(1):22.

Peters, F., Mackenbach, J., and Nusselder, W. (2016). Do life expectancy projections need to account for the impact of smoking. *Netspar Design Papers*, 2016(52):1–54.

Peto, R., Boreham, J., Lopez, A. D., Thun, M., and Heath, C. (1992). Mortality from tobacco in developed countries: indirect estimation from national vital statistics. *The Lancet*, 339(8804):1268–1278.

Peto, R., Lopez, A. D., Boreham, J., and Thun, M. (2006). Mortality from smoking in developed countries. *Population*, 673290(284395):300245.

Peto, R., Lopez, A. D., Boreham, J., Thun, M., and Heath, C. (1994). Mortality from smoking in developed countries 1950-2000. Indirect estimates from national statistics.

Preston, S. H., Glei, D. A., and Wilmoth, J. R. (2009). A new method for estimating smoking-attributable mortality in high-income countries. *International Journal of Epidemiology*, 39(2):430–438.

Preston, S. H., Glei, D. A., and Wilmoth, J. R. (2011). Contribution of smoking to international differences in life expectancy. In Crimmins, E. M., Preston, S. H., and Cohen, B.,

editors, *International Differences in Mortality at Older Ages: Dimensions and Sources*, pages 105–31. The National Academies Press, Washington, DC.

Preston, S. H., Stokes, A., Mehta, N. K., and Cao, B. (2014). Projecting the effect of changes in smoking and obesity on future life expectancy in the United States. *Demography*, 51(1):27–49.

Preston, S. H. and Wang, H. (2006). Sex mortality differences in the United States: The role of cohort smoking patterns. *Demography*, 43(4):631–646.

Raftery, A. E., Chunn, J. L., Gerland, P., and Ševčíková, H. (2013). Bayesian probabilistic projections of life expectancy for all countries. *Demography*, 50(3):777–801.

Raftery, A. E. and Lewis, S. M. (1992). One long run with diagnostics: Implementation strategies for Markov chain Monte Carlo. *Statistical Science*, 7(4):493–497.

Reitsma, M. B., Fullman, N., Ng, M., Salama, J. S., Abajobir, A., Abate, K. H., Abbafati, C., Abera, S. F., Abraham, B., Abyu, G. Y., et al. (2017). Smoking prevalence and attributable disease burden in 195 countries and territories, 1990–2015: a systematic analysis from the global burden of disease study 2015. *The Lancet*, 389(10082):1885–1906.

Rogers, R. G., Hummer, R. A., Krueger, P. M., and Pampel, F. C. (2005). Mortality attributable to cigarette smoking in the United States. *Population and Development Review*, 31(2):259–292.

Rosen, L. (2013). An intuitive approach to understanding the attributable fraction of disease due to a risk factor: the case of smoking. *International Journal of Environmental Research and Public Health*, 10(7):2932–2943.

Shibuya, K., Inoue, M., and Lopez, A. D. (2005). Statistical modeling and projections of lung cancer mortality in 4 industrialized countries. *International Journal of Cancer*, 117(3):476–485.

Smith, T. R. and Wakefield, J. (2016). A review and comparison of age–period–cohort models for cancer incidence. *Statistical Science*, 31(4):591–610.

Stoeldraijer, L., Bonneux, L., van Duin, C., van Wissen, L., and Janssen, F. (2015). The future of smoking-attributable mortality: the case of England & Wales, Denmark and the Netherlands. *Addiction*, 110(2):336–345.

Stoeldraijer, L., van Duin, C., van Wissen, L., and Janssen, F. (2013). Impact of different mortality forecasting methods and explicit assumptions on projected future life expectancy: The case of the Netherlands. *Demographic Research*, 29:323–354.

Tachfouti, N., Raherison, C., Obtel, M., and Nejjari, C. (2014). Mortality attributable to tobacco: review of different methods. *Archives of Public Health*, 72(1):22.

Teng, A., Atkinson, J., Disney, G., Wilson, N., and Blakely, T. (2017). Changing smoking-mortality association over time and across social groups: National census-mortality cohort studies from 1981 to 2011. *Scientific Reports*, 7(1):11465.

United Nations (2017). *World Population Prospects*. United Nations, New York, N.Y. Accessed: Oct. 15, 2018 `http://population.un.org/wpp/Download/Standard/Population/`.

Wang, H. and Preston, S. H. (2009). Forecasting United States mortality using cohort smoking histories. *Proceedings of the National Academy of Sciences*, 106(2):393–398.

Wen, C., Tsai, S., Chen, C., Cheng, T., Tsai, M., and Levy, D. (2005). Smoking attributable mortality for Taiwan and its projection to 2020 under different smoking scenarios. *Tobacco Control*, 14(suppl 1):i76–i80.

World Health Organization (2017). Mortality database. Last accessed: Oct. 15, 2018 `http://www.who.int/healthinfo/statistics/mortality_rawdata/en/`.

Appendices

A Full Bayesian Hierarchical Model

The details of the four-layer Bayesian Hierarchical model described in Section 2.4 are as follows. Here $\mathcal{N}_l^u(a,b)$ represents a normal distribution with mean a and variance b truncated at interval $[l,u]$ ($l(u)$ is omitted if it takes value $-\infty$ (∞)). Gamma(a,b) represents a Gamma distribution with shape a and rate b. Lognormal(a,b) represents a log-normal distribution with parameters a,b. InvGamma(a,b) represents a inverse-Gamma distribution with shape a and scale b.

Level 1: $y_{c,s,t}|h_{c,s,t} \sim \mathcal{N}(h_{c,s,t}, \sigma_c^2)$;

Level 2: $h_{c,s,t_0} = g(t_0|\theta_{c,s}) + \varepsilon^h_{c,s,t_0}$,

$h_{c,s,t} = h_{c,s,t-1} + g(t|\theta_{c,s}) - g(t-1|\theta_{c,s}) + \varepsilon^h_{c,s,t}$ for $t > t_0$,

$\varepsilon^h_{c,s,t} \sim_{ind} \mathcal{N}(0, \sigma_h^2)$;

Level 3:

$a_1^{c,m} \sim \text{Gamma}(2, 2/a_1^m)$, $a_1^{c,f} \sim \text{Gamma}(2, 2/a_1^f)$,

$a_2^{c,m} \sim \mathcal{N}^{65}(a_2^m, \sigma^2_{a_2^m})$, $a_2^{c,f} = a_2^{c,m} + \triangle^c_{a_2}$,

$a_3^{c,m} \sim \text{Gamma}(2, 2/a_3^m)$, $\triangle^c_{a_2} \sim \mathcal{N}(\triangle_{a_2}, \sigma^2_{\triangle_{a_2}})$,

$a_4^{c,m} \sim \mathcal{N}_0^{100}(a_4, \sigma^2_{a_4})$, $a_3^{c,f} \sim \text{Gamma}(2, 2/a_3^f)$,

$k^{c,m} \sim \mathcal{N}_0(k^m, \sigma^2_{k^m})$, $a_4^{c,f} \sim \mathcal{N}_0^{100}(a_4, \sigma^2_{a_4})$,

$\sigma_c^2 \sim \text{Lognormal}(\nu, \rho^2)$, $k^{c,f} \sim \mathcal{N}_0(k^f, \sigma^2_{k^f})$;

Level 4:

$a_1^m \sim \text{Gamma}(1.477, 9.423)$, $a_1^f \sim \text{Gamma}(2.093, 16.302)$,

$a_2^m \sim \mathcal{N}(24.362, 12.488)$, $\triangle_{a_2} \sim \mathcal{N}(12.080, 11.140)$,

$a_3^m \sim \mathcal{N}(1.031, 7.378)$, $a_3^f \sim \text{Gamma}(1.031, 7.378)$,

$a_4 \sim \mathcal{N}(38.362, 19.058)$, $k^f \sim \text{N}(0.362, 0.255)$,

$k^m \sim \mathcal{N}(0.362, 0.255)$, $\sigma^2_{\triangle_{a_2}} \sim \text{InvGamma}(2, 11^2)$,

$\sigma^2_{a_2^m} \sim \text{InvGamma}(2, 12.488^2)$, $\sigma^2_{k^f} \sim \text{InvGamma}(2, 0.255^2)$,

$\sigma^2_{a_4} \sim \text{InvGamma}(2, 19.058^2)$, $\nu \sim \mathcal{N}(-10.414, 1.186)$,

$\sigma^2_{k^m} \sim \text{InvGamma}(2, 0.255^2)$, $\rho^2 \sim \text{InvGamma}(2, 1.186^2)$,

$\sigma_h^2 \sim \text{InvGamma}(2, 0.01^2)$.

B MCMC Convergence Diagnostics

B.1 Hyperparameter Diagnostics

In this section, we present the MCMC convergence diagnostics for the hyperparameters in Level 4 of the model in terms of trace plots, Raftery diagnostic statistics (Raftery and Lewis, 1992), and Gelman diagnostic statistics (Gelman and Rubin, 1992). Table 3 provides the Gelman and Raftery diagnostic statistics for all hyperparameters. We used 3 chains with 2000 burn in iterations and 8000 samples without thinning for the Gelman diagnostics, and randomly chose one of the chain to perform the Raftery diagnostics. Figure 9 shows the trace plots of all 8000 samples of hyperparameters.

Table 3: Convergence diagnostics for hyperparameters. PSRF and 95% UCI are the point estimator and upper bound of the 95% CI of the Gelman potential scale reduction factor. Burn1, Size1, and DF1 are the length of burn in, required sample size, and dependence factor from the Raftery diagnostics with parameters $q = 0.025, r = 0.0125, s = 0.95$. Burn2, Size2, and DF2 are the length of burn in, required sample size, and dependence factor of Raftery diagnostics with parameters $q = 0.975, r = 0.0125, s = 0.95$.

Parameters	Gelman Diag		Raftery Diag					
	PSRF	95% UCI	Burn1	Size1	DF1	Burn2	Size2	DF2
a_1^m	1	1.00	6	1318	2.20	6	1164	1.94
a_2^m	1	1.00	3	710	1.18	6	1504	2.51
a_3^m	1	1.00	6	1584	2.64	6	1424	2.37
a_4	1	1.01	8	1750	2.92	9	2028	3.38
k^m	1	1.01	10	1952	3.25	6	1236	2.06
$\sigma^2_{a_2^m}$	1	1.00	2	640	1.07	6	1730	2.88
$\sigma^2_{a_4}$	1	1.00	21	4410	7.35	12	2132	3.55
$\sigma^2_{k^m}$	1	1.00	6	1334	2.22	8	1448	2.41
a_1^f	1	1.00	2	640	1.07	6	1318	2.20
$\triangle_{a_2}$	1	1.00	4	756	1.26	6	688	1.15
a_3^f	1	1.00	8	1504	2.51	12	1852	3.09
k^f	1	1.00	5	895	1.49	2	640	1.07
$\sigma^2_{\triangle_{a_2}}$	1	1.00	3	696	1.16	4	839	1.40
$\sigma^2_{k^f}$	1	1.00	2	640	1.07	6	1376	2.29
ν	1	1.00	8	1518	2.53	8	1934	3.22
ρ^2	1	1.00	6	1270	2.21	6	1392	2.32
σ_h^2	1	1.00	10	1872	3.12	12	2337	3.90

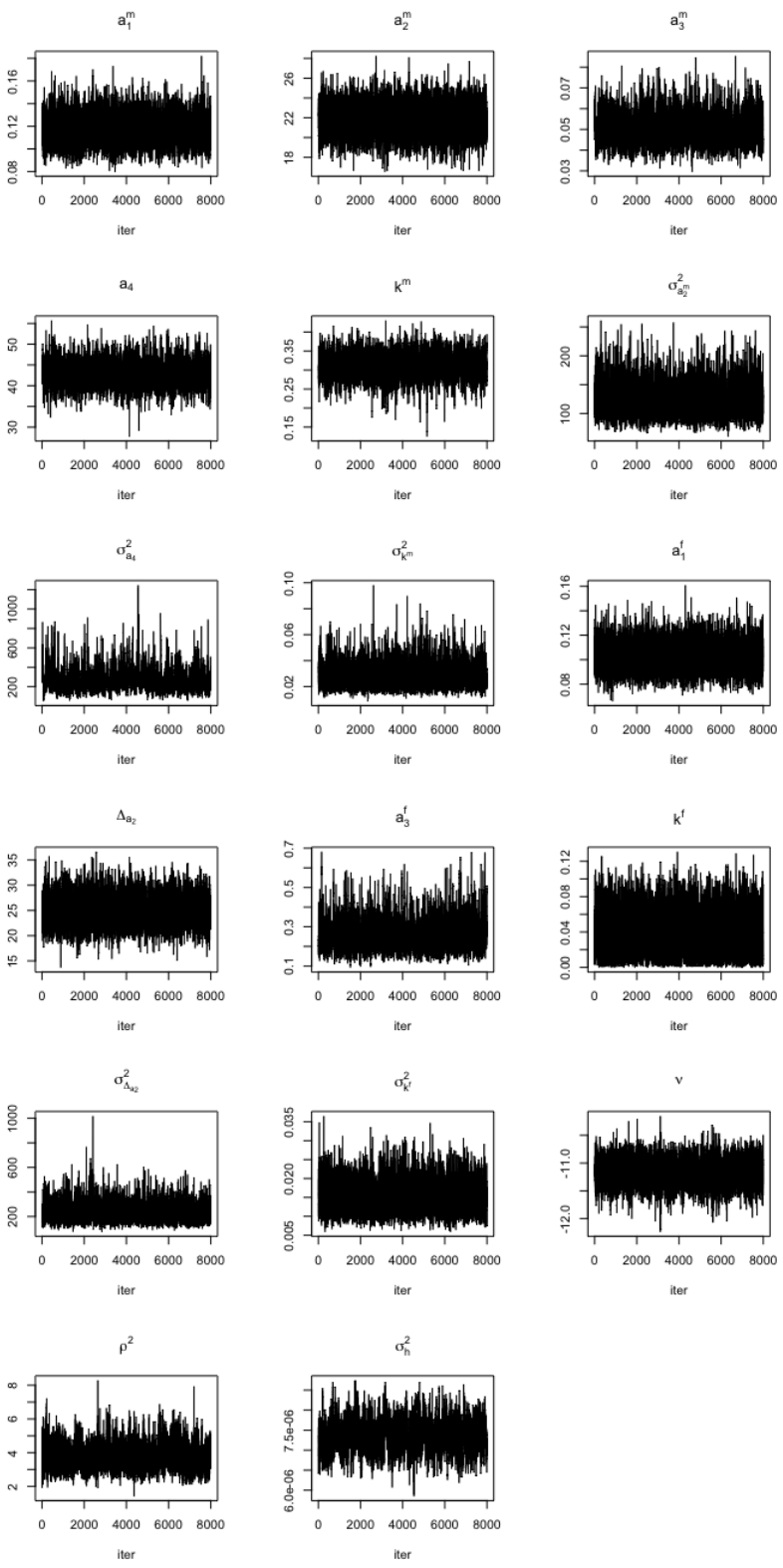

Figure 9: Trace plots for the hyperparameters.

B.2 Country-specfic Parameter Diagnostics

Here we present the MCMC convergence diagnostics for country-specific parameters in terms of trace plots and Gelman and Raftery convergence diagnostics. Table 4 provides the Gelman and Raftery diagnostic statistics for country-specific parameters of the United States for males and females. The chains are the same as in the previous section. Figure 10 shows the trace plots for all 8000 samples of country-specific paremeters for males and females in the United States.

Table 4: Convergence diagnostics for country-specific parameters for the United States. PSRF and 95% UCI are the point estimator and upper bound of the 95% CI of the Gelman potential scale reduction factor. Burn1, Size1, and DF1 are the length of burn in, required sample size, and dependence factor from the Raftery diagnostics with parameters $q = 0.025, r = 0.0125, s = 0.95$. Burn2, Size2, and DF2 are the length of burn in, required sample size, and dependence factor from the Raftery diagnostics with parameters $q = 0.975, r = 0.0125, s = 0.95$.

Parameters	Gelman Diag		Raftery Diag					
	PSRF	95% UCI	Burn1	Size1	DF1	Burn2	Size2	DF2
a_1^m	1	1.00	4	830	1.38	2	640	1.07
a_2^m	1	1.00	6	1326	2.21	4	756	1.26
a_3^m	1	1.00	4	822	1.37	2	633	1.06
a_4^m	1	1.00	2	614	1.02	4	772	1.29
k^m	1	1.00	6	1106	1.10	2	621	1.03
a_1^f	1	1.00	3	661	1.10	2	614	1.02
a_2^f	1	1.00	2	627	1.04	2	614	1.02
a_3^f	1	1.00	2	627	1.04	6	1314	2.19
a_4^f	1	1.00	3	661	1.10	4	848	1.41
k^f	1	1.00	3	668	1.11	6	1444	2.41
σ_c^2	1.01	1.03	96	15198	25.30	24	3834	6.39

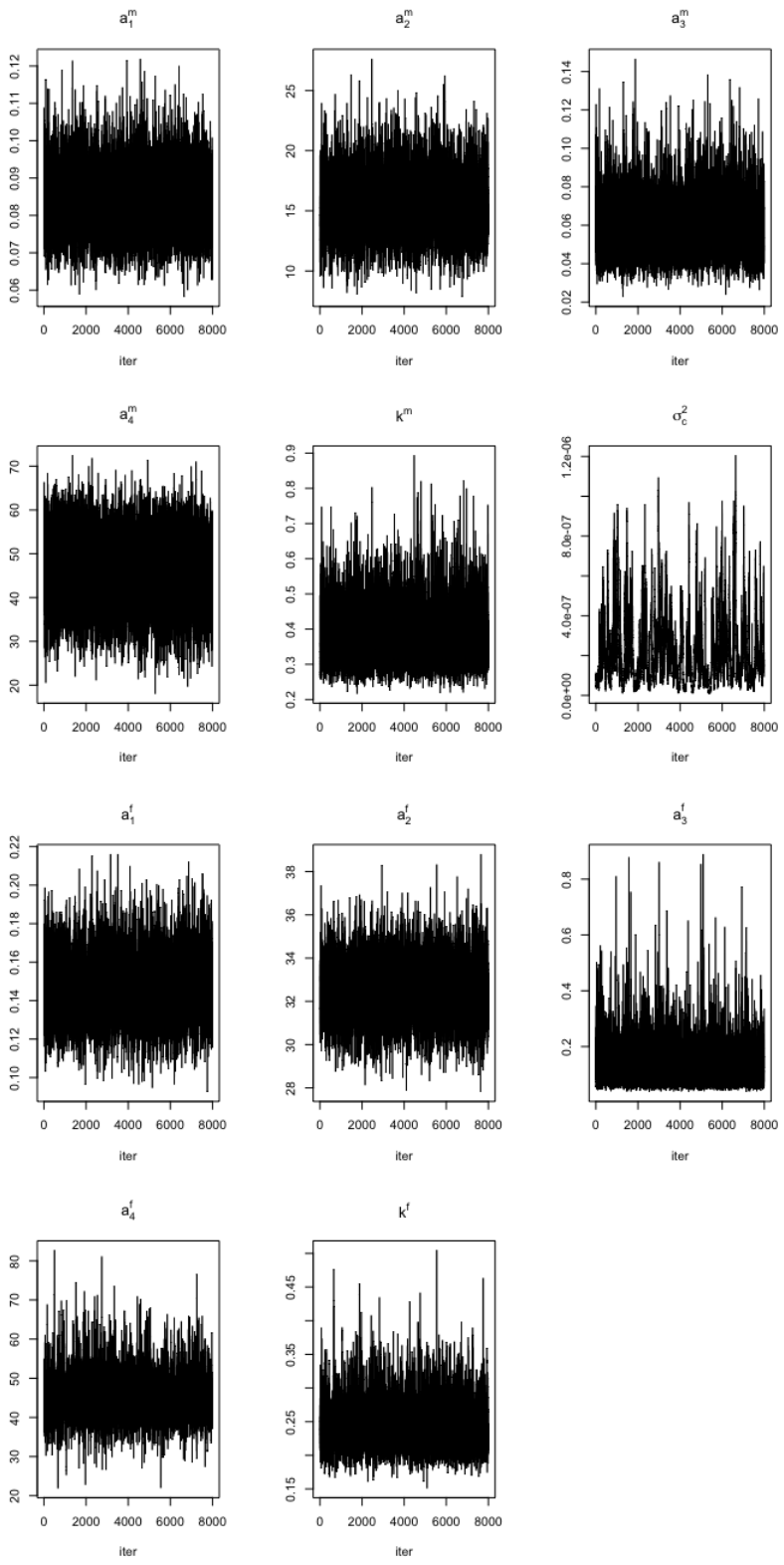

Figure 10: Trace plots for the country-specific parameters of the United States.

C All-age Smoking Attribuable Fraction Projection for 69 countries

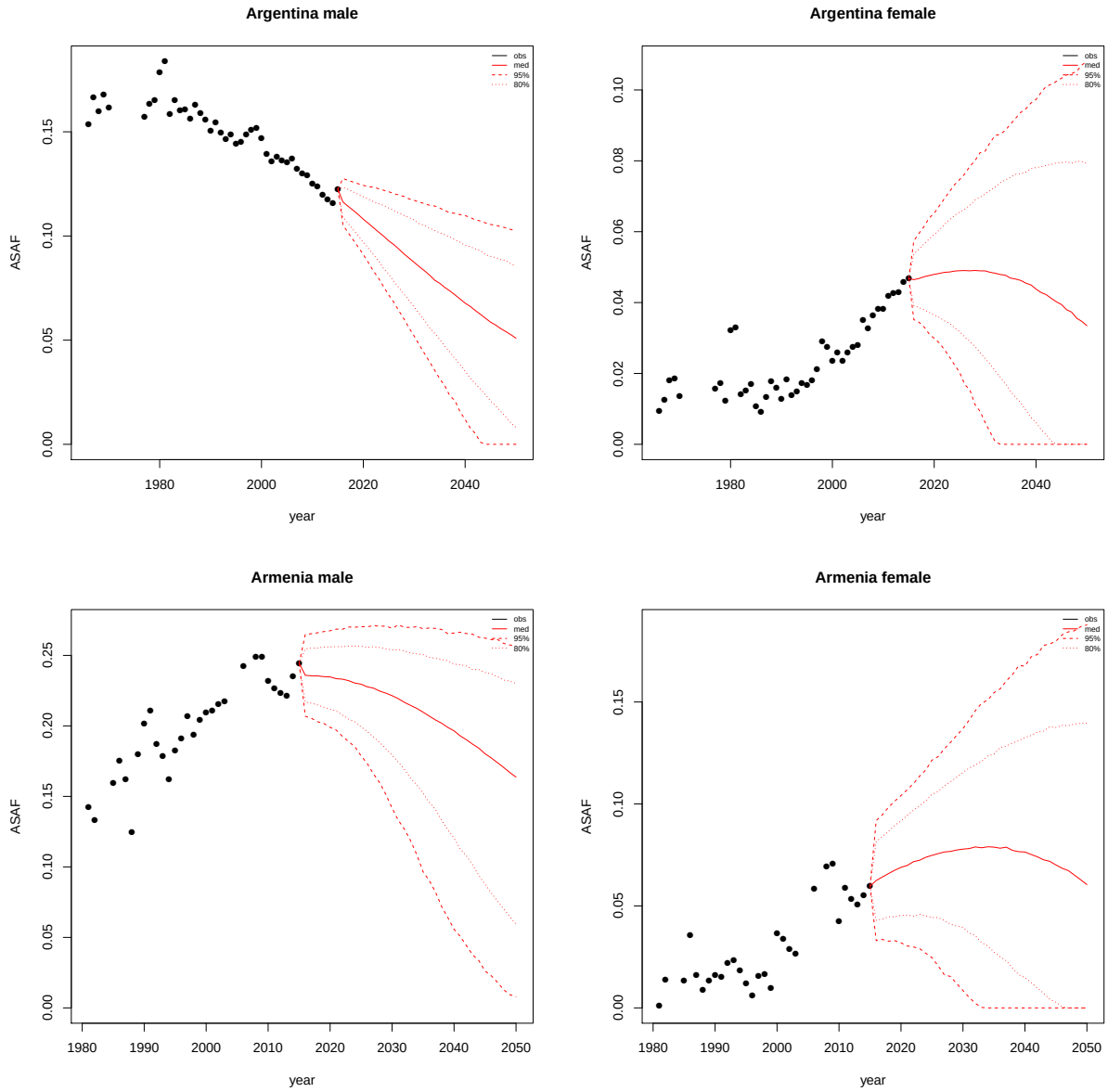

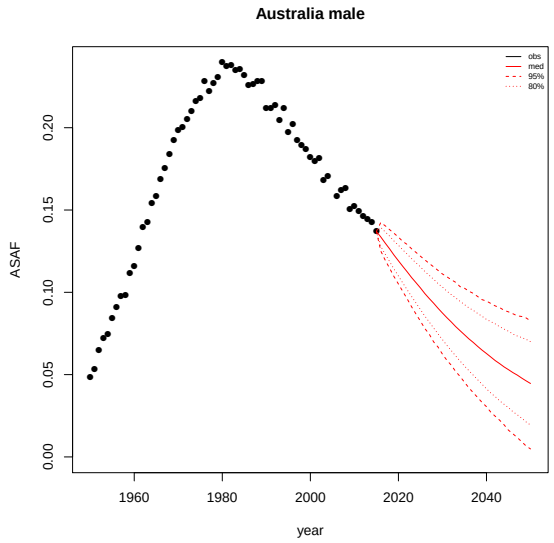
Australia male
obs
med
95%
80%
ASAF
0.00
0.05
0.10
0.15
0.20
1960
1980
2000
2020
2040
year

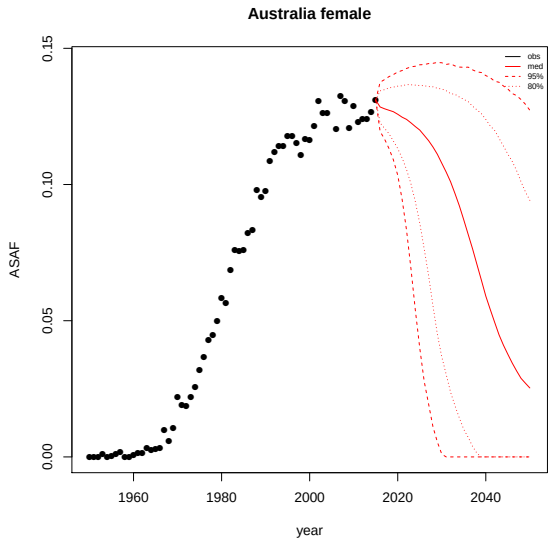
Australia female
obs
med
95%
80%
ASAF
0.00
0.05
0.10
0.15
1960
1980
2000
2020
2040
year

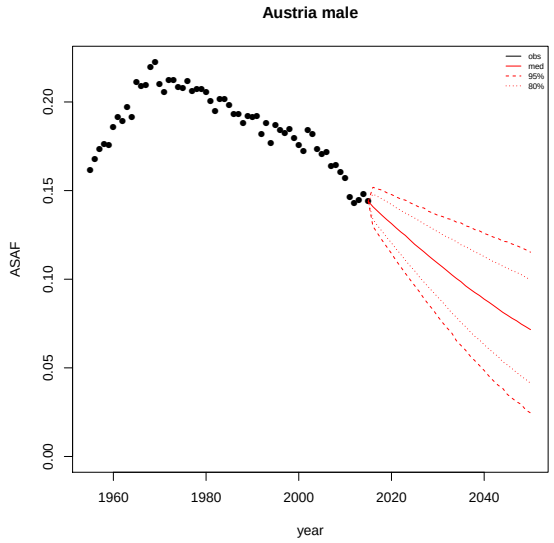
Austria male
obs
med
95%
80%
ASAF
0.00
0.05
0.10
0.15
0.20
1960
1980
2000
2020
2040
year

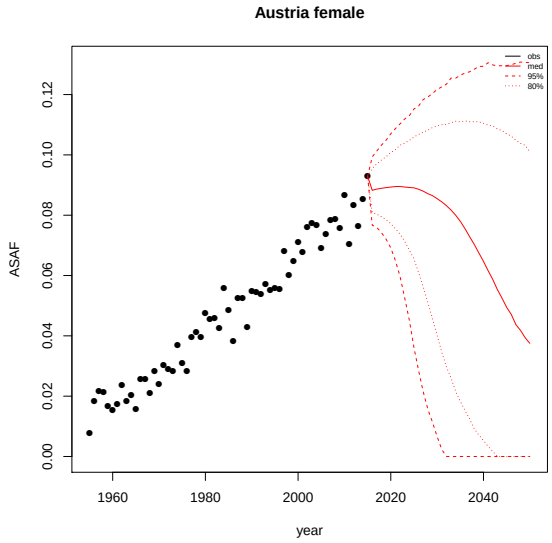
Austria female
obs
med
95%
80%
ASAF
0.00
0.02
0.04
0.06
0.08
0.10
0.12
1960
1980
2000
2020
2040
year

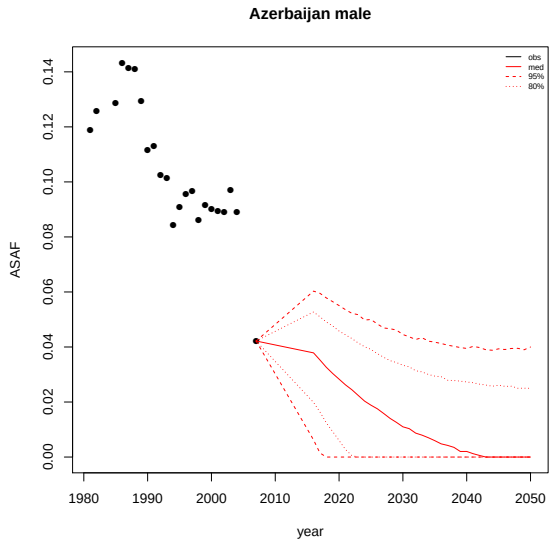
Azerbaijan male
obs
med
95%
80%
ASAF
0.00
0.02
0.04
0.06
0.08
0.10
0.12
0.14
1980
1990
2000
2010
2020
2030
2040
2050
year

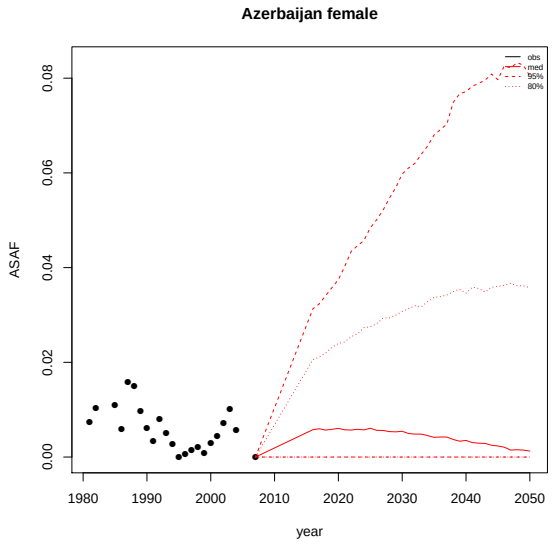
Azerbaijan female
obs
med
95%
80%
ASAF
0.00
0.02
0.04
0.06
0.08
1980
1990
2000
2010
2020
2030
2040
2050
year

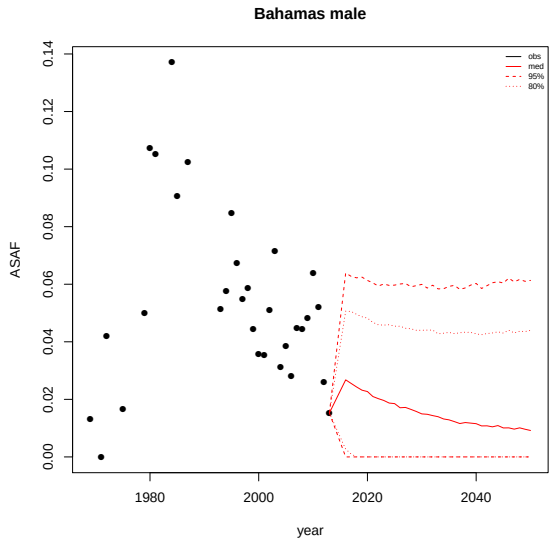
Bahamas male
ASAF
year
obs
med
95%
80%

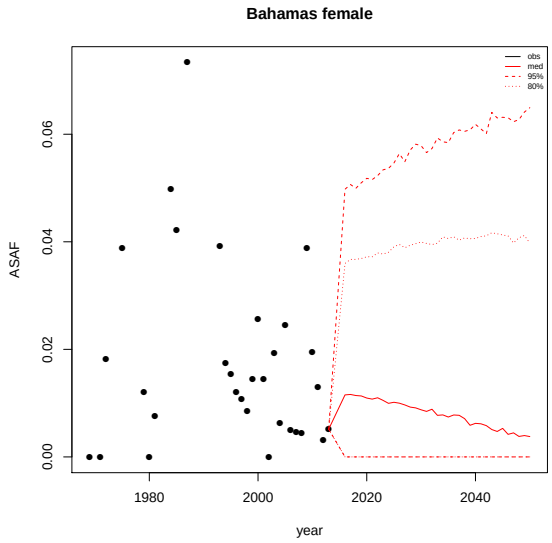
Bahamas female
ASAF
year
obs
med
95%
80%

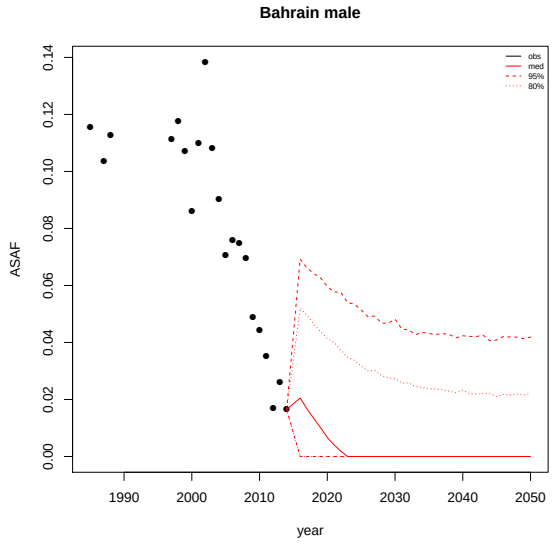
Bahrain male
ASAF
year
obs
med
95%
80%

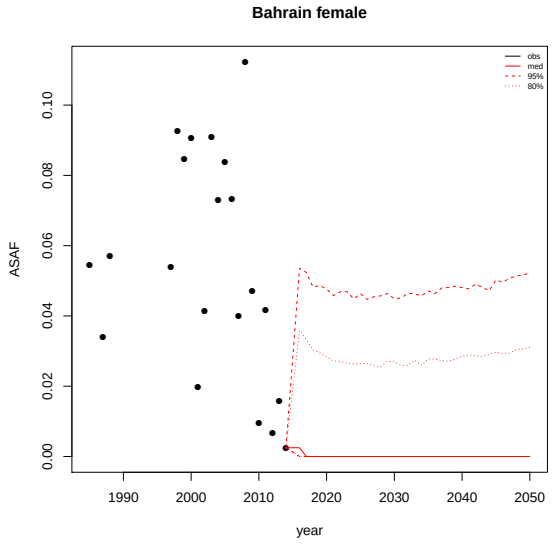
Bahrain female
ASAF
year
obs
med
95%
80%

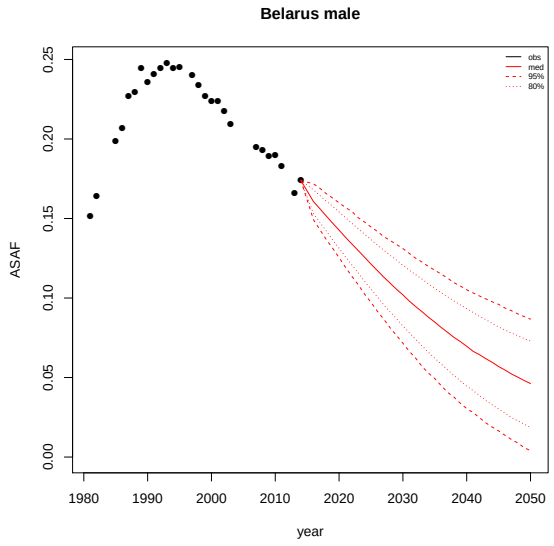
Belarus male
ASAF
year
obs
med
95%
80%

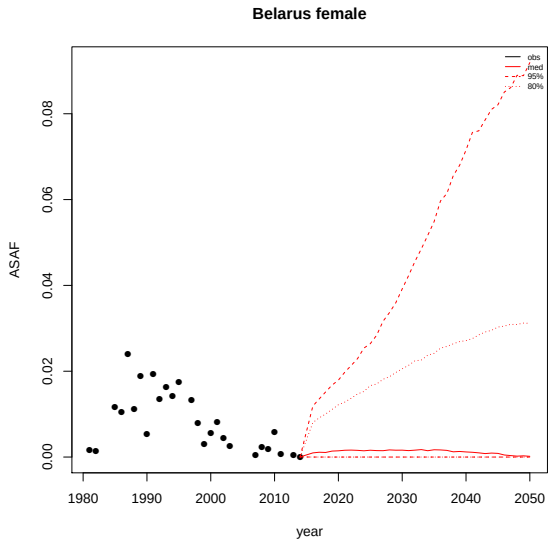
Belarus female
ASAF
year
obs
med
95%
80%

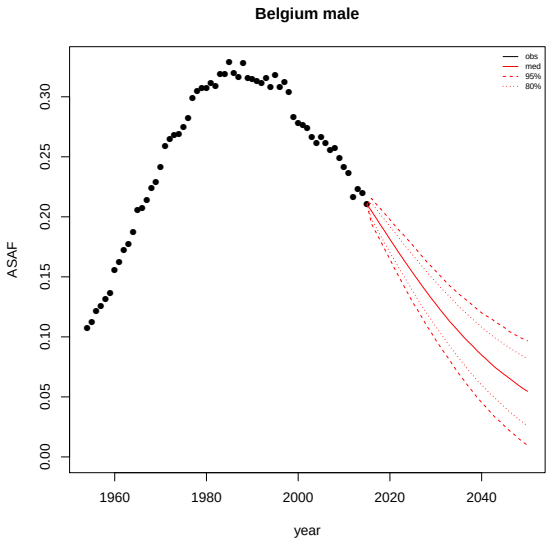
Belgium male
obs
med
95%
80%
ASAF
0.00
0.05
0.10
0.15
0.20
0.25
0.30
1960
1980
2000
2020
2040
year

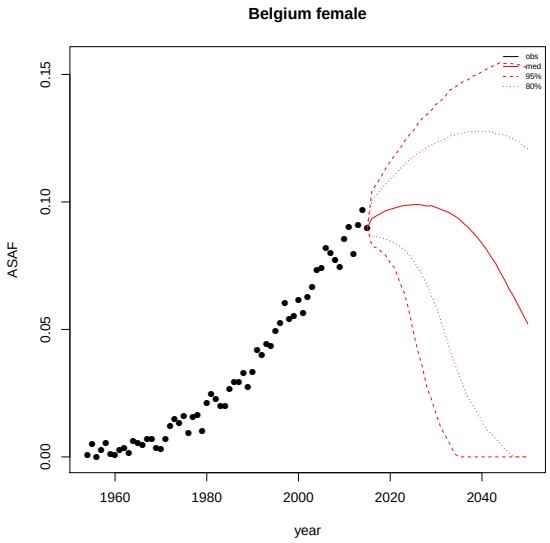
Belgium female
obs
med
95%
80%
ASAF
0.00
0.05
0.10
0.15
1960
1980
2000
2020
2040
year

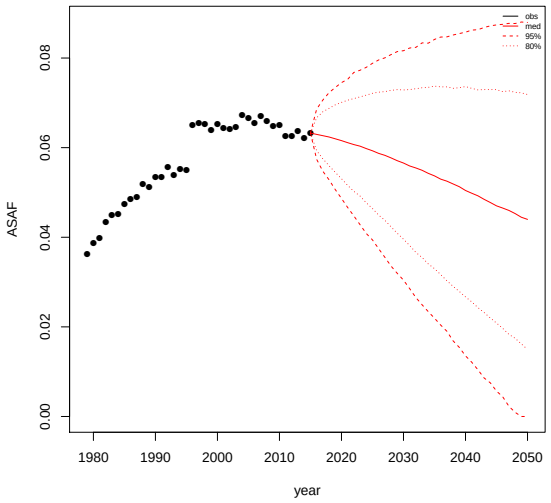
Brazil male
obs
med
95%
80%
ASAF
0.00
0.02
0.04
0.06
0.08
1980
1990
2000
2010
2020
2030
2040
2050
year

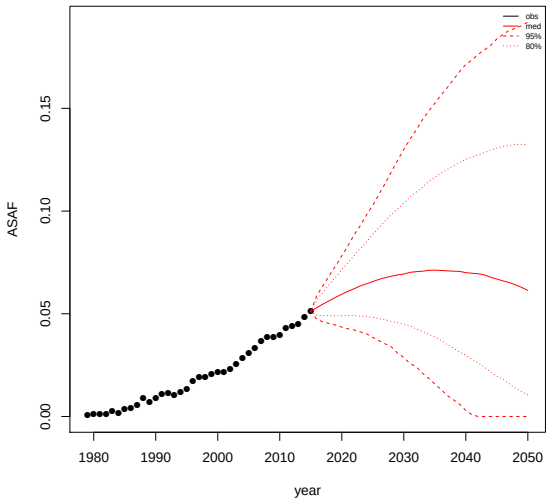
Brazil female
obs
med
95%
80%
ASAF
0.00
0.05
0.10
0.15
1980
1990
2000
2010
2020
2030
2040
2050
year

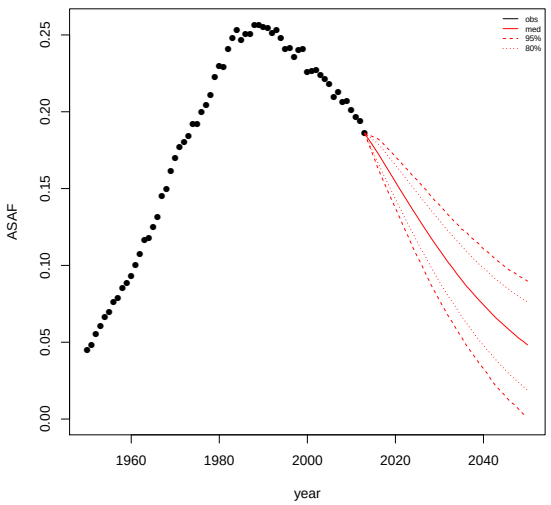
Canada male
obs
med
95%
80%
ASAF
0.00
0.05
0.10
0.15
0.20
0.25
1960
1980
2000
2020
2040
year

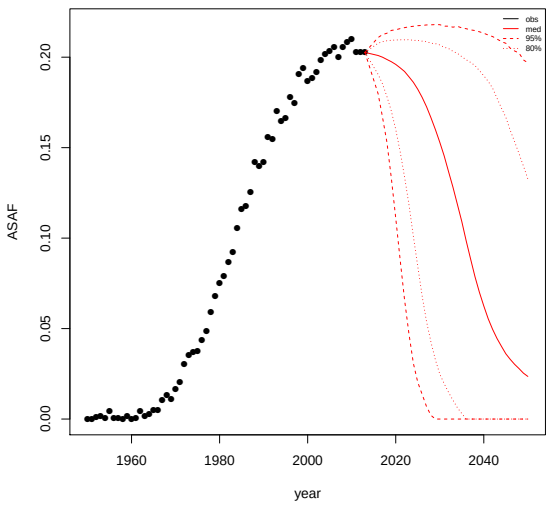
Canada female
obs
med
95%
80%
ASAF
0.00
0.05
0.10
0.15
0.20
1960
1980
2000
2020
2040
year

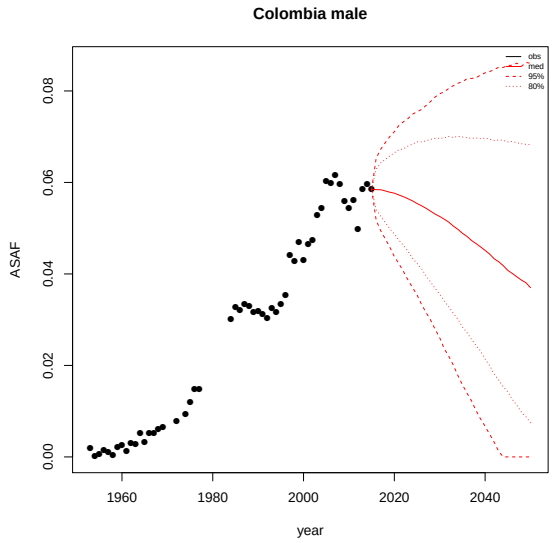
Colombia male
ASAF
year
obs
med
95%
80%

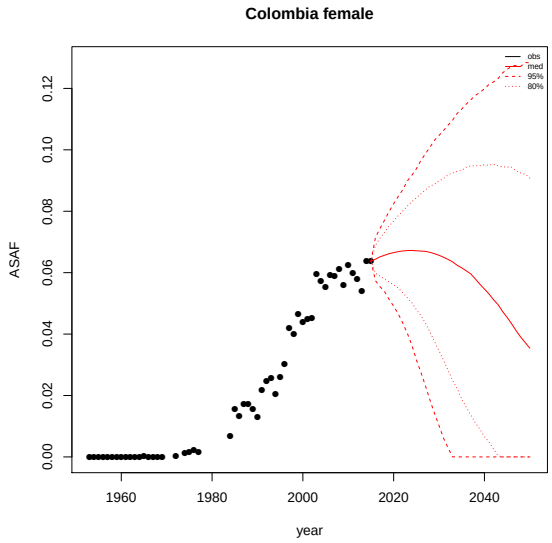
Colombia female
ASAF
year
obs
med
95%
80%

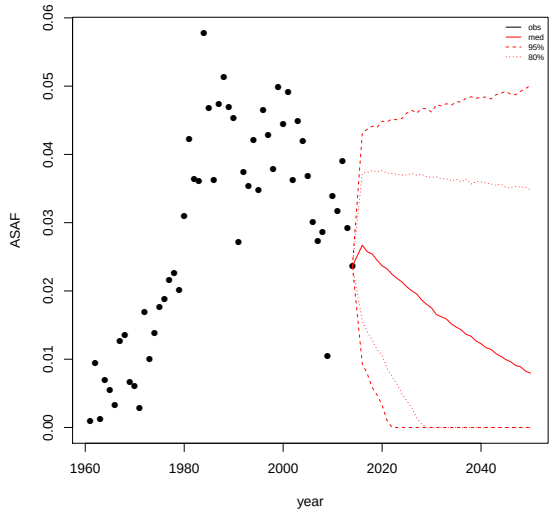
Costa Rica male
ASAF
year
obs
med
95%
80%

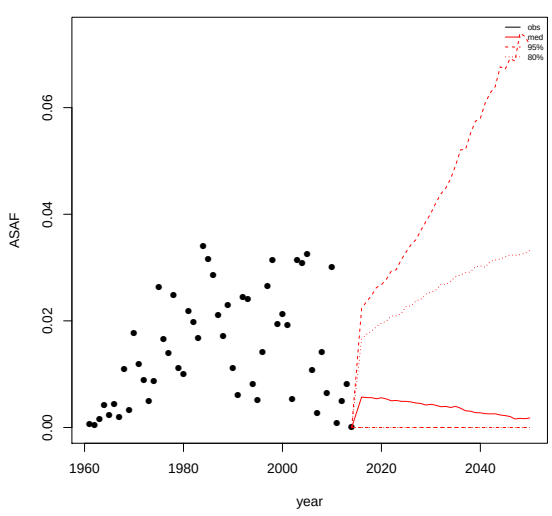
Costa Rica female
ASAF
year
obs
med
95%
80%

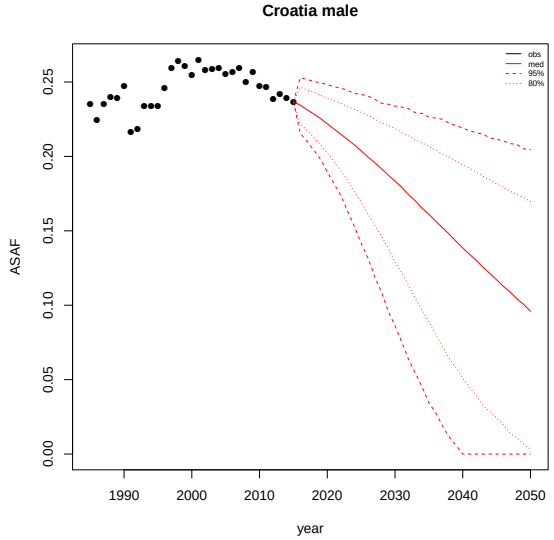
Croatia male
ASAF
year
obs
med
95%
80%

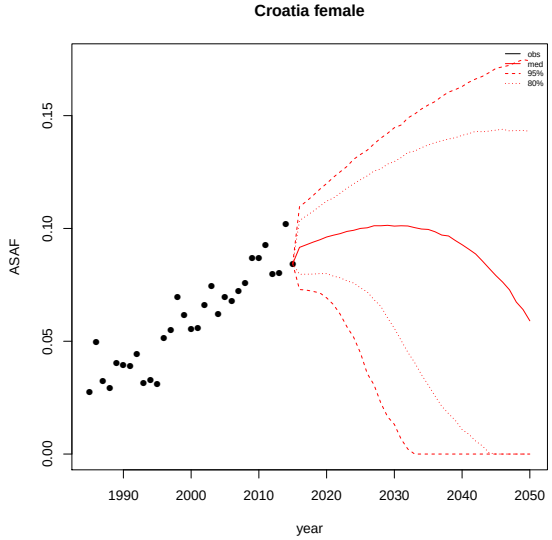
Croatia female
ASAF
year
obs
med
95%
80%

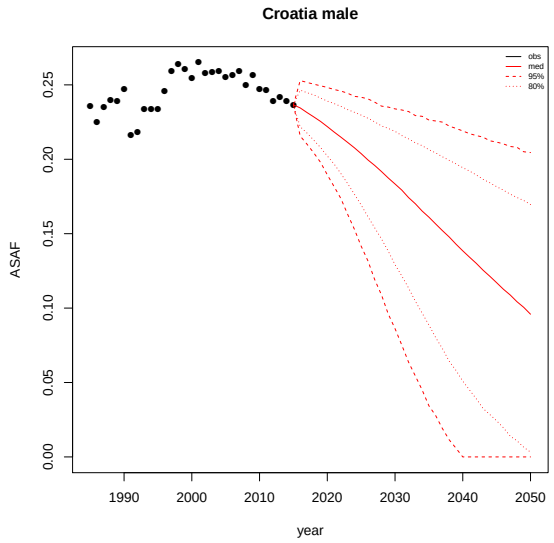
Croatia male
obs
med
95%
80%
ASAF
0.00
0.05
0.10
0.15
0.20
0.25
1990
2000
2010
2020
2030
2040
2050
year

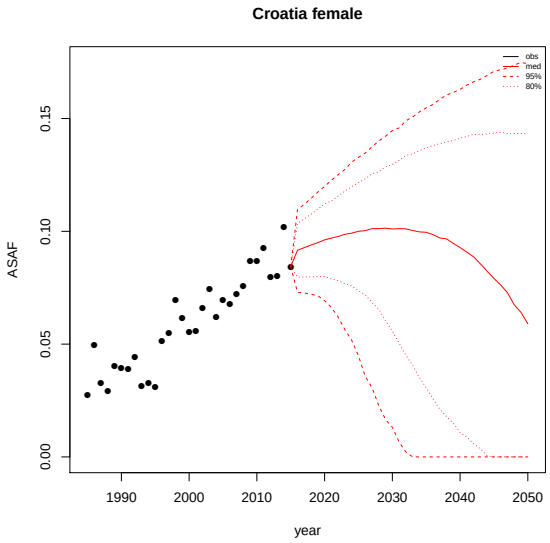
Croatia female
obs
med
95%
80%
ASAF
0.00
0.05
0.10
0.15
1990
2000
2010
2020
2030
2040
2050
year

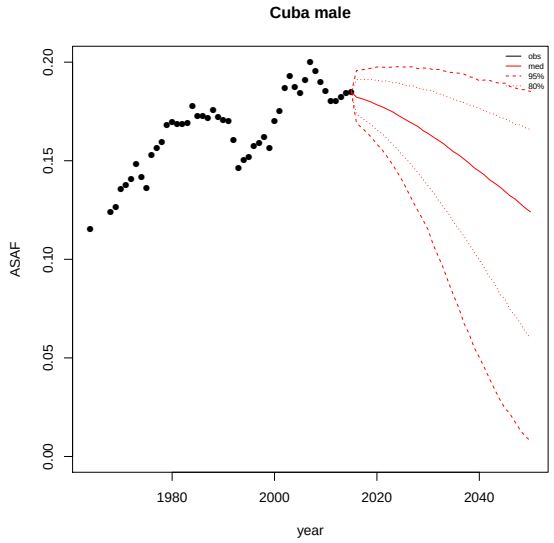
Cuba male
obs
med
95%
80%
ASAF
0.00
0.05
0.10
0.15
0.20
1980
2000
2020
2040
year

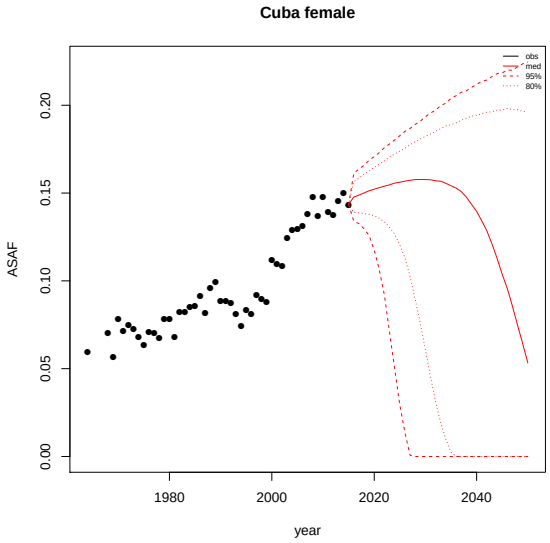
Cuba female
obs
med
95%
80%
ASAF
0.00
0.05
0.10
0.15
0.20
1980
2000
2020
2040
year

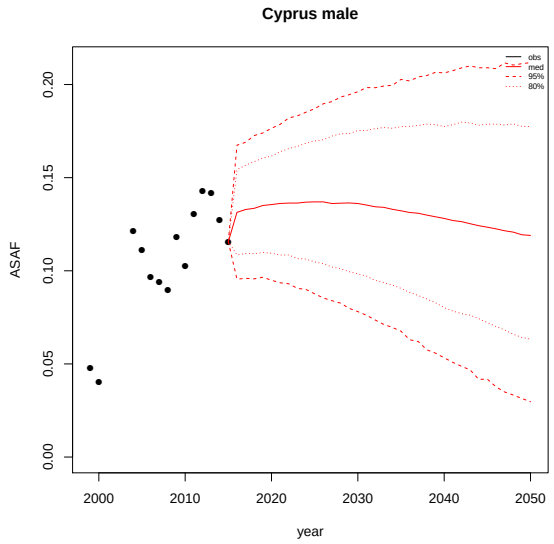
Cyprus male
obs
med
95%
80%
ASAF
0.00
0.05
0.10
0.15
0.20
2000
2010
2020
2030
2040
2050
year

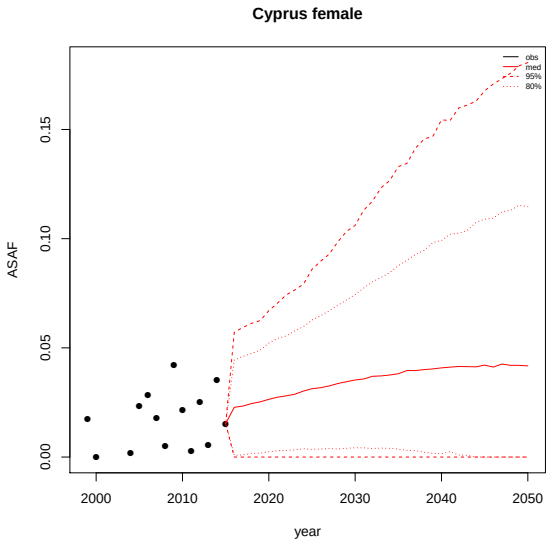
Cyprus female
obs
med
95%
80%
ASAF
0.00
0.05
0.10
0.15
2000
2010
2020
2030
2040
2050
year

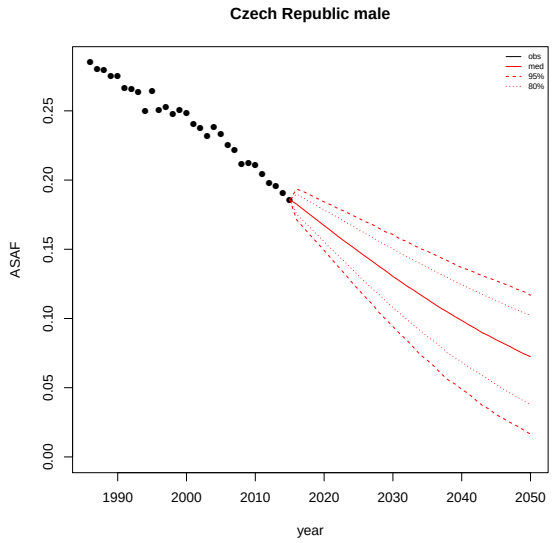
Czech Republic male
obs
med
95%
80%
ASAF
0.00
0.05
0.10
0.15
0.20
0.25
1990
2000
2010
2020
2030
2040
2050
year

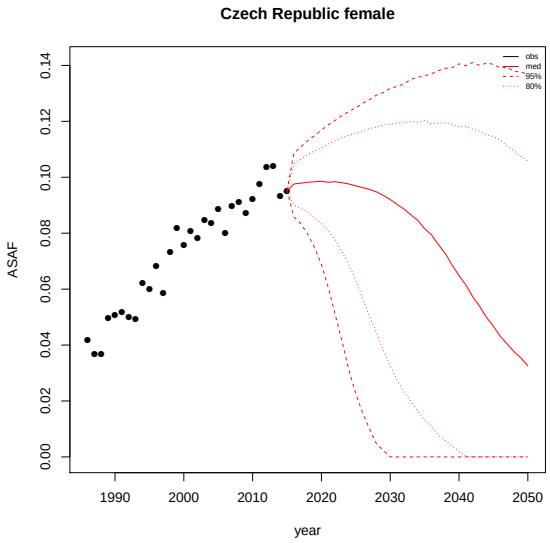
Czech Republic female
obs
med
95%
80%
ASAF
0.00
0.02
0.04
0.06
0.08
0.10
0.12
0.14
1990
2000
2010
2020
2030
2040
2050
year

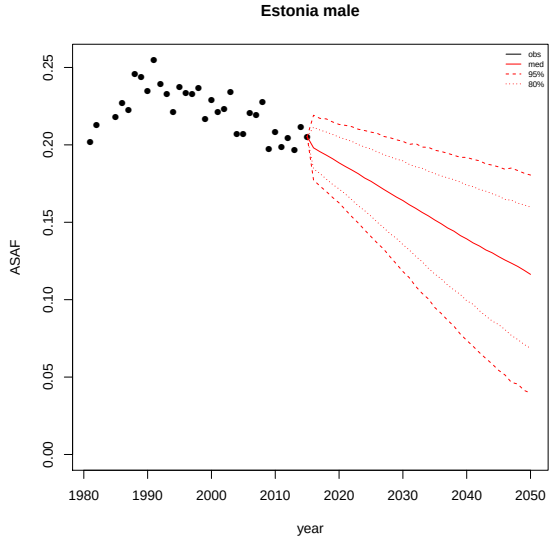
Estonia male
obs
med
95%
80%
ASAF
0.00
0.05
0.10
0.15
0.20
0.25
1980
1990
2000
2010
2020
2030
2040
2050
year

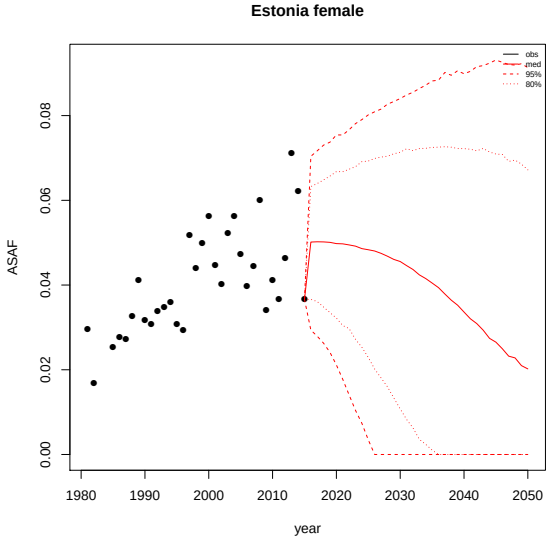
Estonia female
obs
med
95%
80%
ASAF
0.00
0.02
0.04
0.06
0.08
1980
1990
2000
2010
2020
2030
2040
2050
year

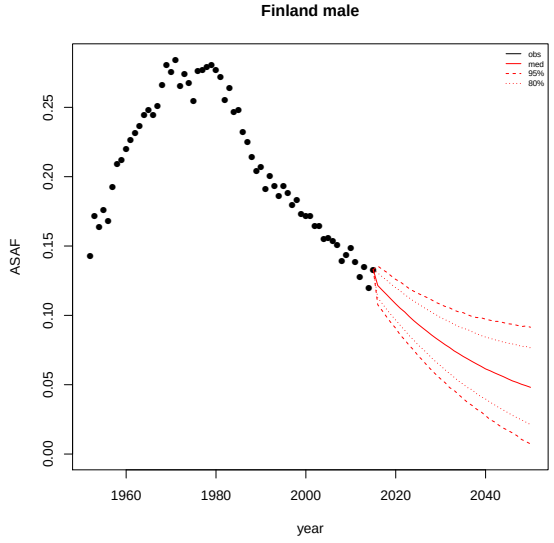
Finland male
obs
med
95%
80%
ASAF
0.00
0.05
0.10
0.15
0.20
0.25
1960
1980
2000
2020
2040
year


Finland female
obs
med
95%
80%
ASAF
0.00
0.02
0.04
0.06
0.08
0.10
0.12
1960
1980
2000
2020
2040
year

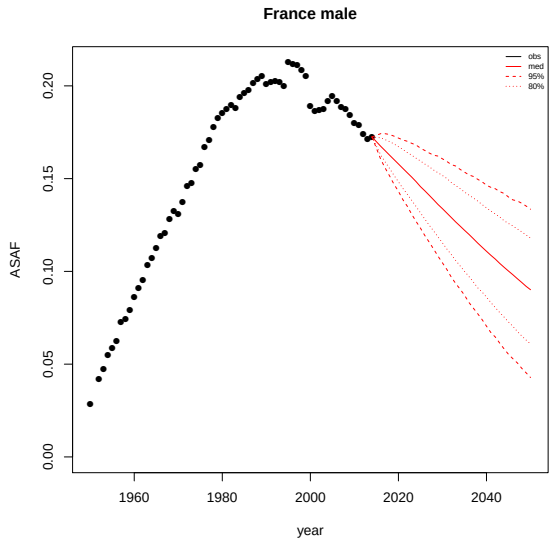
France male
obs
med
95%
80%
ASAF
0.00
0.05
0.10
0.15
0.20
1960
1980
2000
2020
2040
year

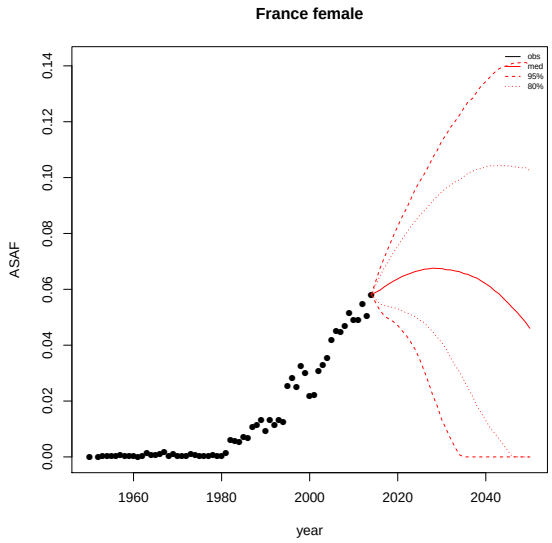
France female
obs
med
95%
80%
ASAF
0.00
0.02
0.04
0.06
0.08
0.10
0.12
0.14
1960
1980
2000
2020
2040
year

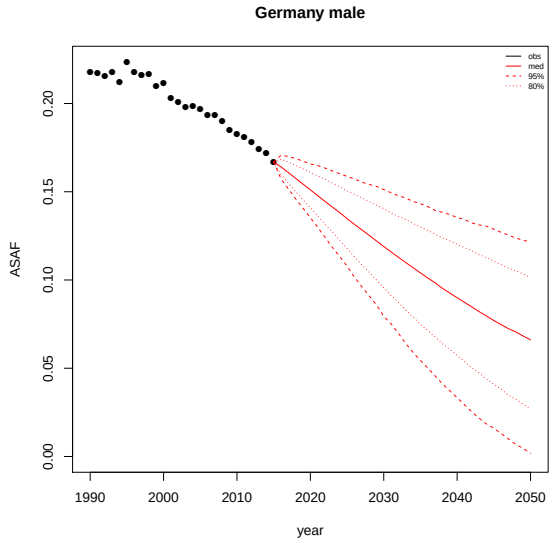
Germany male
obs
med
95%
80%
ASAF
0.00
0.05
0.10
0.15
0.20
1990
2000
2010
2020
2030
2040
2050
year

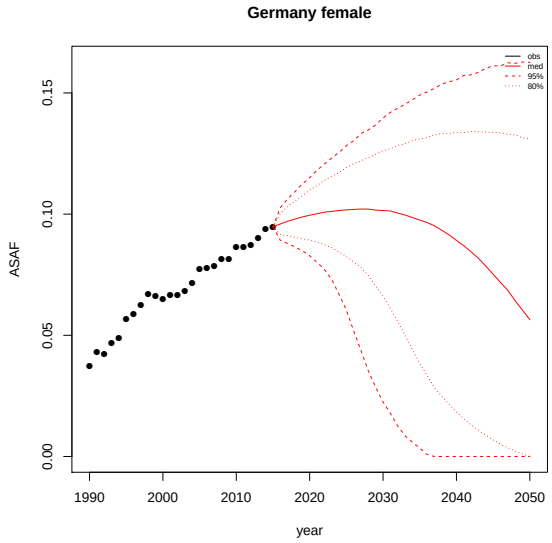
Germany female
obs
med
95%
80%
ASAF
0.00
0.05
0.10
0.15
1990
2000
2010
2020
2030
2040
2050
year

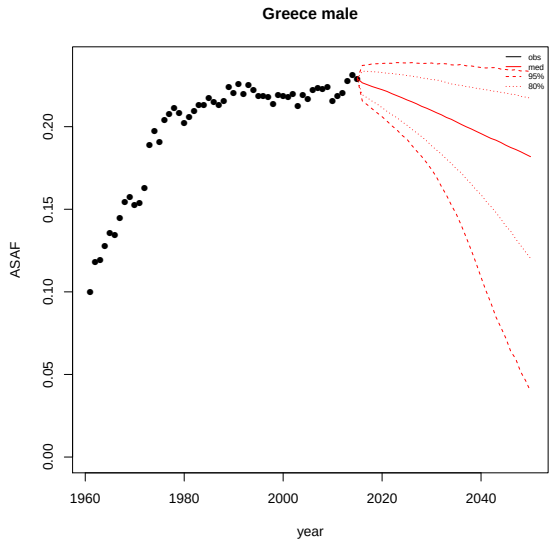
Greece male
obs
med
95%
80%
ASAF
0.00
0.05
0.10
0.15
0.20
1960
1980
2000
2020
2040
year

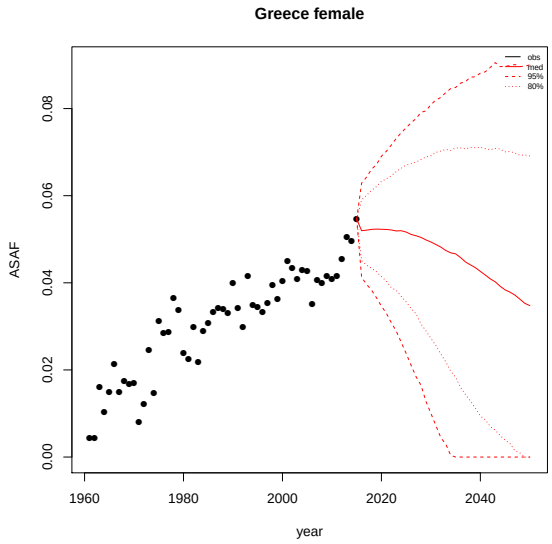
Greece female
obs
med
95%
80%
ASAF
0.00
0.02
0.04
0.06
0.08
1960
1980
2000
2020
2040
year

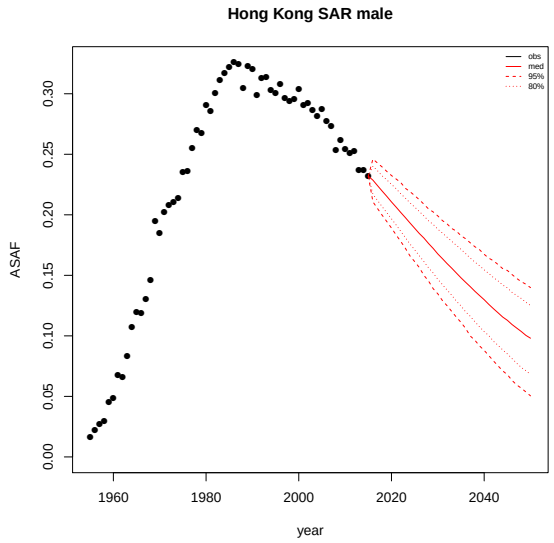
Hong Kong SAR male
obs
med
95%
80%
ASAF
0.00
0.05
0.10
0.15
0.20
0.25
0.30
1960
1980
2000
2020
2040
year

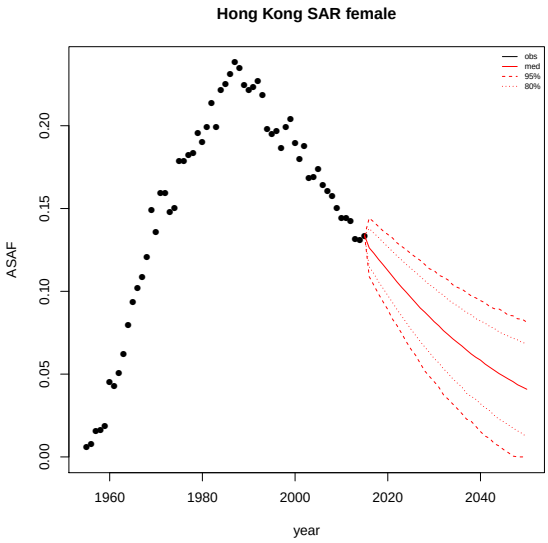
Hong Kong SAR female
obs
med
95%
80%
ASAF
0.00
0.05
0.10
0.15
0.20
1960
1980
2000
2020
2040
year

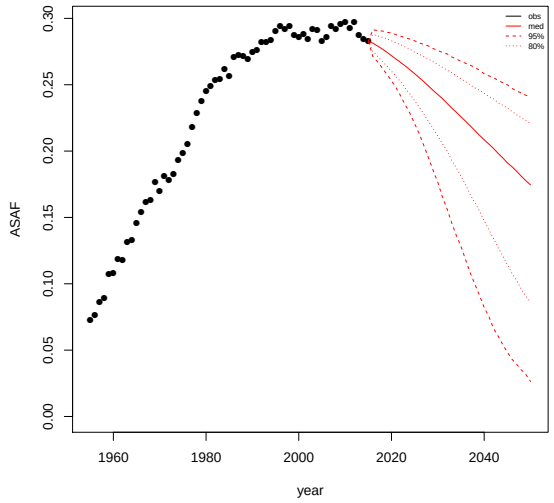
Hungary male
obs
med
95%
80%
ASAF
0.00
0.05
0.10
0.15
0.20
0.25
0.30
1960
1980
2000
2020
2040
year

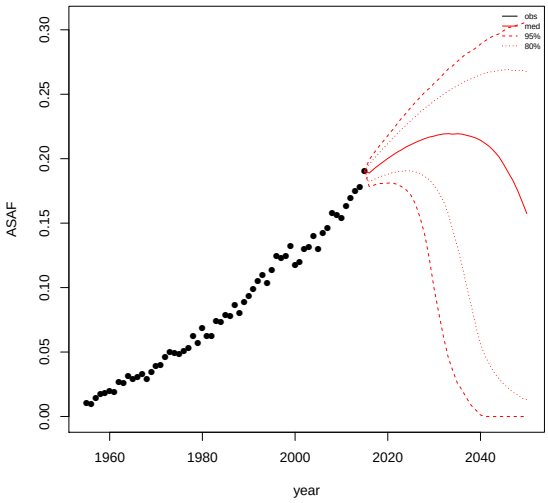
Hungary female
obs
med
95%
80%
ASAF
0.00
0.05
0.10
0.15
0.20
0.25
0.30
1960
1980
2000
2020
2040
year

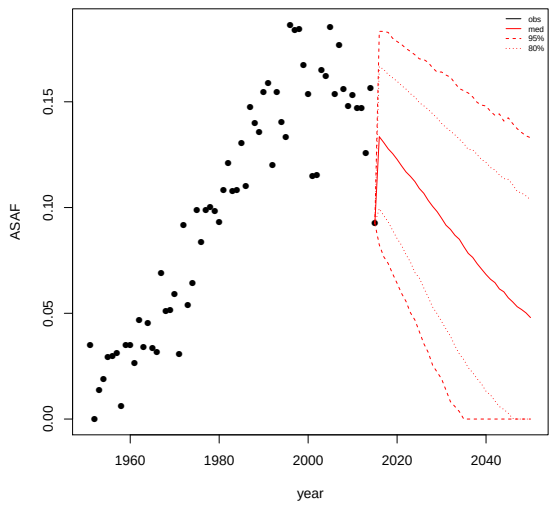
Iceland male
obs
med
95%
80%
ASAF
0.00
0.05
0.10
0.15
1960
1980
2000
2020
2040
year

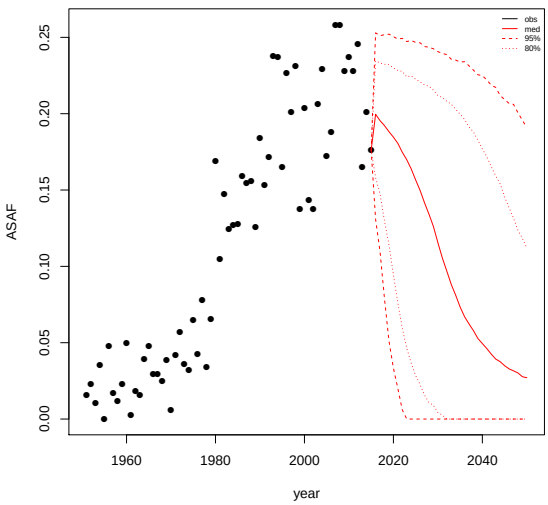
Iceland female
obs
med
95%
80%
ASAF
0.00
0.05
0.10
0.15
0.20
0.25
1960
1980
2000
2020
2040
year

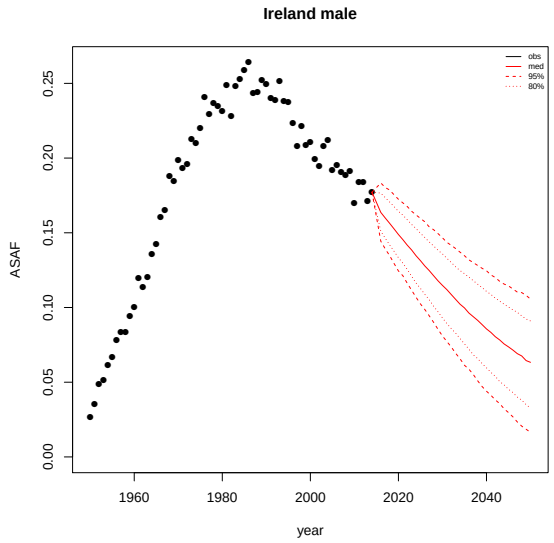
Ireland male
ASAF
year
obs
med
95%
80%

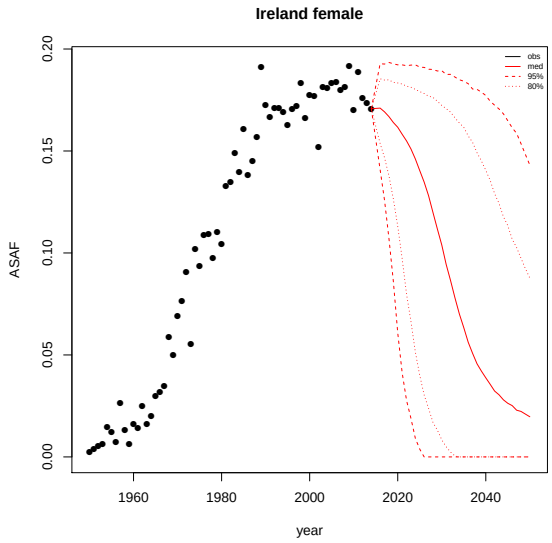
Ireland female
ASAF
year
obs
med
95%
80%

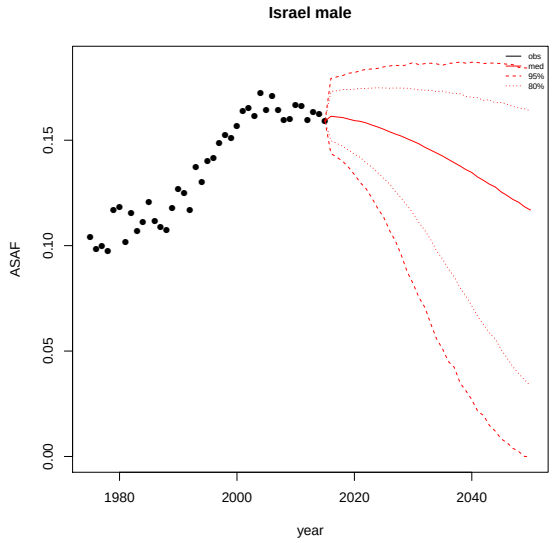
Israel male
ASAF
year
obs
med
95%
80%

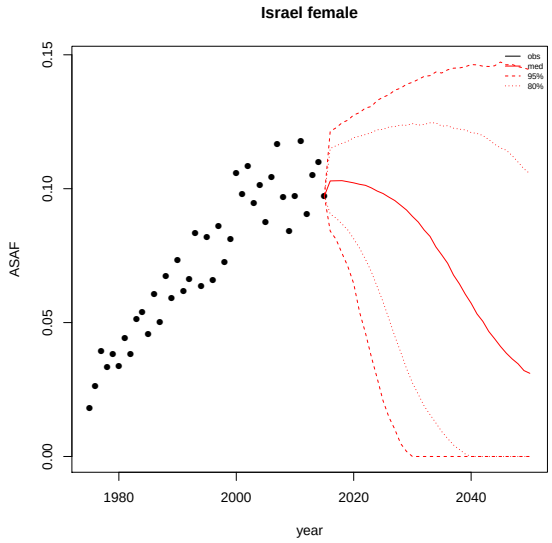
Israel female
ASAF
year
obs
med
95%
80%

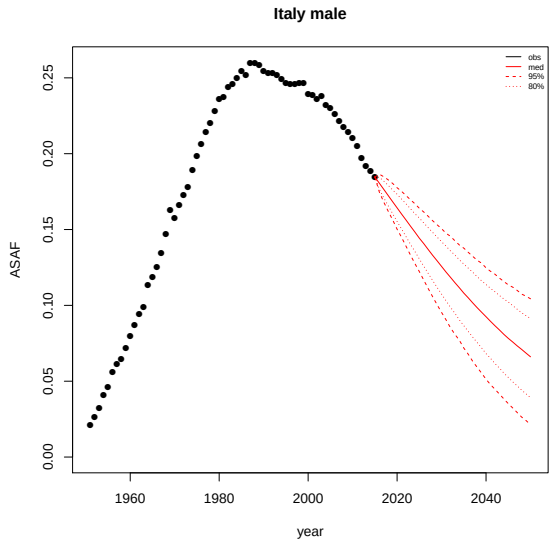
Italy male
ASAF
year
obs
med
95%
80%

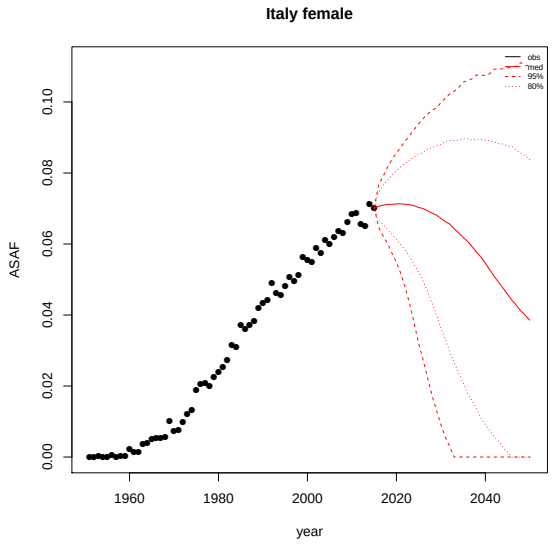
Italy female
ASAF
year
obs
med
95%
80%

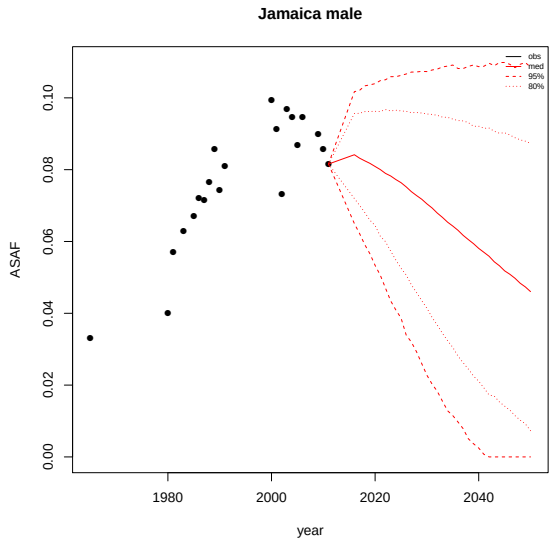
Jamaica male
obs
med
95%
80%
ASAF
0.00
0.02
0.04
0.06
0.08
0.10
1980
2000
2020
2040
year

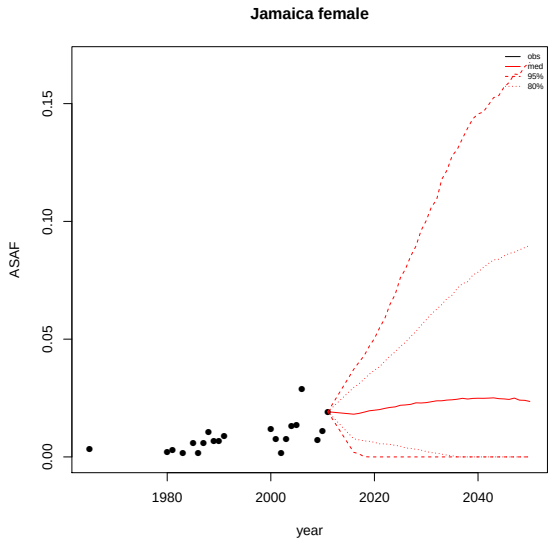
Jamaica female
obs
med
95%
80%
ASAF
0.00
0.05
0.10
0.15
1980
2000
2020
2040
year

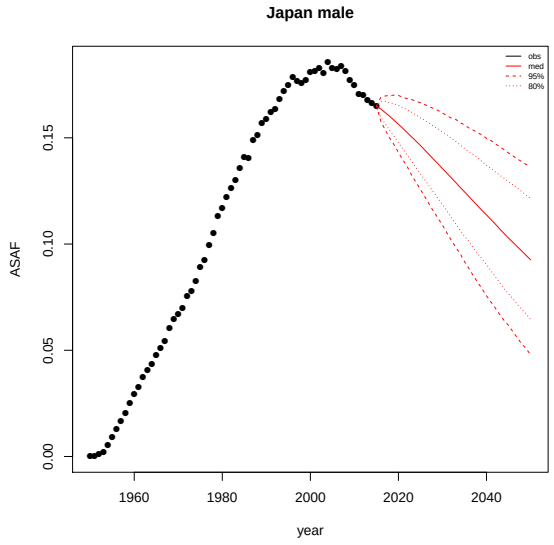
Japan male
obs
med
95%
80%
ASAF
0.00
0.05
0.10
0.15
1960
1980
2000
2020
2040
year

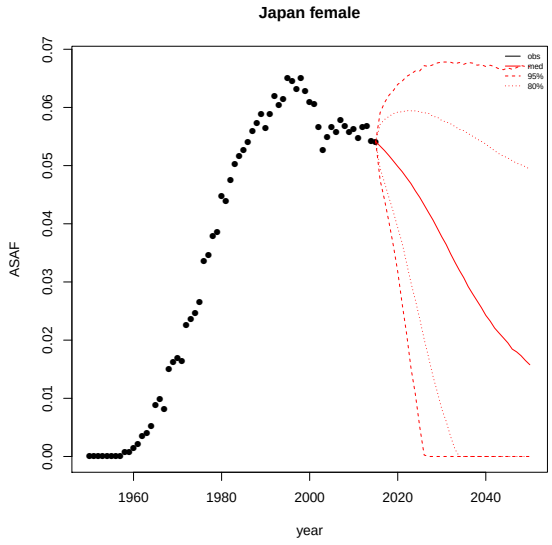
Japan female
obs
med
95%
80%
ASAF
0.00
0.01
0.02
0.03
0.04
0.05
0.06
0.07
1960
1980
2000
2020
2040
year

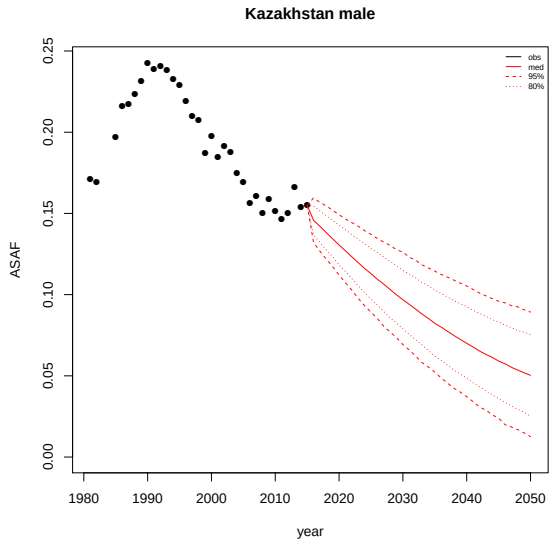
Kazakhstan male
obs
med
95%
80%
ASAF
0.00
0.05
0.10
0.15
0.20
0.25
1980
1990
2000
2010
2020
2030
2040
2050
year

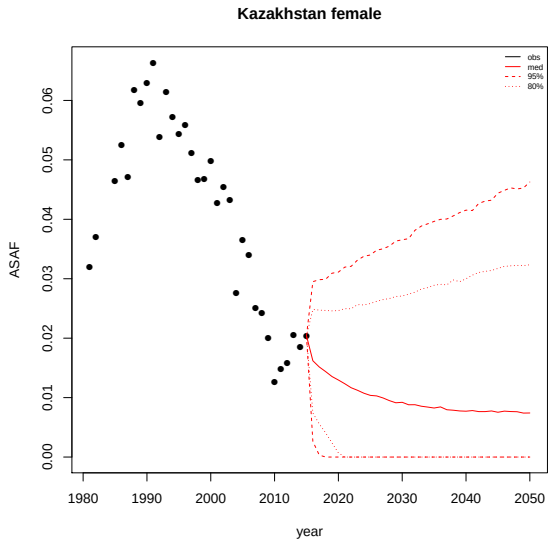
Kazakhstan female
obs
med
95%
80%
ASAF
0.00
0.01
0.02
0.03
0.04
0.05
0.06
1980
1990
2000
2010
2020
2030
2040
2050
year

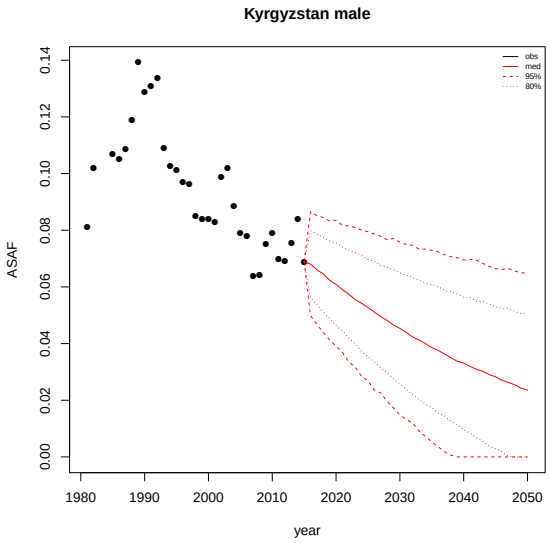
Kyrgyzstan male
obs
med
95%
80%
ASAF
0.00
0.02
0.04
0.06
0.08
0.10
0.12
0.14
1980
1990
2000
2010
2020
2030
2040
2050
year

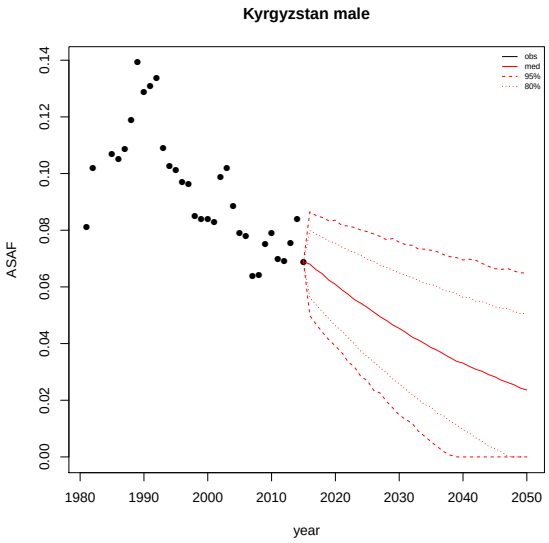
Kyrgyzstan male
obs
med
95%
80%
ASAF
0.00
0.02
0.04
0.06
0.08
0.10
0.12
0.14
1980
1990
2000
2010
2020
2030
2040
2050
year

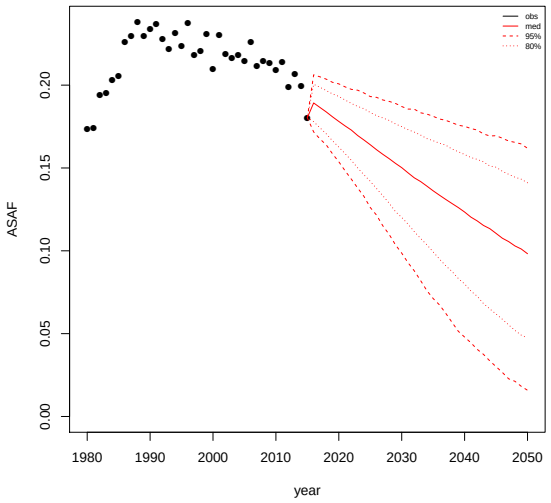
Latvia male
obs
med
95%
80%
ASAF
0.00
0.05
0.10
0.15
0.20
1980
1990
2000
2010
2020
2030
2040
2050
year

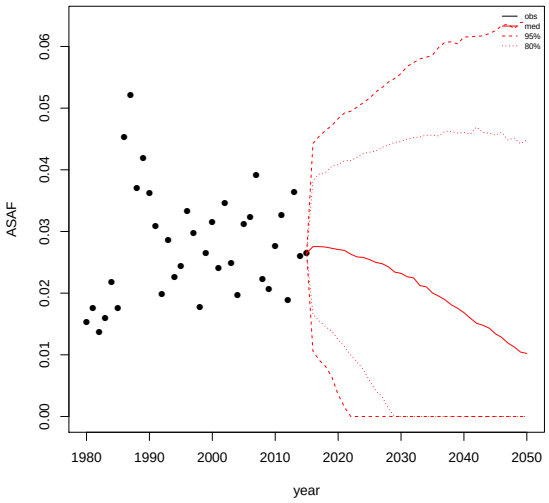
Latvia female
obs
med
95%
80%
ASAF
0.00
0.01
0.02
0.03
0.04
0.05
0.06
1980
1990
2000
2010
2020
2030
2040
2050
year

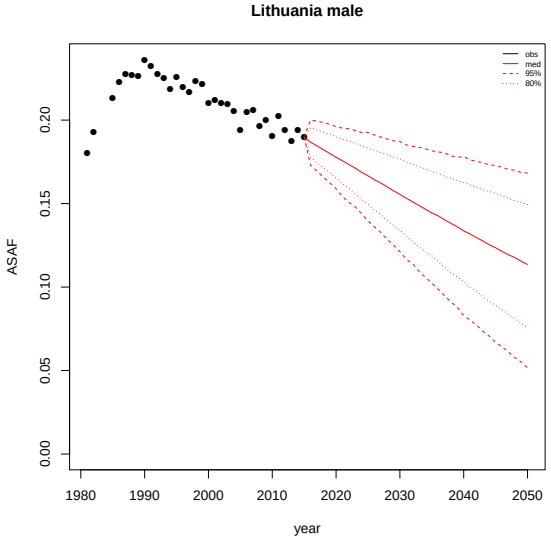
Lithuania male
obs
med
95%
80%
ASAF
0.00
0.05
0.10
0.15
0.20
1980
1990
2000
2010
2020
2030
2040
2050
year

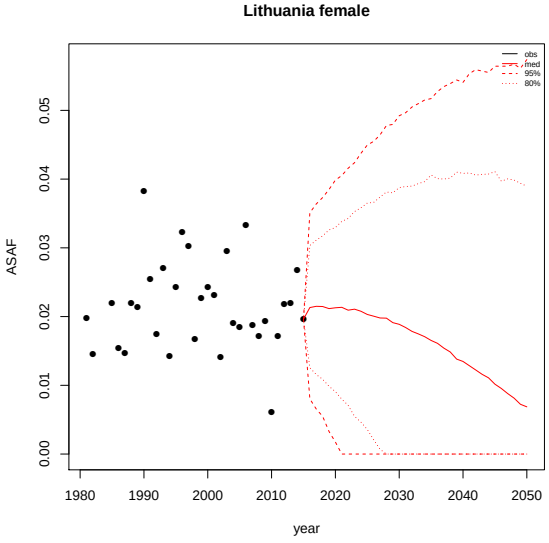
Lithuania female
obs
med
95%
80%
ASAF
0.00
0.01
0.02
0.03
0.04
0.05
1980
1990
2000
2010
2020
2030
2040
2050
year

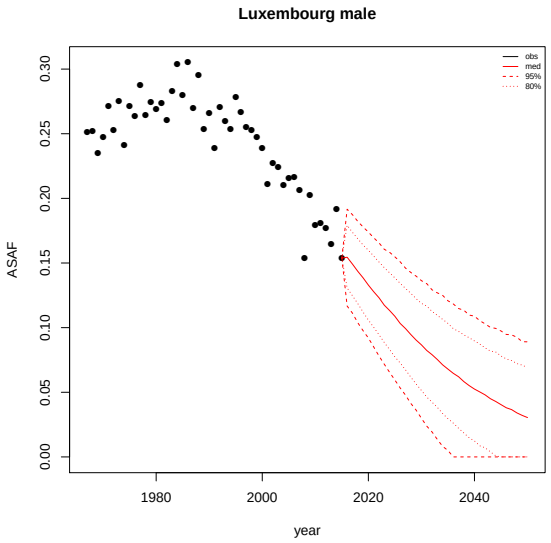
Luxembourg male
ASAF
year
obs
med
95%
80%

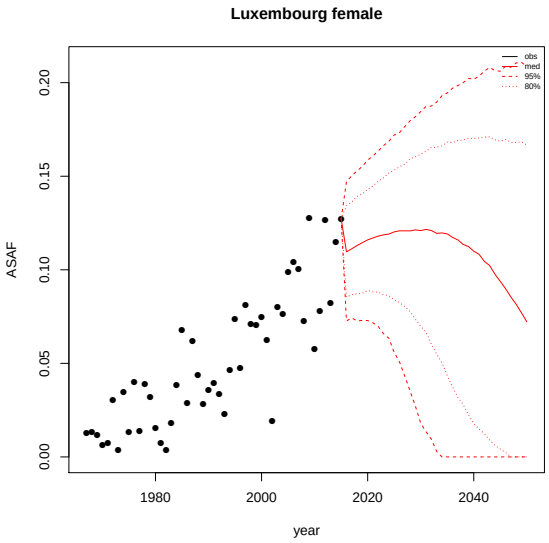
Luxembourg female
ASAF
year
obs
med
95%
80%

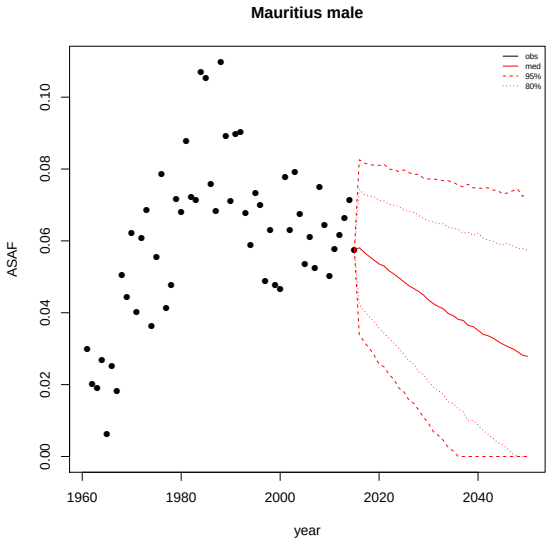
Mauritius male
ASAF
year
obs
med
95%
80%

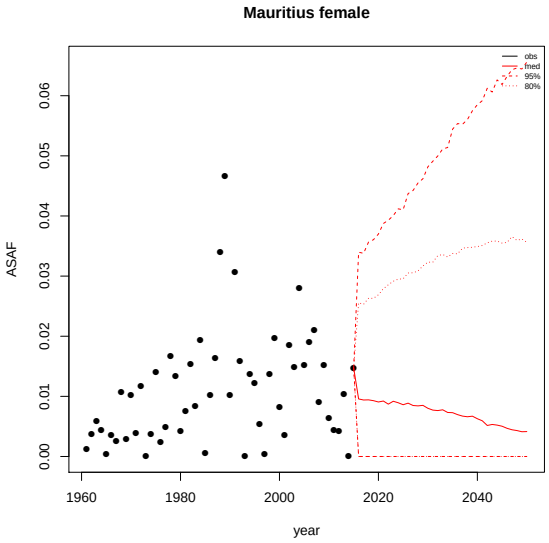
Mauritius female
ASAF
year
obs
med
95%
80%

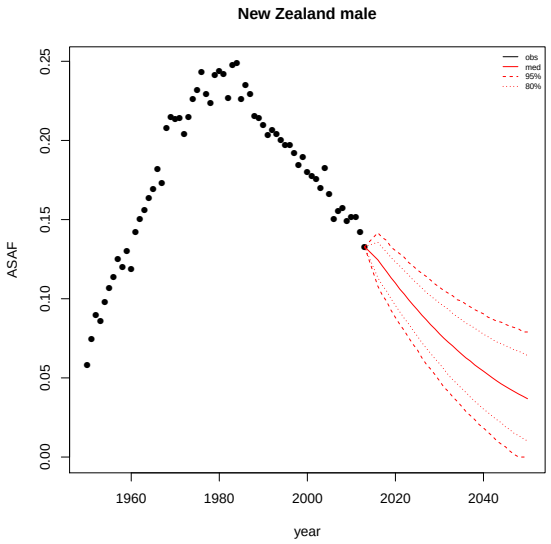
New Zealand male
ASAF
year
obs
med
95%
80%

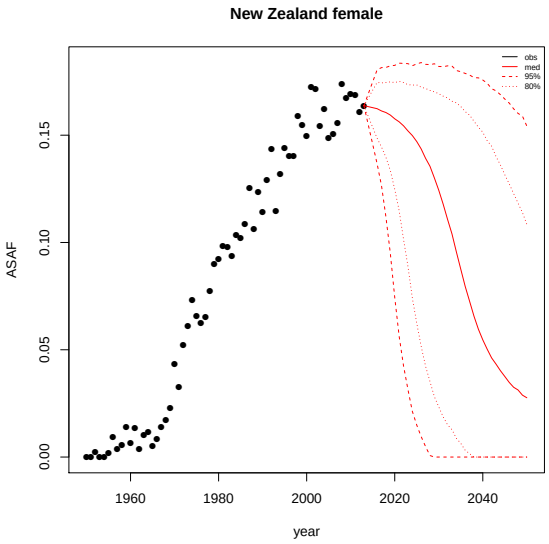
New Zealand female
ASAF
year
obs
med
95%
80%

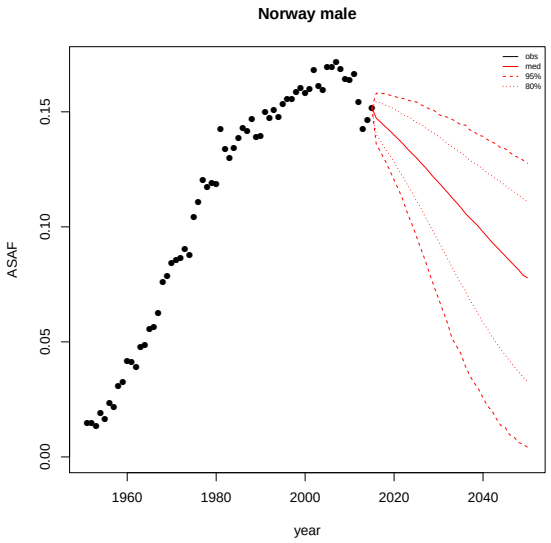
Norway male
ASAF
year
obs
med
95%
80%

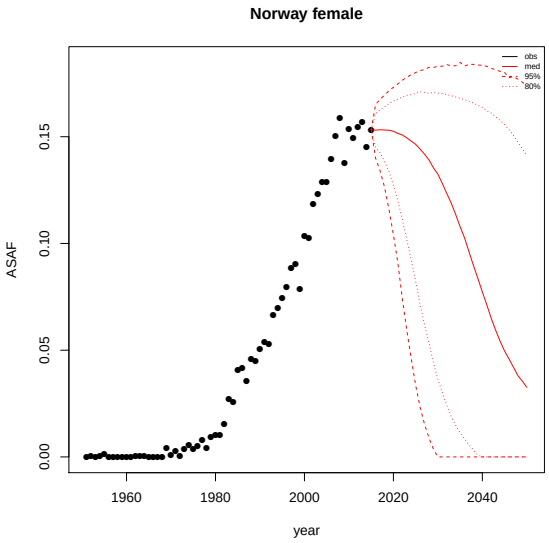
Norway female
ASAF
year
obs
med
95%
80%

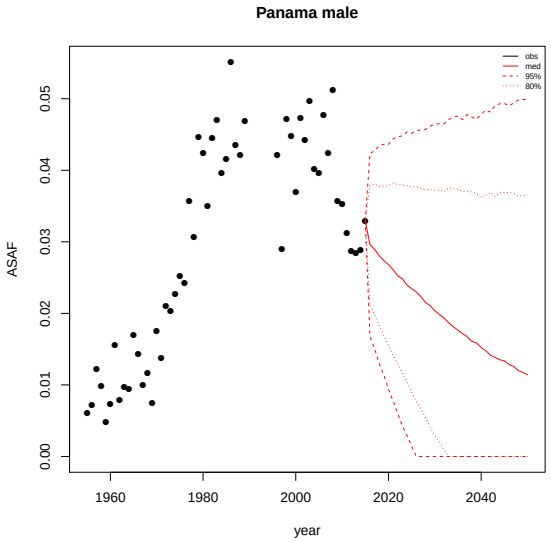
Panama male
ASAF
year
obs
med
95%
80%

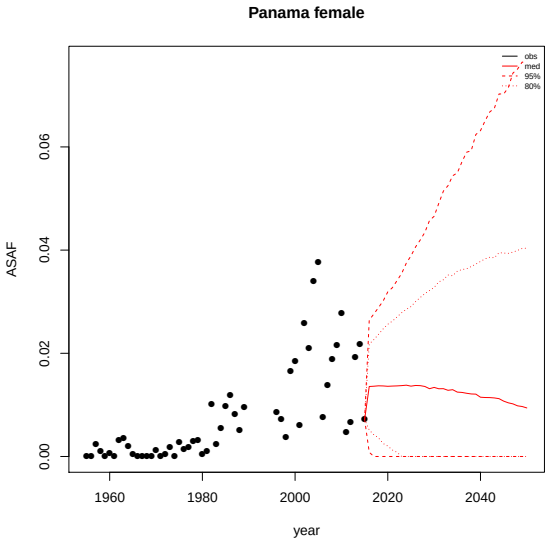
Panama female
ASAF
year
obs
med
95%
80%

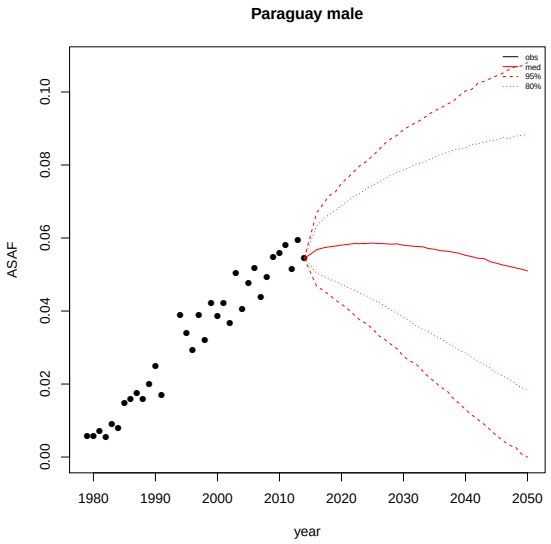
Paraguay male
ASAF
year
obs
med
95%
80%

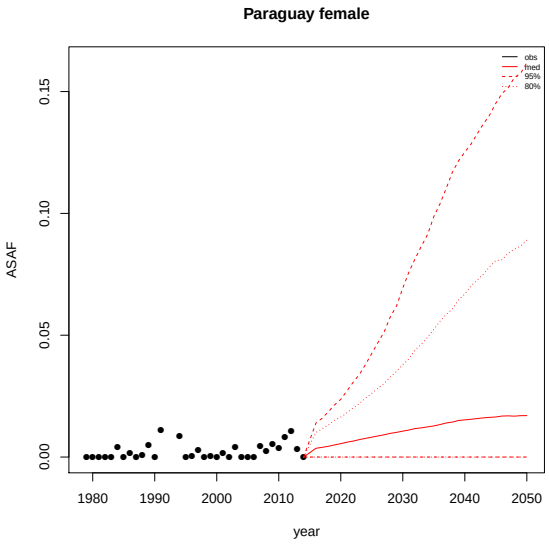
Paraguay female
ASAF
year
obs
med
95%
80%

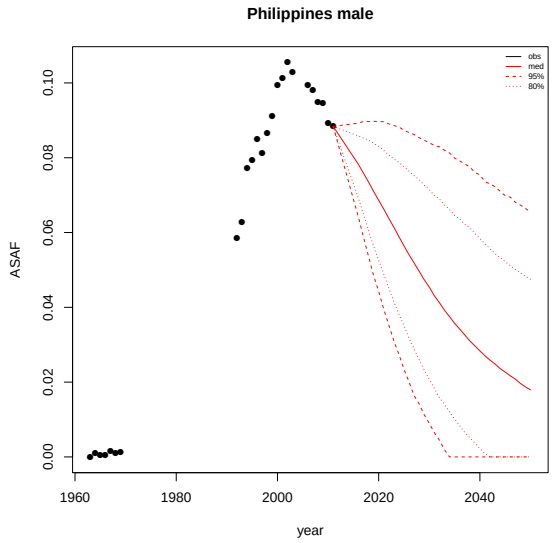
Philippines male
obs
med
95%
80%
ASAF
0.00
0.02
0.04
0.06
0.08
0.10
1960
1980
2000
2020
2040
year

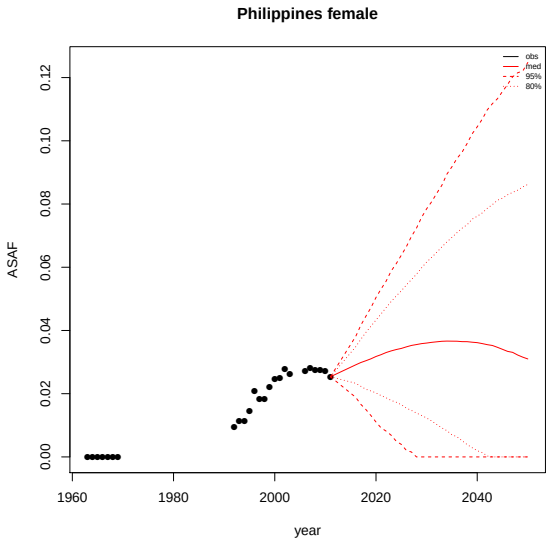
Philippines female
obs
med
95%
80%
ASAF
0.00
0.02
0.04
0.06
0.08
0.10
0.12
1960
1980
2000
2020
2040
year

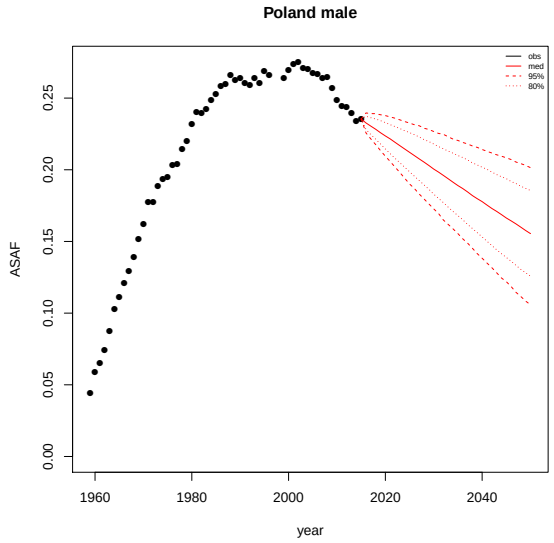
Poland male
obs
med
95%
80%
ASAF
0.00
0.05
0.10
0.15
0.20
0.25
1960
1980
2000
2020
2040
year

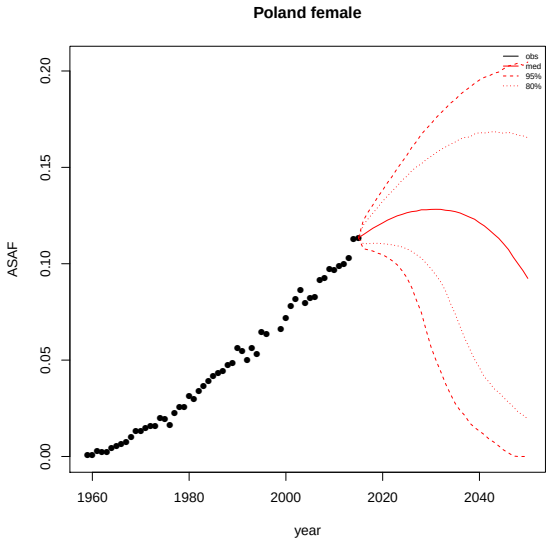
Poland female
obs
med
95%
80%
ASAF
0.00
0.05
0.10
0.15
0.20
1960
1980
2000
2020
2040
year

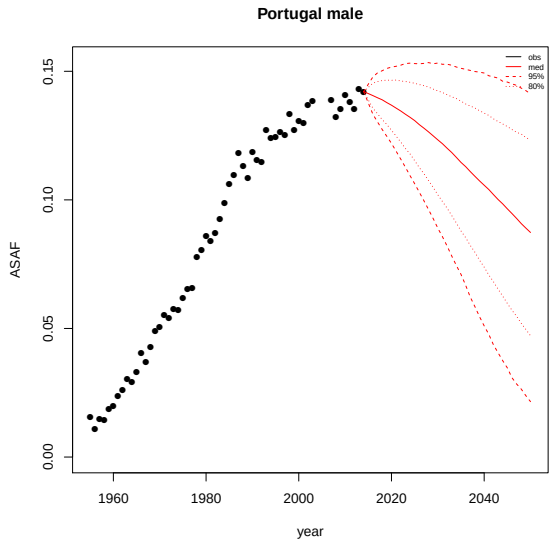
Portugal male
obs
med
95%
80%
ASAF
0.00
0.05
0.10
0.15
1960
1980
2000
2020
2040
year

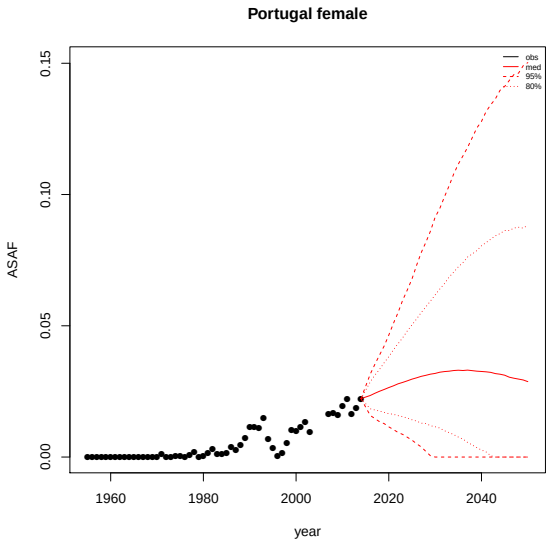
Portugal female
obs
med
95%
80%
ASAF
0.00
0.05
0.10
0.15
1960
1980
2000
2020
2040
year

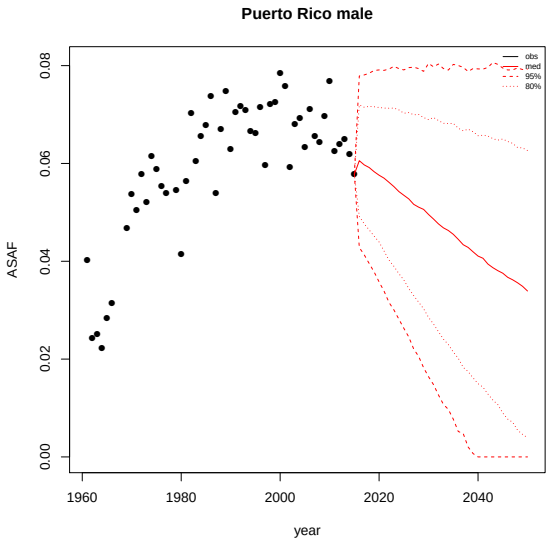
Puerto Rico male
ASAF
year
obs
med
95%
80%

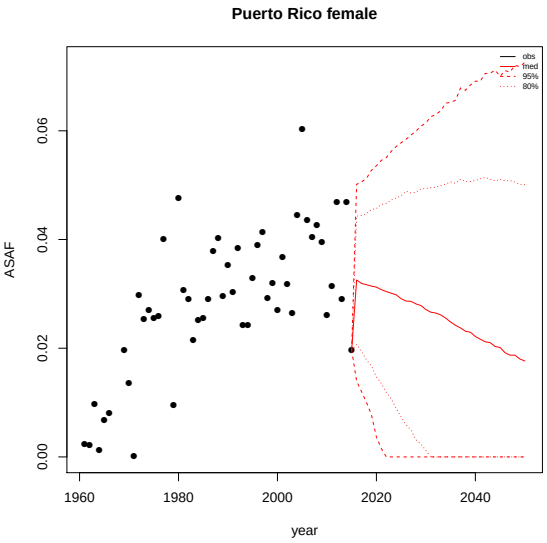
Puerto Rico female
ASAF
year
obs
med
95%
80%

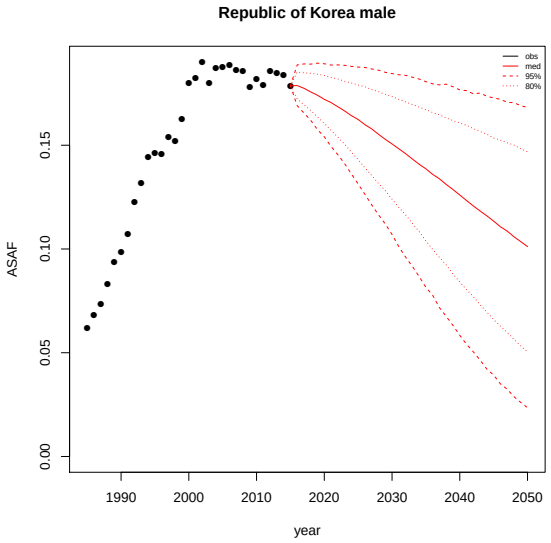
Republic of Korea male
ASAF
year
obs
med
95%
80%

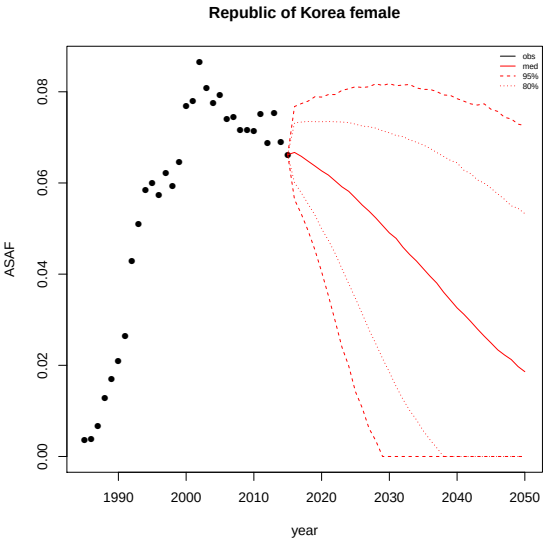
Republic of Korea female
ASAF
year
obs
med
95%
80%

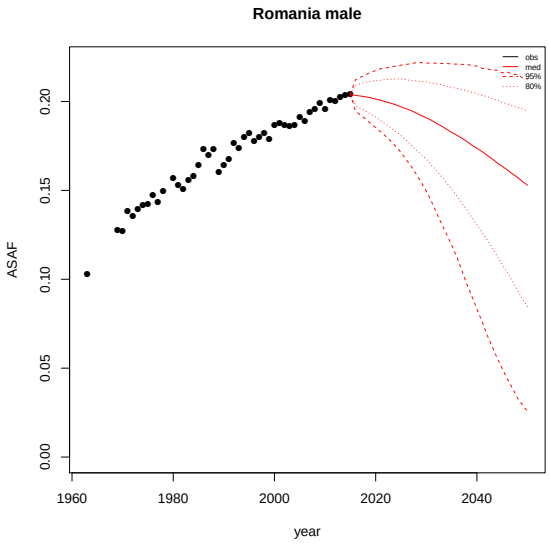
Romania male
ASAF
year
obs
med
95%
80%

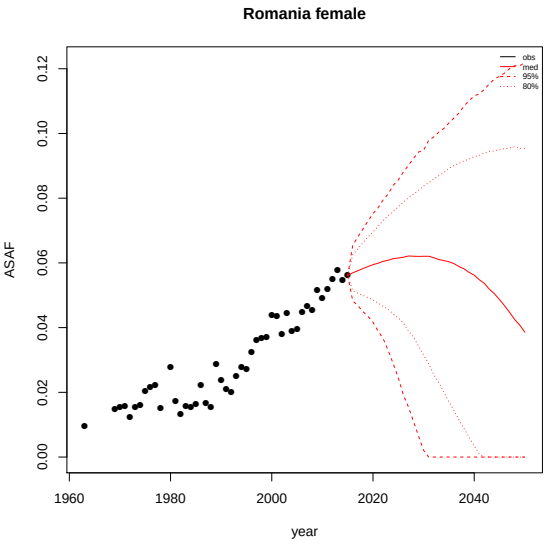
Romania female
ASAF
year
obs
med
95%
80%

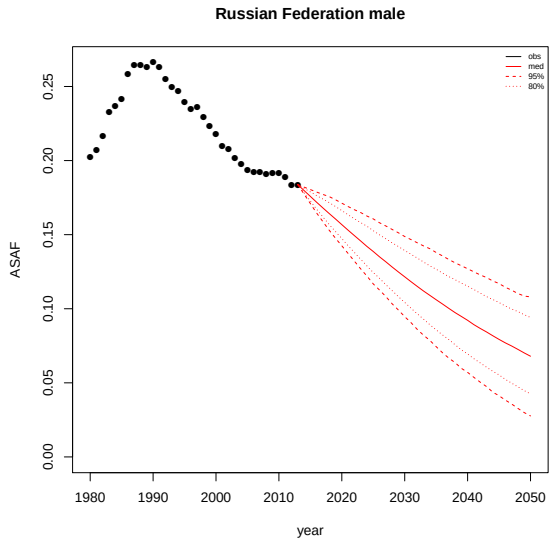
Russian Federation male
obs
med
95%
80%
ASAF
0.00
0.05
0.10
0.15
0.20
0.25
1980
1990
2000
2010
2020
2030
2040
2050
year

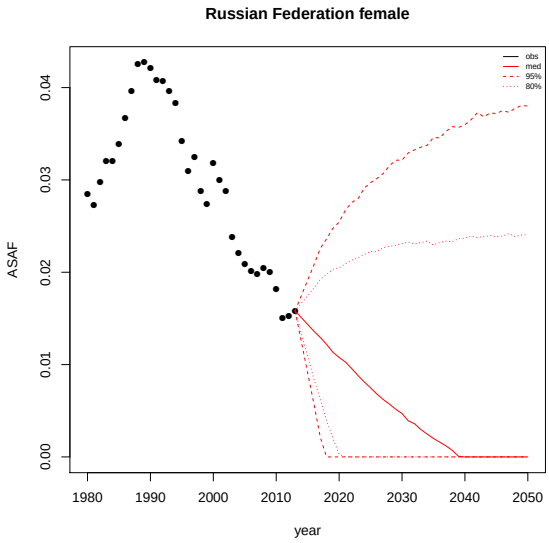
Russian Federation female
obs
med
95%
80%
ASAF
0.00
0.01
0.02
0.03
0.04
1980
1990
2000
2010
2020
2030
2040
2050
year

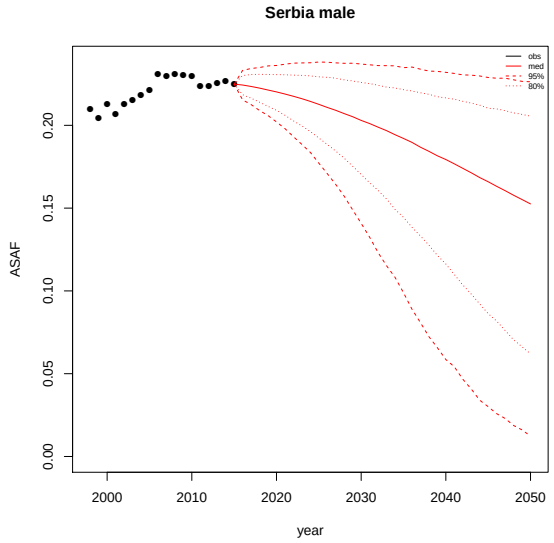
Serbia male
obs
med
95%
80%
ASAF
0.00
0.05
0.10
0.15
0.20
2000
2010
2020
2030
2040
2050
year

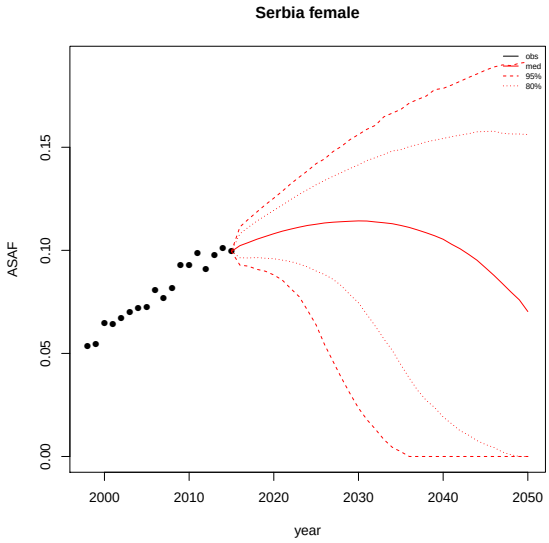
Serbia female
obs
med
95%
80%
ASAF
0.00
0.05
0.10
0.15
2000
2010
2020
2030
2040
2050
year

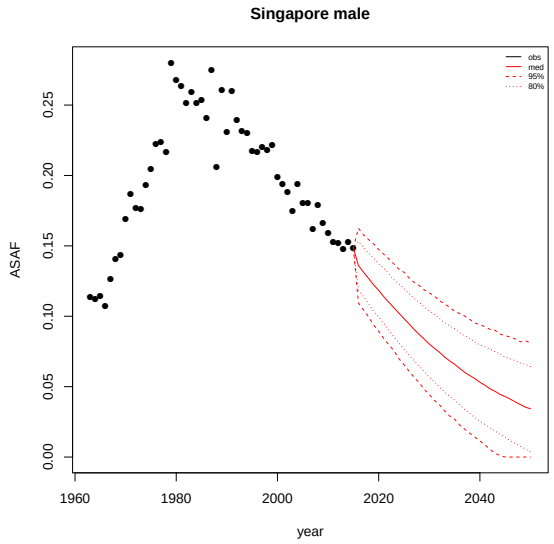
Singapore male
obs
med
95%
80%
ASAF
0.00
0.05
0.10
0.15
0.20
0.25
1960
1980
2000
2020
2040
year

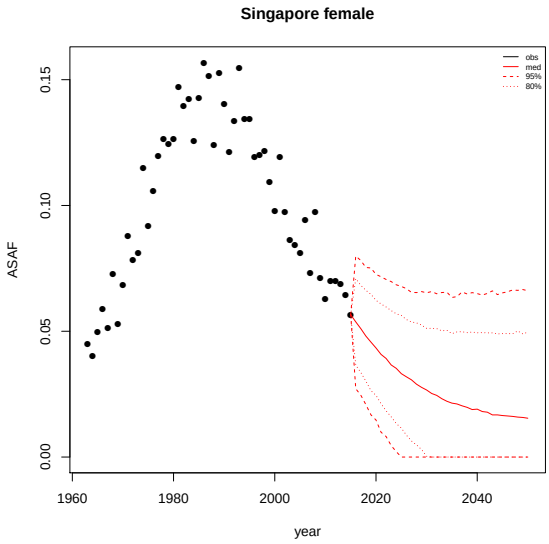
Singapore female
obs
med
95%
80%
ASAF
0.00
0.05
0.10
0.15
1960
1980
2000
2020
2040
year

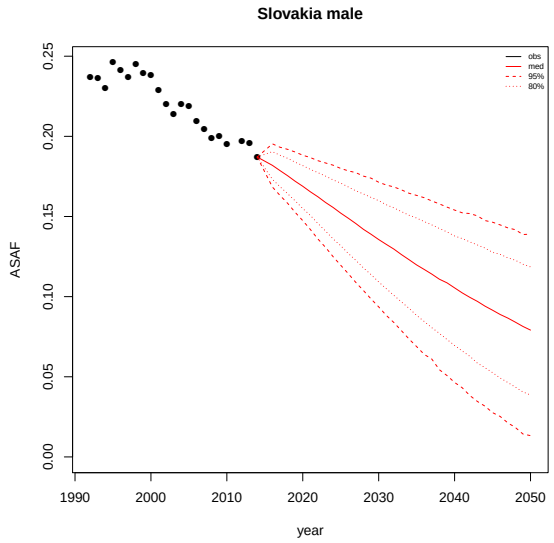
Slovakia male
ASAF
year
obs
med
95%
80%

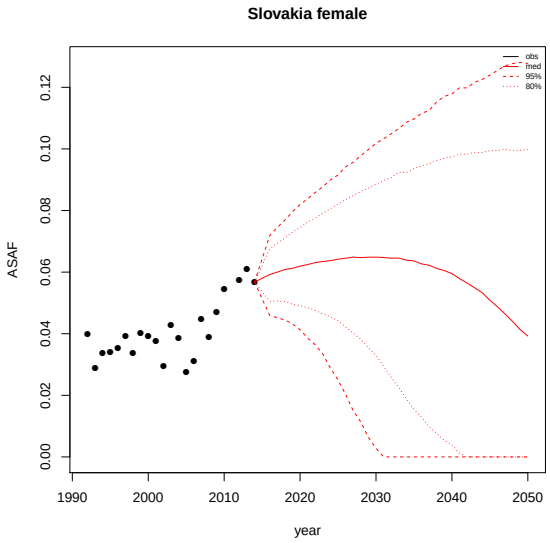
Slovakia female
ASAF
year
obs
med
95%
80%

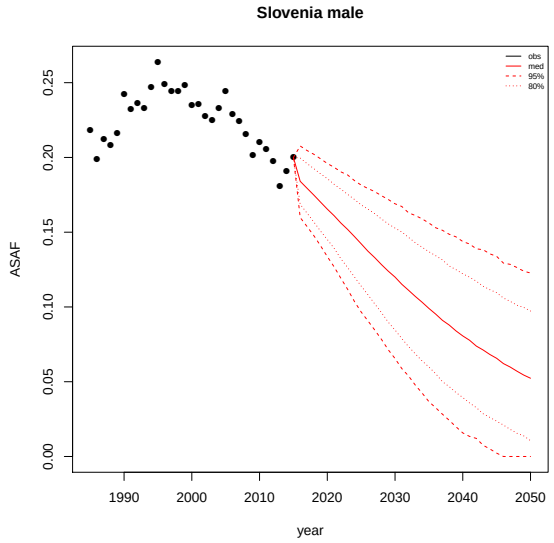
Slovenia male
ASAF
year
obs
med
95%
80%

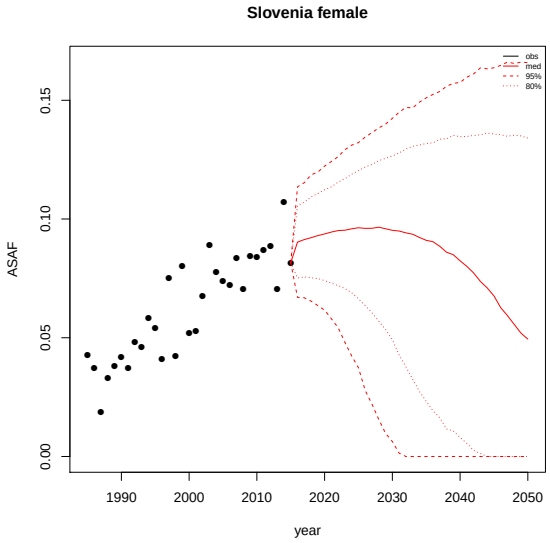
Slovenia female
ASAF
year
obs
med
95%
80%

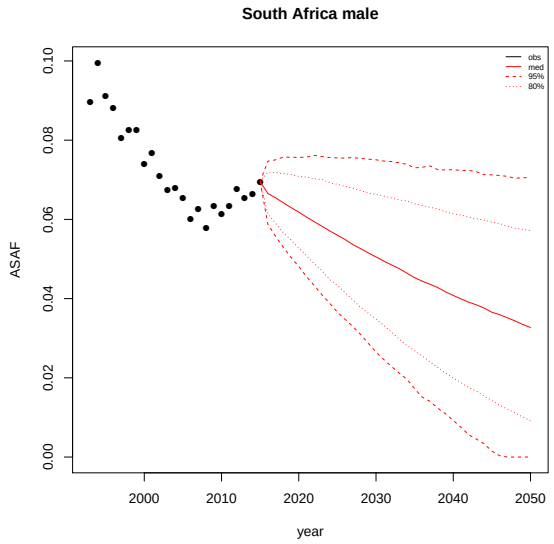
South Africa male
ASAF
year
obs
med
95%
80%

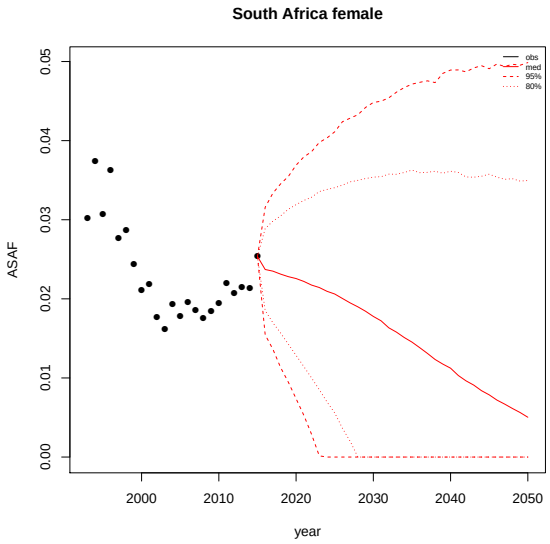
South Africa female
ASAF
year
obs
med
95%
80%

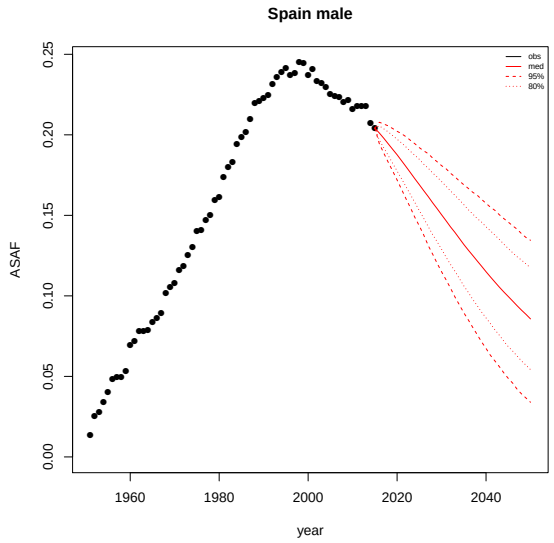
Spain male
ASAF
year
obs
med
95%
80%

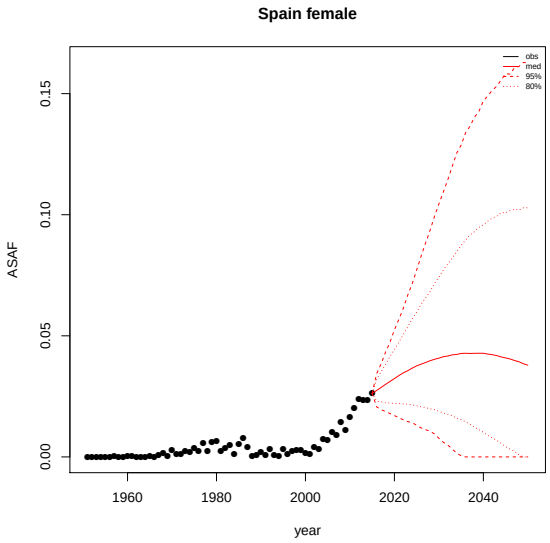
Spain female
ASAF
year
obs
med
95%
80%


Sweden male
ASAF
year
obs
med
95%
80%

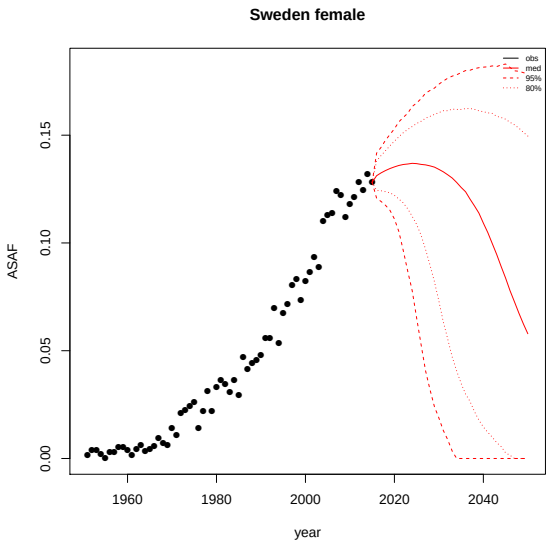
Sweden female
ASAF
year
obs
med
95%
80%

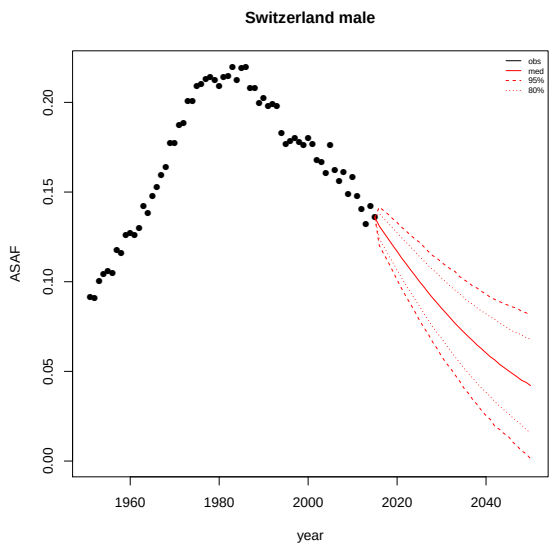
Switzerland male
ASAF
year
obs
med
95%
80%

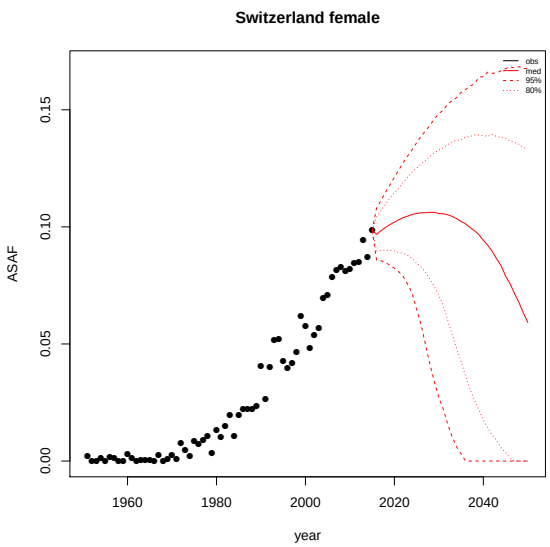
Switzerland female
ASAF
year
obs
med
95%
80%

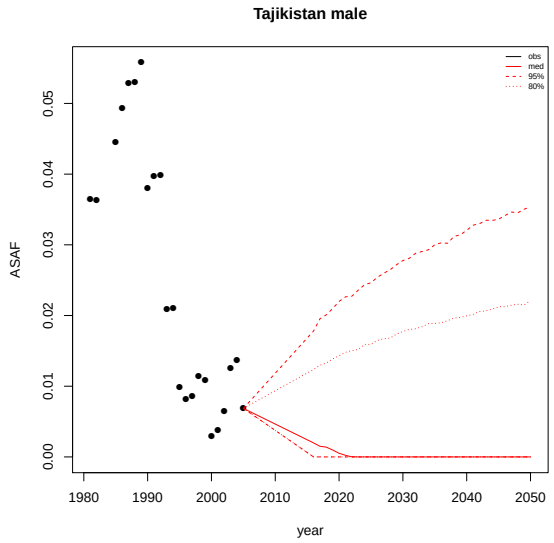
Tajikistan male
obs
med
95%
80%
ASAF
0.00
0.01
0.02
0.03
0.04
0.05
1980
1990
2000
2010
2020
2030
2040
2050
year

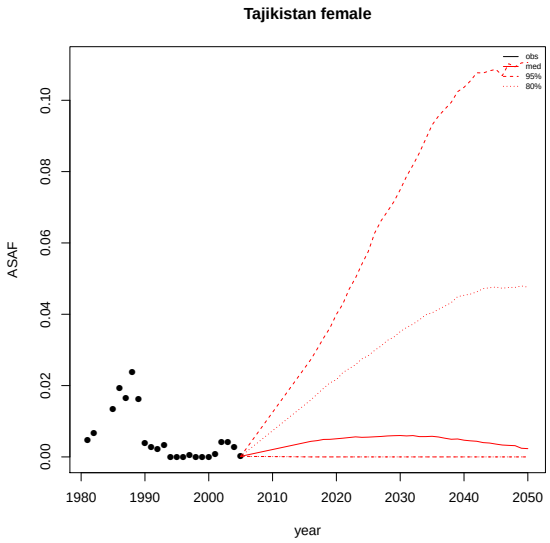
Tajikistan female
obs
med
95%
80%
ASAF
0.00
0.02
0.04
0.06
0.08
0.10
1980
1990
2000
2010
2020
2030
2040
2050
year

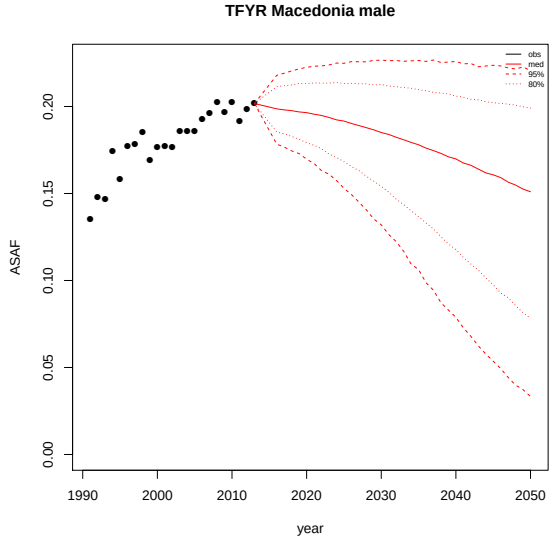
TFYR Macedonia male
obs
med
95%
80%
ASAF
0.00
0.05
0.10
0.15
0.20
1990
2000
2010
2020
2030
2040
2050
year

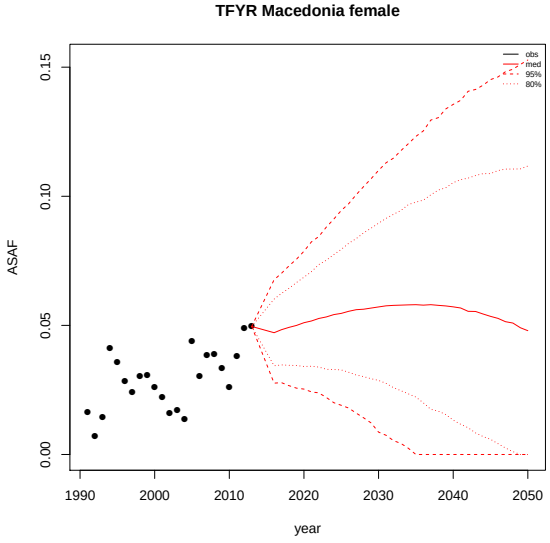
TFYR Macedonia female
obs
med
95%
80%
ASAF
0.00
0.05
0.10
0.15
1990
2000
2010
2020
2030
2040
2050
year

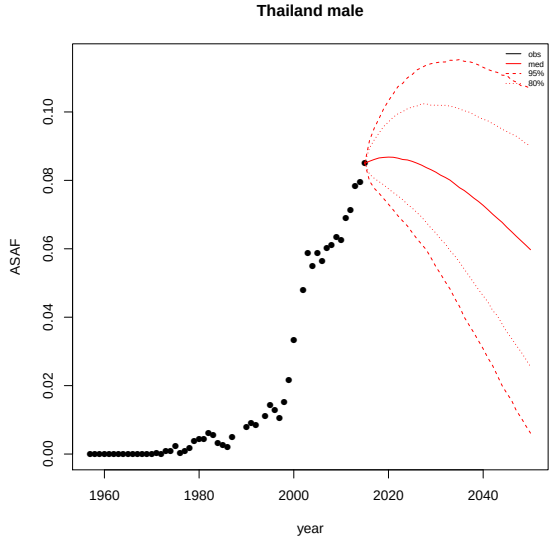
Thailand male
obs
med
95%
80%
ASAF
0.00
0.02
0.04
0.06
0.08
0.10
1960
1980
2000
2020
2040
year

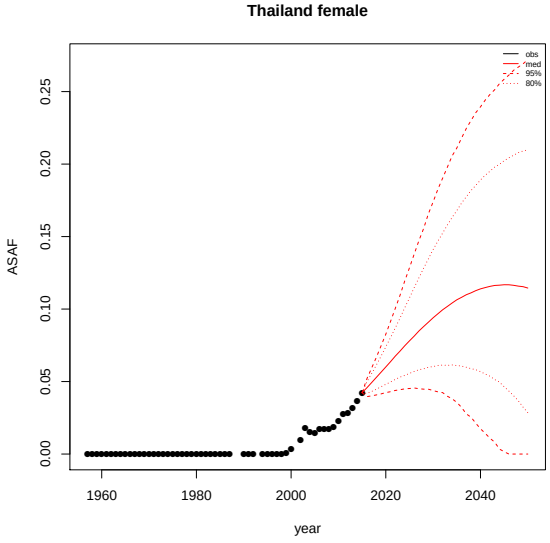
Thailand female
obs
med
95%
80%
ASAF
0.00
0.05
0.10
0.15
0.20
0.25
1960
1980
2000
2020
2040
year

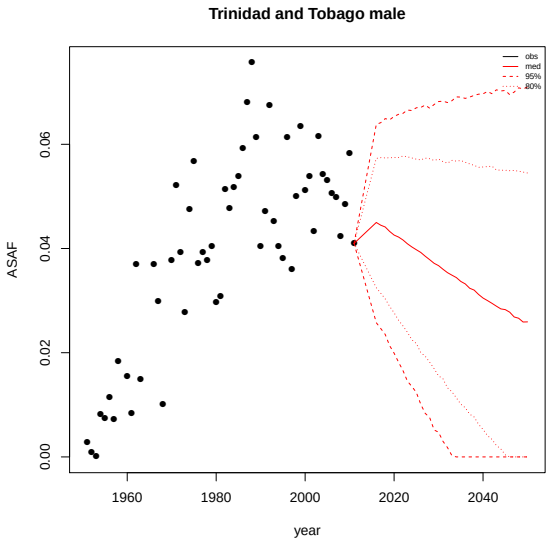
Trinidad and Tobago male
obs
med
95%
80%
ASAF
0.00
0.02
0.04
0.06
1960
1980
2000
2020
2040
year

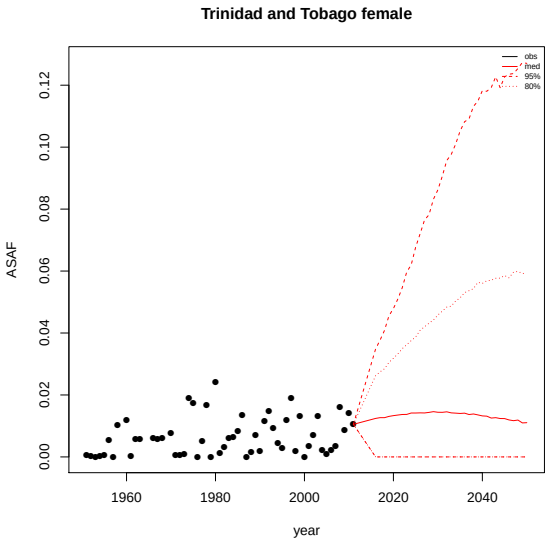
Trinidad and Tobago female
obs
med
95%
80%
ASAF
0.00
0.02
0.04
0.06
0.08
0.10
0.12
1960
1980
2000
2020
2040
year

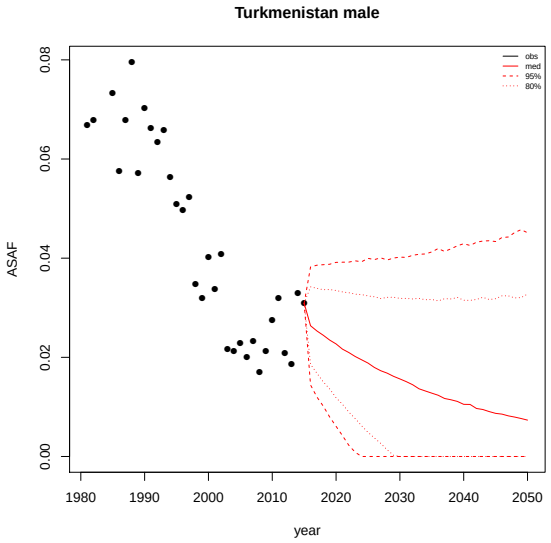
Turkmenistan male
obs
med
95%
80%
ASAF
0.00
0.02
0.04
0.06
0.08
1980
1990
2000
2010
2020
2030
2040
2050
year

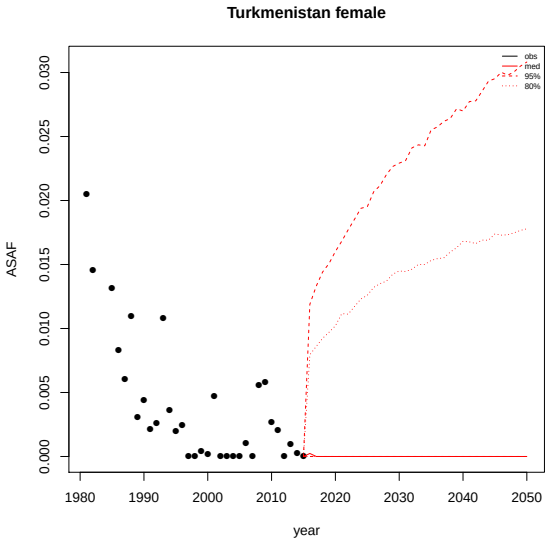
Turkmenistan female
obs
med
95%
80%
ASAF
0.000
0.005
0.010
0.015
0.020
0.025
0.030
1980
1990
2000
2010
2020
2030
2040
2050
year

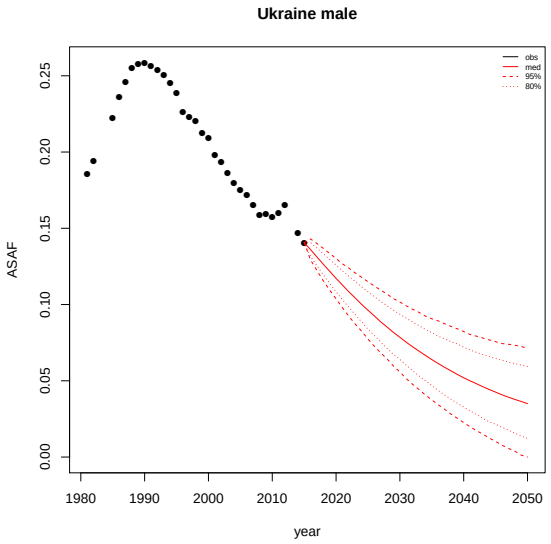
Ukraine male
obs
med
95%
80%
ASAF
0.00
0.05
0.10
0.15
0.20
0.25
1980
1990
2000
2010
2020
2030
2040
2050
year

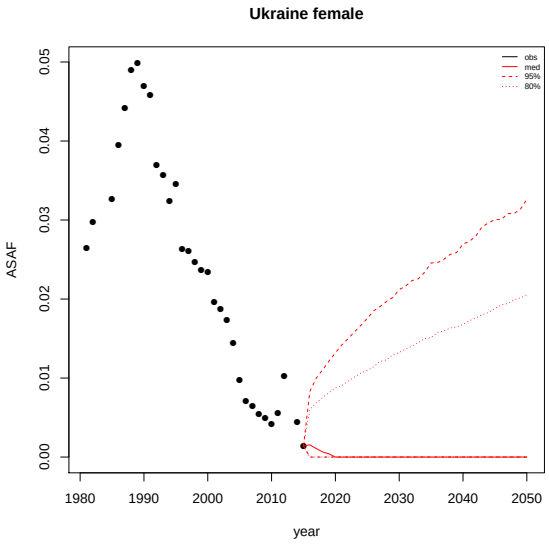
Ukraine female
obs
med
95%
80%
ASAF
0.00
0.01
0.02
0.03
0.04
0.05
1980
1990
2000
2010
2020
2030
2040
2050
year

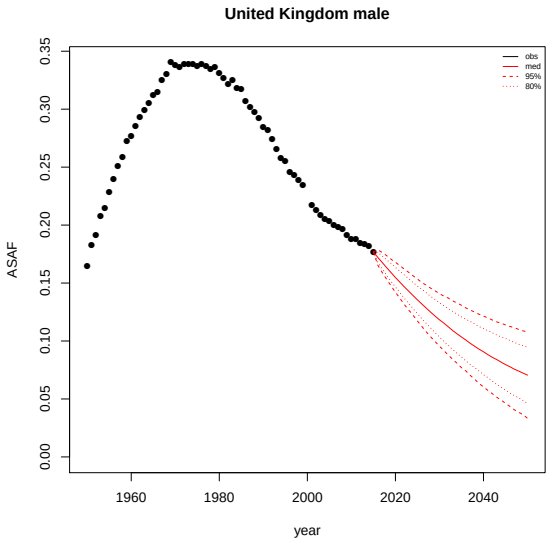
United Kingdom male
ASAF
year
obs
med
95%
80%

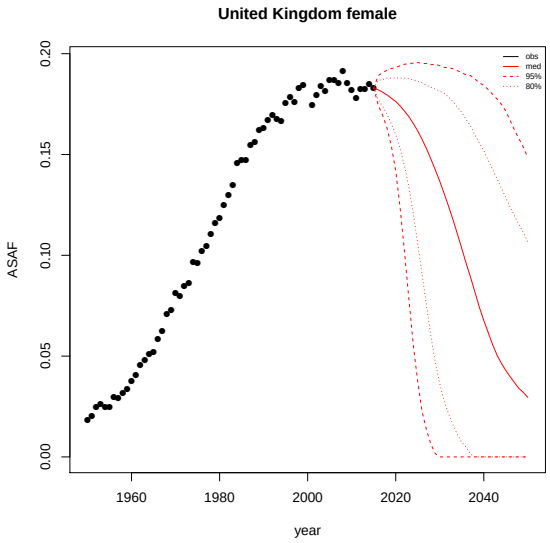
United Kingdom female
ASAF
year
obs
med
95%
80%

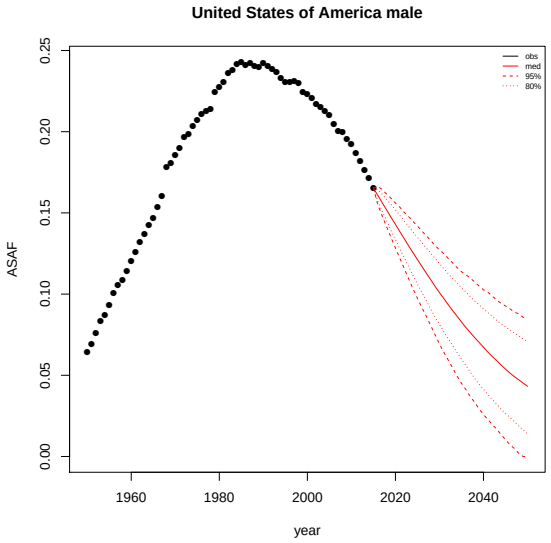
United States of America male
ASAF
year
obs
med
95%
80%

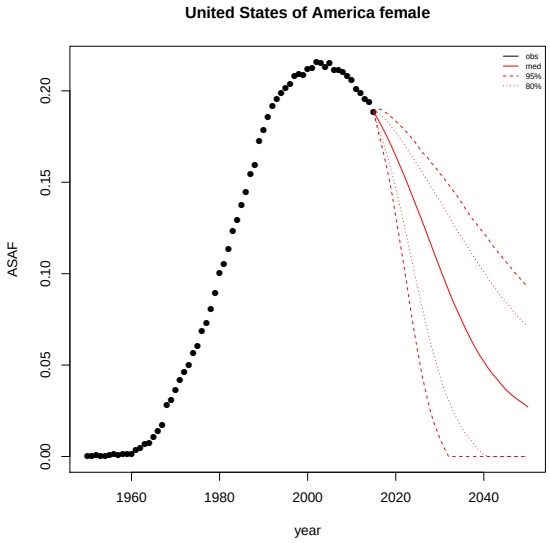
United States of America female
ASAF
year
obs
med
95%
80%

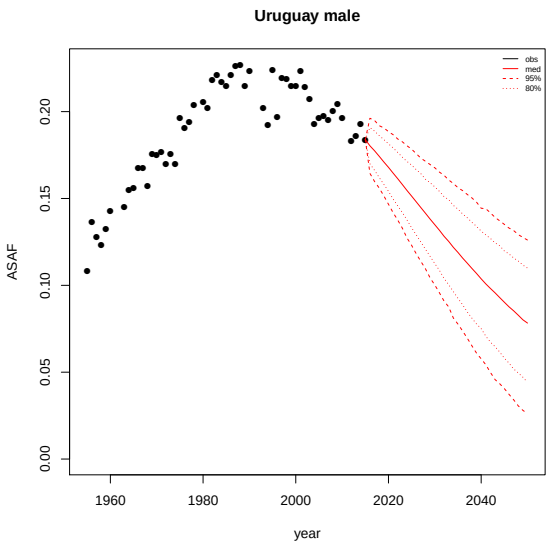
Uruguay male
ASAF
year
obs
med
95%
80%

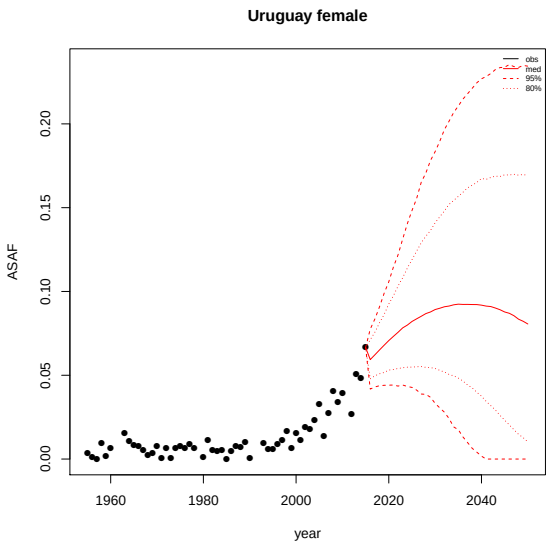
Uruguay female
ASAF
year
obs
med
95%
80%

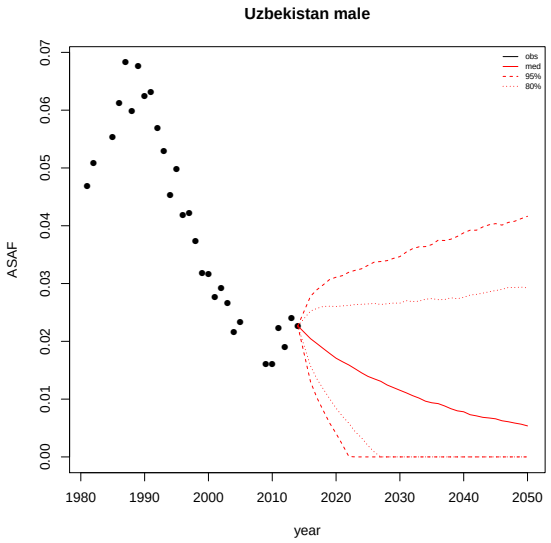
Uzbekistan male
ASAF
year
obs
med
95%
80%

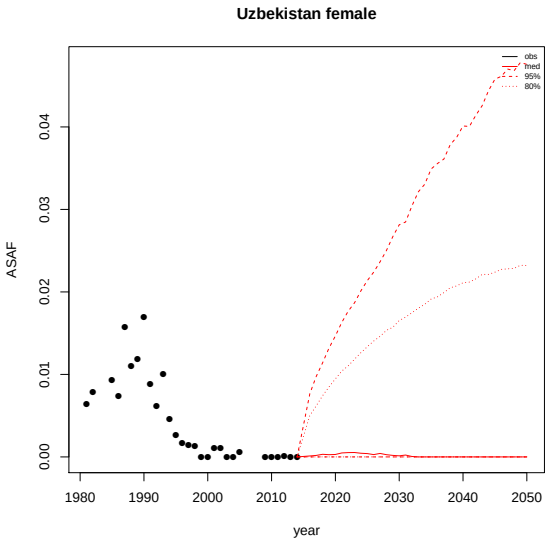
Uzbekistan female
ASAF
year
obs
med
95%
80%

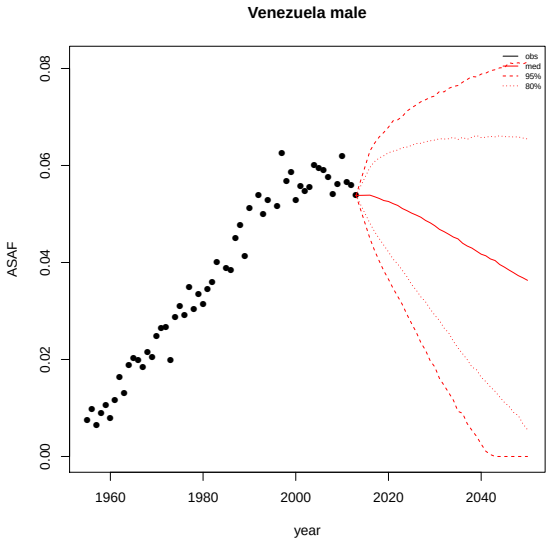
Venezuela male
ASAF
year
obs
med
95%
80%

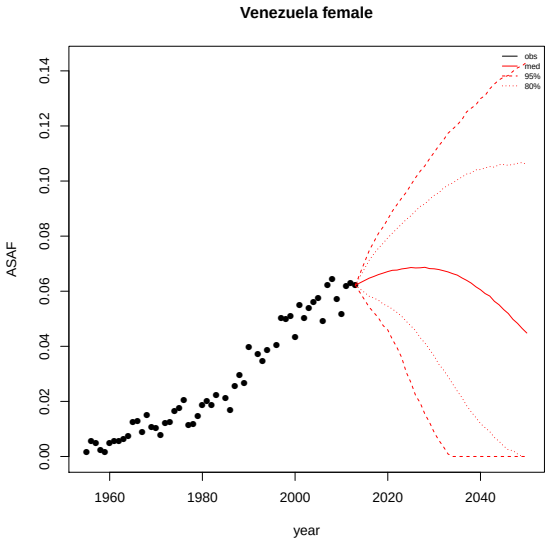
Venezuela female
ASAF
year
obs
med
95%
80%